

2020

Cytotoxicity and genotoxicity induced by silica nanoparticles in human dental pulp cell culture

<https://hdl.handle.net/2144/41352>

"Downloaded from OpenBU. Boston University's institutional repository."

BOSTON UNIVERSITY
HENRY M. GOLDMAN SCHOOL OF DENTAL MEDICINE

DISSERTATION

**CYTOTOXICITY AND GENOTOXICITY INDUCED BY SILICA
NANOPARTICLES IN HUMAN DENTAL PULP CELL CULTURE**

by

OMAR RIFAT ALKHATTAB

BDS, King Abdulaziz University, 2013
CAGS, Boston University School of Dental Medicine, 2020

Submitted in partial fulfillment of the requirements for the degree of

Doctor of Science in Dentistry
In the Department of Restorative Sciences and Biomaterials

2020

First Reader

Laisheng Chou, DMD, CAGS, PhD
Professor, Department of Restorative Sciences and Biomaterials
Professor and Director of Oral Medicine
Goldman School of Dental Medicine
Professor of materials science and engineering,
College of Engineering
Boston University

Second Reader

Sami Chogle, BDS, DMD, MSD, CAGS
Herbert Schilder Professor in Endodontics
Chair, Department of Endodontics
Associate professor of Endodontics
Director, Advanced Education Program in Endodontics
Boston University Goldman School of Dental Medicine

Third Reader

Russell Giordano, DMD, CAGS, DMSc
Associate Professor of Restorative Sciences and biomaterials
Director of Biomaterials
Assistant Dean, Biomaterials and biomaterials research
Goldman School of Dental Medicine
Associate professor in materials science and engineering
College of Engineering
Boston University

ACKNOWLEDGMENTS

I wish to express my sincere appreciation and gratitude to those who helped me complete this Doctorate of Science in Dentistry thesis and enriched my experience at the Department of Restorative Sciences and Biomaterials.

Professor Laisheng Chou, my mentor and research advisor, for his support, knowledge, guidance, and utmost patience in the process of the research project and thesis. I am lucky to be one of his students.

Professor Dan Nathanson, for accepting me in his department, for his encouragement and inspiration, and his valuable comments during research presentations throughout the years that made me a more knowledgeable dentist.

Dr. Sami Chogle, for believing in me and giving me the opportunity to be part of this program and for his support and guidance. It is a privilege to have such a role model in the field of endodontics who always helped me to step forward.

Mrs. Claire Zhang for all her help with my experiments and for sharing her knowledge and support and answering all my questions.

The staff and colleagues of the Department of Restorative Sciences and Biomaterials for their knowledge, kindness, and encouragement.

This achievement would not be possible without the unconditional love of my parents and brother and sisters, who always supported me and boosted my confidence while encouraging me to be the best in my field and reminding me the importance of education.

CYTOTOXICITY AND GENOTOXICITY INDUCED BY SILICA NANOPARTICLES
IN HUMAN DENTAL PULP CELL CULTURE

OMAR R. ALKHATTAB

Boston University, Henry M. Goldman School of Dental Medicine, 2020

Major Professor: Dr. Laisheng Chou, Professor, Department of Restorative Sciences and
Biomaterials

ABSTRACT

This study was designed to evaluate the cell attachment efficiency, cell proliferation, cytotoxicity and genotoxicity of different sizes and doses of silica on human dental pulp cell culture. Human dental pulp cells (HDPCs) derived from extracted third molars were cultured in growth media and supplemented with two sizes of silica particles (70 nm – 225 nm) and (1 μ m – 5 μ m) in different doses: (12.5 μ g/mL, 50 μ g/mL, 100 μ g/mL and 1000 μ g/mL) and media without silica particles as a control, for the time intervals of 16h, 24h, 7 and 14 days. Attachment efficiency and cell proliferation were measured by comparing optical density of crystal violet stained cells. Cytotoxicity was measured using water-soluble dye that changes its absorption spectra upon cellular reduction. Genotoxicity was measured using specific antibody-based detection. Cultures with Si-np50, Si-np100, Si- μ p12.5, Si- μ p50, Si- μ p100 at 16h yielded significantly higher attachment efficiency compared to the other doses. Cultures with Si-np50 and Si-np100 showed increased attachment efficiency compared to cultures with their larger

microparticles counterparts ($P < 0.05$). Cultures with Si- μ p12.5 displayed similar proliferation compared to the control at day 14. Higher doses showed significant reduction in proliferation compared to lower doses in all sizes of Si-np and Si- μ p at day 14. All the silica nanoparticles groups showed lower proliferation when compared to their larger microparticles counterparts at 14 days ($P < 0.05$). When comparing different doses in the cytotoxicity assay all the groups displayed cytotoxicity by day 14, except the Si- μ p12.5 group. And when comparing different sizes, all the doses of Si-np showed higher levels of cytotoxicity when compared to Si- μ p at day 14 ($P < 0.05$). Cultures with 1000 μ g/mL group displayed significantly higher genotoxicity in both sizes when compared to lower doses at day 1. When comparing both sizes to each other, nanoparticles showed a higher genotoxicity than microparticles ($p < 0.05$). In conclusion, the higher doses of silica nanoparticles significantly decreased proliferation and increased cytotoxicity and genotoxicity on normal HDPCs in a dose and size dependent manner. This is the first report to demonstrate the effect of dose and size of silica particles on the proliferation, cytotoxicity and genotoxicity of normal HDPCs.

Table of Contents

ACKNOWLEDGMENTS	iii
ABSTRACT	iv
Table of Contents.....	vi
LIST OF FIGURES	xi
LIST OF PHOTOS	xiv
LIST OF ABBREVIATIONS.....	xv
Chapter 1: INTRODUCTION	2
1.1 Nanotechnology	2
1.2 Physicochemical Characteristics of Nanoparticles	3
1.2.1 Size.....	3
1.3 Silicon	5
1.4 Silica	6
1.5 Silica Genotoxicity.....	7
1.6 Silica Cytotoxicity	8
1.7 Dental Pulp.....	9
1.7.1 Morphologic Zones of the Pulp.....	9
1.7.3 The pulp interstitium and ground substance.	12
1.7.5 Innervation.	12
1.7.6 Vascular supply.....	13
1.7.7 Lymphatics.	13

1.7.8 Pulp Functions	13
1.9 Experimental Basic Research in Regenerative Endodontics Field	16
1.9.1 Scaffolds	16
1.9.2 Morphogens/Growth Factors	17
1.9.3 Stem Cells	18
1.9.4 Delivery systems	20
1.10 Rationale and clinical significance for this research:	22
Chapter 2: HYPOTHESIS	24
Chapter 3: OBJECTIVES OF THE STUDY	26
Chapter 4: MATERIALS AND METHODS	29
2.1 Materials	29
2.1.1 Table 1 : List of materials	29
2.1.2 Table 2 : List of chemicals, enzymes, growth media and kits	32
2.1.3 Table 3 : List of equipment used.....	34
2.2 Approvals and training.....	36
2.3 Methods.....	37
2.3.1. Silica particles characterization	37
2.3.2 Growth media preparation	38
2.3.3 Cell culture preparation	39
2.3.4 Determination of the optimal cell seeding concentration	47
2.3.5 Silica particles preparation	48
2.3.6 Groups of materials: as shown in (Photo 4)	48

2.3.7 Attachment efficiency assay	50
2.3.8 Proliferation rates with crystal violet staining assay	51
2.3.9 Cytotoxicity Assay	53
2.3.10 Genotoxicity Assay	54
2.4 STATISTICAL ANALYSIS	57
Chapter 5: RESULTS	59
3.1 Characterization of silica particles	59
3.1.1 SEM, TEM.....	59
3.1.2 DLS	66
3.2 Attachment efficiency	69
3.2.1 Attachment efficiency of normal human dental pulp cells affected by different doses of silica nanoparticles at 16 hours	69
3.2.2 Attachment efficiency of normal human dental pulp cells affected by different doses of silica microparticles at 16 hours	71
3.2.3 Attachment efficiency of normal human dental pulp cells affected by different sizes of silica particles at 16 hours	73
3.3 Proliferation	76
3.3.1 Proliferation of normal human dental pulp cells affected by different doses of silica nanoparticles at different time intervals:	76
3.3.2 Proliferation of normal human dental pulp cells affected by different doses of silica microparticles at different time intervals:	82

3.3.3 Proliferation of normal human dental pulp cells affected by different sizes of silica particles at different time intervals:	88
3.4 Cytotoxicity.....	95
3.4.1 Cytotoxicity of normal human dental pulp cells affected by different doses of silica nanoparticles at different time intervals:	95
3.4.2 Cytotoxicity of normal human dental pulp cells affected by different doses of silica microparticles at different time intervals:	101
3.4.3 Cytotoxicity of normal human dental pulp cells affected by different sizes of silica particles at different time intervals :	107
3.5 Genotoxicity.....	114
3.5.1 Genotoxicity of normal human dental pulp cells affected by different doses of silica nanoparticles at different time intervals:	114
3.5.2 Genotoxicity of normal human dental pulp cells affected by different doses of silica microparticles at different time intervals:	116
3.5.3 Genotoxicity of normal human dental pulp cells affected by different sizes of silica particles at different time intervals:	118
Chapter 6: DISCUSSION	121
Chapter 7: CONCLUSIONS.....	133
REFERENCES	136
CURRICULUM VITAE.....	153

LIST OF TABLES

2.1.1 Table 1 : List of materials	29
2.1.2 Table 2 : List of chemicals, enzymes, growth media and kits	32
2.1.3 Table 3 : List of equipment used.....	34

LIST OF FIGURES

Figure 1 : The size distribution of the nanoparticles group, immediately after sonication in culture medium, ranging from 14 nm to 70 nm with a mean of 32 nm	67
Figure 2 : The size distribution of the nanoparticles group, after 3 days, ranging from 38 nm to 225 nm with a mean of 92 nm.	68
Figure 3 : Attachment efficiency of normal human dental pulp cells exposed to different doses of Silica Nanoparticles at 16 hours:	70
Figure 4 : Attachment efficiency of normal human dental pulp cells affected by different doses of silica microparticles at 16 hours	72
Figure 5 : Attachment efficiency of normal human dental pulp cells affected by different sizes of silica particles at 16 hours.....	74
Figure 6 : Proliferation of normal human dental pulp cells affected by different doses of silica nanoparticles at 24 hours:	77
Figure 7 : Proliferation of normal human dental pulp cells affected by different doses of silica nanoparticles at 7 days:	79
Figure 8 : Proliferation of normal human dental pulp cells affected by different doses of silica nanoparticles at 14 days:	81
Figure 9 : Proliferation of normal human dental pulp cells affected by different doses of silica microparticles at 24 hours:	83
Figure 10 : Proliferation of normal human dental pulp cells affected by different doses of silica microparticles at 7 days	85

Figure 11 : Proliferation of normal human dental pulp cells affected by different doses of silica microparticles at 14 days	87
Figure 12 : Proliferation of normal human dental pulp cells affected by different sizes of silica particles at 24 hours:.....	89
Figure 13 : Proliferation of normal human dental pulp cells affected by different sizes of silica particles at 7 days:	91
Figure 14 : Proliferation of normal human dental pulp cells affected by different sizes of silica particles at 14 days:	93
Figure 15 : Cytotoxicity of normal human dental pulp cells affected by different doses of silica nanoparticles at 24 hours	96
Figure 16 : Cytotoxicity of normal human dental pulp cells affected by different doses of silica nanoparticles at 7 days.....	98
Figure 17 : Cytotoxicity of normal human dental pulp cells affected by different doses of silica nanoparticles at 14 days.....	100
Figure 18 : Cytotoxicity of normal human dental pulp cells affected by different doses of silica microparticles at 24 hours	102
Figure 19 : Cytotoxicity of normal human dental pulp cells affected by different doses of silica microparticles at 7 days	104
Figure 20 : Cytotoxicity of normal human dental pulp cells affected by different doses of silica microparticles at 14 days	106
Figure 21 : Cytotoxicity of normal human dental pulp cells affected by different sizes of silica particles at 24 hours.....	108

Figure 22 : Cytotoxicity of normal human dental pulp cells affected by different sizes of silica particles at 7 days	110
Figure 23 : Cytotoxicity of normal human dental pulp cells affected by different sizes of silica particles at 14 days	112
Figure 24 : Genotoxicity of normal human dental pulp cells affected by different doses of silica nanoparticles at 24 hours:	115
Figure 25 Genotoxicity of normal human dental pulp cells affected by different doses of silica microparticles at 24 hours:	117
Figure 26 Genotoxicity of normal human dental pulp cells affected by different sizes of silica particles at 24 hours	119

LIST OF PHOTOS

Photo 1 : Steps of human dental pulp cells extraction.	40
Photo 2 : Display of primary cell culture in 12.5cm ² flask	42
Photo 3 : Secondary cell culture showing 70-80% confluence.....	44
Photo 4 : 96 well plates design representing each experimental group (n=4)	49
Photo 5 : SEM images of SiO ₂ microparticles (1 - 5 μm) dispersed in DI water were analyzed to verify their morphology and size taken at lower magnification x2.00k. 60	
Photo 6 : SEM images of aggregated Si-np (70-225 nm) dispersed in DI water prior to particles sonication treatment.	61
Photo 7 : SEM images of SiO ₂ nanoparticles (70-225 nm) dispersed in DI water were analyzed to verify their morphology and size.	62
Photo 8 : TEM images of SiO ₂ NPs (70-225 nm) to verify their size and shape.....	63
Photo 9 : TEM images of SiO ₂ NPs (70-225 nm) to verify their size and shape.	64
Photo 10 : TEM images of SiO ₂ NPs (70-225 nm) to verify their size and shape.	65

LIST OF ABBREVIATIONS

ALP: alkaline phosphatase

AMP: Adenosine monophosphate

ANOVA: analysis of variance

BME: basal Medium Eagle

BMMSC: bone marrow derived mesenchymal stem cells

BSP: bone sialoprotein

CS: calcium silicate

CITI: collaborative institutional training Initiative

Ca (OH)₂: calcium hydroxide

DFPC: dental follicle progenitor cells

DLS: dynamic light scattering

DSP: double strand break

DPMSC: dental pulp mesenchymal stem cells

ECM: extracellular matrix

EDTA: ethylenediamine tetra-acetic acid

EDS: energy dispersive X-ray spectroscopy

ES: embryonic stem cells

FBS: fetal bovine serum

FE-SEM: field emission scanning electron microscope

PGA: polyglycolic acid

PLA: polylactic acid

PLGA: polylactic-co-glycolic acid

HA: hydroxyapatite

HR: hours

IBC: institutional biosafety committee

IRB: institutional review board

IPS: induced pluripotent stem cells

MTA: mineral trioxide aggregate

MSC: mesenchymal stem cells

NaOCL: sodium hypochlorite

Np: nanoparticles

OCN: osteocalcin

OPN: osteopontin

PRP: Platelet rich plasma

PBS: phosphate buffered saline solution

PDi: polydispersity index

RES: reticulo-endothelial system

RT: room temperature

RPM: rounds per minute

SCAP: stem cells of the apical papilla

SEM: scanning electron microscope

SHED: stem cells of human exfoliated deciduous teeth

SiO₂: silica (silicon dioxide)

TEM: transmission electron microscope

TRITC: tetramethylrhodamine

Si-np: Silica nanoparticles

Si- μ p: Silica microparticles

Si-np12.5: 12.5 μ g/mL Silica nanoparticles

Si-np50: 50 μ g/mL Silica nanoparticles

Si-np100: 100 μ g/mL Silica nanoparticles

Si-np1000: 1000 μ g/mL Silica nanoparticles

Si- μ p12.5: 12.5 μ g/mL Silica microparticles

Si- μ p50: 50 μ g/mL Silica microparticles

Si- μ p100: 100 μ g/mL Silica microparticles

Si- μ p1000: 1000 μ g/mL Silica microparticles

INTRODUCTION

Chapter 1: INTRODUCTION

1.1 Nanotechnology

Nanotechnology is a rapidly developing interdisciplinary field that became an important tool for a diverse range of applications in medical, chemical, aerospace engineering, electronics, sport and consumer products. The European Commission's defines "nanomaterial" as natural, incidental, or manufactured materials containing particles in an unbound state, as an aggregate or as an agglomerate, and where for 50% or more of the particles in the number size distribution, one or more of their external dimensions is ranges from 1 nm to 100 nm (1–5).

This rapid development in the field of nanotechnology enabled us to synthesize nanomaterials with unique physical, chemical, and biological properties due to the enhanced surface-to-volume ratio compared to their larger counterparts and to the quantum phenomena of nanoparticles (6–10). The behavior of nanoparticles is different from their larger counterparts due to two effects. The first is the lower stability of surface atoms compared to the bulk atoms because they have few neighbors, which results in unsatisfied bonds. The second is the quantum confinement effect in materials with delocalized electrons (11,12).

Based on the structural dimensions, nanomaterials can be classified into three categories: 1) zero-dimensional nanostructures such as nanoparticles, 2) one-dimensional nanostructures such as nanorods, and 3) two-dimensional nanostructures such as thin films (13,14). Based on the activity, they can be classified into bioactive nanomaterials and

bioinert nanomaterials. The former include hydroxyapatite, bioglass and tricalcium phosphate, and the latter include titanium, alumina, zirconia, and vitreous carbon (15).

1.2 Physicochemical Characteristics of Nanoparticles

The characterization of properties and effects of nanoparticles is an important step in their synthesis for medical use because it will affect their behavior in biological tissues in regards to size. The optimal size of nanoparticles for in vivo delivery is in the range of 10-100 nm, smaller particles (<10 nm) will be subjected to renal elimination while bigger ones (>200 nm) will be affected by reticulo-endothelial system (RES) sequestration(16). The life span and fate of nanoparticles in the circulation are determined by another factor, the surface characteristics, in order to inhibit the uptake by RES and avoid the interactions with plasma proteins. The surface of nanoparticles must ideally be hydrophilic (17). Nanoparticles planned to be used in actively targeting specific receptors on cells must be incorporated with appropriate ligands on their surface. Finally, it is important to study the biocompatibility of those particles on cells and tissues.

1.2.1 Size

The size of nanoparticles is considered one of the most important factors that determines their distribution in biological systems and interactions with cells. Size also plays an important role in the vascular extravasation and clearance from the human body, which is crucial during nanoparticles' application as drug carriers. Dynamic light scattering (DLS) and electron microscopy are the most commonly used tools for nanoparticles size measurements (18).

DLS is a very popular, rapid technique that requires minimal sample preparation and can be done on small volumes. It monitors the fluctuations in the intensity of the scattered light with a photon detector when a laser beam is directed at the dispersion and relates it to the size of a hypothetical hard sphere that diffuses at the same fashion of those particles being measured. It then quantifies the Brownian motion of the nanoparticles in a dispersion and relates the translational diffusion coefficient or velocity to the size of nanoparticles using the Stokes-Einstein.

Unfortunately, the results of the DLS can be distorted by the presence of the aggregates and that's why it's so essential to make sure that the sample is well dispersed. Another cause for data misrepresentation is the presence of multimodal particle size distribution. For example, when measuring a mixture of 100 nm and 20 nm, smaller particles' signals were lost because the larger particles masked the scattering intensity of these small particles (19).

Another factor that can affect the hydrodynamic size is the concentration of the dispersion, as a highly concentrated sample would present multiple scattering while an extra-diluted sample might not be sufficient to produce scattering(19). A number of researchers assessed the stability of nanoparticles in different types of media using DLS (20–22).

In order to complement the particle size measurements that were obtained using DLS, electron microscopy can be used. Scanning electron microscope (SEM) provides valuable information about the particles' sizes and shapes, including surface features and composition., It operates at a high vacuum when a high-energy electron beam is directed

to the surface of the sample. The backscattered electrons, x-rays, and secondary electrons that result from the interactions with the sample are collected, and the samples of the SEM are mounted on a sample holder and should be electrically conductive or sputter coated with a conductive layer (13).

Transmission electron microscope (TEM) is another method to analyze the nanoparticles in a higher resolution at the atomic scale to provide more information on the structure of the nanoparticles. It also utilizes an electron beam that interacts with the sample in high vacuum, but the difference here is that the transmitted electrons are detected (13).

1.3 Silicon

Silicon is one of the most abundant elements on earth, and it is found in connective and osseous tissues. It also plays a role in the early stages of bone formation, including stimulation of calcification in human tissues (23,24). Its absence has been linked to the development of many human disorders, including esophageal cancer, fibrotic lung disease, silicosis, and asbestosis. Silicon ions induce osteogenesis that causes higher levels of ALP and osteocalcin DSP, therefore leading to mineralization.

The significance of silicon in bone development has been widely studied, silicon is required for cell proliferation and regulation of DNA replication, as well as increased cyclic AMP levels(25) . Silicon has also been shown to stimulate DNA synthesis and encourage growth in fibroblastic and osteoblastic cells(26,27).

Clinical applications of bioactive silicon are widespread in the field of dentistry. These have been used for endosseous implants and in other periodontal procedures, including sinus lifts and bone grafting with high success rates(28).

1.4 Silica

Elemental silicon, or silica, is commonly used in manufacturing computer chips and solar cells. In its elemental form, it is a lightweight silver-colored metal normally found bound to four oxygen atoms forming silica. This silica tetrahedron forms the basis for most silicate minerals through the binding of silicon to four oxygen atoms in a tetrahedron pyramid. But a silica tetrahedron is more than just a stable pyramid. Just as every silicon atom needs to engage itself in four bonds, and each oxygen atom needs two. This means each oxygen atom in a single silica tetrahedron is unsatisfied. None of the oxygen atoms in a single silica tetrahedron have more than their single bond with the central silicon. One alternative is for a number of silica tetrahedra to come together so that each oxygen atom binds with two silicon atoms(29).

Silica nanoparticles are some of the most utilized nanomaterials in the field of nanotechnology. They can occur in numerous forms, including crystalline, simple amorphous, or mesoporous forms (30). Generally, mesoporous silica has a well-defined nanoporous structure and has been shown to be an effective drug carrier (31) and a nucleic acid delivery vehicle (32). Amorphous silica nanoparticles, on the other hand, are characterized by a non-crystalline structure and are currently employed in a wide range of industrial and biomedical applications (30). The relative ease by which as nanoparticles can be produced in different sizes and with different surface modifications has led to their widespread use in cosmetics (sunscreens), dentistry (toothpaste) and paints, as well as a food and animal feed additive (33). In biomedicine, silica nanoparticles are used as drug delivery systems (34,35), especially in cancer therapy and diagnostics (36,37).

1.5 Silica Genotoxicity

Genotoxicity is defined as a double strand break (DSB) in DNA that is a harmful lesion in mammalian cells. One of the common responses to DSB formation is phosphorylation of H2A histones. Genotoxic agents promote phosphorylation of histone variant H2AX that forms micronuclei at the site of DNA DSB. Phosphorylated H2AX aids in the assembly of proteins that are essential for DSB repair. An HCS DNA Damage Kit (Invitrogen) was used to detect and measure genotoxicity through specific antibody-based detection of phosphorylated H2AX in the nucleus is used for measuring DNA damage, which is accomplished by using pH2AX monoclonal antibody.

The genotoxic potential of silica nanoparticles was investigated. However, the results are not consistent. Amorphous silica nanoparticles in two different sizes, 30 nm and 80 nm, were genotoxic in 3T3-L1 mouse embryonic fibroblasts carrying lacZ reporter gene(38).

On the contrary, no genotoxic findings have been observed after mouse fibroblasts cells were exposed to alumina-coated silica nanoparticles ranging in size from 20 nm to 250 nm as measured by Comet Assay(39).

Similarly, no significant increase in the micronucleus formation was found in mouse fibroblasts exposed to 15-300 nm SiNP despite their cellular internalization(30).

1.6 Silica Cytotoxicity

The ever-increasing globalization of silica nanoparticles in industrial and commercial application has augmented human exposure to silica nanoparticles in environmental and vocational settings. Evidence is mounting regarding the induction of cytotoxicity by silica nanoparticles. Studies using in vitro models have reported cytotoxic results after exposure of silica nanoparticles to different cell lineages (40).

Numerous studies have demonstrated nanoparticles unique physical chemical properties, including size and surface characteristics, that ultimately amplify their potential to induce cytotoxicity(40). Numerous other studies have shown that amorphous silica has the potential to reduce the viability of many different human cell types or increase the reactive oxidative species concentration(41–45). Initial studies of silicon nanoparticles' effect on rodent-derived cells have shown that these nanoparticles impair cell viability and induce proinflammatory cytokines such as interleukin-1, as well as increase the secretion of ROS (46–50).

Exposure to silica nanoparticles should be reduced to avoid unwanted effects. In a study that compared different doses and sizes (20 nm and 80 nm) of silica nanoparticles on HFL-1 cells, a significant ROS release occurred. In addition, the induction of p53, Bax expression, inhibition of cl-2 production and activation of caspase 9 eventually resulted in the apoptosis of HFL-1 cells in a size-associated and dose-dependent manner, where the higher the concentration (from 250 mg/L to 2000 mg/L). The smaller the dimensions of particles, the greater the inhibition and apoptosis were found (51).

Considering the existence of different toxicity levels between micro and nano scales, as demonstrated for TiO₂ (52) , polystyrene nanoparticles (53), it is likely that nanosized silica can have a different effect than microscale sizes. This issue becomes important because of the increasing use of silica nanoparticles in different industries, as was mentioned earlier.

Different forms of silica nanoparticles have different effects at the cellular level. Amorphous silica nanoparticles were found to be cytotoxic in a number of studies. In a study that compared 15 nm and 46 nm to A549 human lung cancer cells, silica nanoparticles were found cytotoxic after 48 and 72 hours of exposure to concentrations of 10 micrograms per milliliter(44).

1.7 Dental Pulp

Dental pulp is a unique connective tissue of mesenchymal origin that is enclosed within a hard tissue (enamel, dentin, and cementum) that protects it from the external microbial-rich environment. The pulp is a unique sensory organ that includes a variety of tissue elements, including ground substance, connective tissue fibers, vascular tissue, axons, and various types of cell (54–57)

1.7.1 Morphologic Zones of the Pulp

Pulp-dentin complex. Pulp is protected by dentin, which is produced by odontoblasts that play an important role in the pulp-dentin complex. These are located in the periphery of the dental pulp and extend into the dentin. Thus, they function as a single unit.

Odontoblast layer. The odontoblast layer is located next to the predentin. It is the outermost layer of cells in healthy dental pulp and contains the cell bodies of odontoblasts, the processes of which pass through the predentin into dentin. It also contains nerve fibers and capillaries among the odontoblast cell bodies.

Cell-poor zone. The presence or absence of this zone depends on the status of the pulp (63). It is a narrow zone located adjacent to the odontoblast layer that is free of cells and is crossed by nerve fibers, blood capillaries, and fibroblast cellular processes.

Cell-rich zone. This zone contains a variety of cells, including macrophages, dendritic cells, undifferentiated mesenchymal stem cells, and fibroblasts, more of which are in this zone than in the most central part of the dental pulp.

Pulp proper. This zone represents the central area of the dental pulp. It contains nerves, larger blood vessels, and loose connective tissue. Fibroblasts are the most prominent cells in this zone.

1.7.2 Pulp Cells

Odontoblasts. These are the most specialized cells in the pulp-dentin complex and play a major role in dentinogenesis by producing a matrix of collagen fibrils, proteoglycans, and noncollagenous proteins. They exhibit the ultrastructural characteristics of protein secreting cells, the nuclei of which contain one or more prominent nucleoli that are rich in RNA, numerous mitochondria, a prominent golgi complex, and highly ordered RER. Odontoblasts secrete acid phosphatase and alkaline phosphatase(58), dentin sialoprotein, phosphophoryn(59),collagen (primarily type I)(60,61) and proteoglycans(62–64).

Pulp fibroblasts. Fibroblasts are the most abundant type of cells in the dental pulp. They appear to be tissue specific and can be differentiated if given the proper signal. They synthesize Types I and III collagen, GAGs, and proteoglycans, and play a role in phagocytosis that enables them to control collagen turnover. Further, they produce the matrix proteins of the interstitium at the ultrastructural level. Mature fibroblasts exhibit properties of protein secreting cells and appear stellate in shape, with a large golgi complex and RER.

Macrophages. Macrophages are found adjacent to blood vessels. They are monocytes that move from the bloodstream to the tissues and are differentiated into many subpopulations. Because of their phagocytic activity and mobility, they act as scavengers for extravasated red blood cells, foreign bodies, and dead cells. A major subpopulation plays an important role in endocytosis and phagocytosis, while another subset has an important immune role in processing antigens and presenting them to memory T cells(65).

Dendritic cells. Dendritic cells are identified by their cytoplasmic processes and the class II MHC complex on their cell surface. They occupy the periphery of the coronal pulp next to the predentin and move to the center after initiation of an immune response(66). They serve an important function in T cell-dependent immunity in antigen presentation.

Lymphocytes. The predominant T-lymphocyte in the human dental pulp is T8 (suppressor) lymphocytes(67).

Mast cells. Mast cells are found routinely in chronically inflamed pulp(68), and rarely in normal pulp tissue. They exist in small groups adjacent to blood vessels and are

distributed in the connective tissue. They play an important role in inflammatory reactions, and their granules contain histamine, heparin, and other chemicals.

1.7.3 The pulp interstitium and ground substance.

The interstitium is amorphous and is considered a gel rather than a solid. It consists of an interstitial (extracellular) matrix and interstitial fluid, and occupies the extravascular and extracellular space. Its major structural component is collagen.

Glycoproteins. These constitute the largest number of proteins in the ECM(69). Proteoglycans are an important subclass of glycoproteins that determine the physical characteristics of a tissue because they regulate the dispersion of interstitial matrix solutes, water, and colloids. They also control a variety of cellular interactions and provide cellular support (64).

1.7.4 Connective Tissue Fibers of the Pulp

Collagen and elastin are two types of structural proteins found in the dental pulp. Odontoblasts synthesize Type I collagen, and fibroblasts synthesize Types I, III, V, and VII, while elastin is a structural protein that is confined in the walls of the arterioles.

1.7.5 Innervation.

The nerve fibers enter through the radicular pulp with blood vessels and spread out beneath the cell-rich zone once they reach the coronal pulp. The innervation of the pulp is composed of autonomic or efferent neurons(70), which produce neurogenic balance in the microcirculation and inflammatory reactions(71), while afferent neurons process sensory impulses. The pulp contains two types of sensory nerve fibers: unmyelinated (C fibers) and

myelinated (A fibers)(70–75).

1.7.6 Vascular supply.

The apical foramen is the main entrance for blood from the dental artery, which enters in arterioles with nerve bundles. Another entrance is via the lateral or accessory canals for the smaller vessels. Neuronal control dominates the blood flow(76–80).

Arterioles access the center of the radicular pulp and disperse branches to the odontoblast layer(81). They diminish in size and branch out toward the dentin as they pass into the coronal pulp(82). Venules become larger as they reach the center of the pulp and usually have thin, muscular, discontinuous walls to facilitate fluids' movement in and out of the vessels.

1.7.7 Lymphatics.

The pulpal lymphatic system plays an important role in the body's immune defense. Its vasculature forms a network of vessels in the interstitium that collects filtered fluid and proteins and returns them through large lymphatics that leave the pulp via the apical foramen and lateral canals of the root(83,84).

1.7.8 Pulp Functions

The function of the pulp can be divided into 5 categories:

1. **Induction.** Pulp serves a major function in dentin's initiation and development, and after the dentin is formed, it also participates in the formation of enamel (85).
2. **Formation.** The pulp's specialized cells, the odontoblasts, which form dentin by secreting the inorganic matrix and transporting the organic components to it, leads

ultimately to its mineralization. They also retain the ability to form dentin throughout life, which allows the pulp to compensate for loss in the hard tissue areas of the tooth that protects it. The dentin formed in this case is called secondary (physiologic) dentin or tertiary (pathologic) dentin(85).

3. **Nutrition.** The pulp supplies nutrients that are important for dentin formation and thus maintain its integrity(85).
4. **Defense.** Pulp is composed of cellular components that are important for initial recognition and processing of antigens. T cells are the primary immune cells, and the dendritic cells are the major antigen presenting cells. Another defense mechanism of the pulp tissue is evident in the formation of dentin in response to caries, trauma, or aging, as explained previously(85).
5. **Sensation.** Pulp is a sensory organ that is sensitive to thermal changes. It registers different impulses as common sensation (pain) regardless of the nature of the stimuli (thermal, traumatic, or mechanical deformation), and the proprioceptive function of the pulp also limits the load of the masticatory muscles, thus protecting the teeth. The nerves in the pulp respond to stimuli that act on it directly or through enamel and dentin (85).

1.8 Regenerative Endodontics

Regenerative endodontics can be defined as “biologically based procedures designed to replace damaged structures such as dentin, root structures, and cells of the pulp dentin complex” (86).

Replacement of the affected or infected parts of a tooth with biocompatible materials has been the goal of dental treatment throughout history. In contrast, regenerative endodontics aims to replace those parts with biologically induced mechanisms (87).

Like most of the developing fields, basic research in regenerative endodontics outperformed the translation of this scope into clinical studies and validated dental treatments (88).

Two methods in regenerative endodontics have been proposed by Nakahara. The first approach is based on the principles of tissue engineering through the use of scaffolds, growth factors, and stem cells. The second approach is based on mimicking the embryonic tooth formation through natural development (89). A third approach is based on the regeneration of a functional dentin-pulp complex and its normal functions in the patient’s existing tooth.

1.9 Experimental Basic Research in Regenerative Endodontics Field

Applying tissue engineering concepts forms the basis of these regenerative endodontic procedures that aim to form tissues through the use of scaffolds, growth factors, and stem cells(86).

To identify the key factors responsible for cellular behavior, such as attachment, differentiation, migration, and proliferation, a considerable number of in vitro studies were conducted, and the data obtained from animal studies in endodontic regeneration seem promising(88).

1.9.1 Scaffolds

An important element in tissue engineering is a physical scaffold (90,91) in which cells grow in a three-dimensional structure. They have to be uniquely developed to allow cellular proliferation, differentiation, migration, and attachment in the correct position(92,93) and selective binding and localization of cells (94). It must be biocompatible, biodegradable, provide structural integrity for new tissue formation and angiogenesis, diffusion of nutrients and oxygen that are essential for cellular growth and metabolism, regulate morphogenic signals that will guide stem cells differentiation and can be functionalized to enhance their function in tissue regeneration (95).

Scaffolds can be divided into natural or synthetic. Examples of synthetic scaffolds include bio-ceramics (95), hydroxyapatite/tricalcium phosphate (96), titanium(97) polyglycolic acid (PGA), polylactic acid (PLA), polylactic-co-glycolic acid (PLGA), poly-epsilon caprolactone (98), and hydrogels like alginate (99,100).

The second category of scaffolds are the natural scaffolds that include glycosaminoglycan, demineralized or native dentin matrix (101–103)(104,105), collagen (103,104) and fibrin.

Platelet rich plasma (PRP) has shown promising results when used in endodontic regeneration. It fills most of the criteria listed for the ideal scaffold like providing a three-dimensional fibrin matrix, being autologous, rich in growth factors, and easy to prepare and handle in the dental clinic(106,107).

1.9.2 Morphogens/Growth Factors

Morphogens are extracellular secreted inductive signals that act as growth factors that trigger the differentiation of stem cells into odontoblasts.

Studies have shown that the pulp chamber size decreased with a fivefold increase of the predentin layer's thickness in patients treated with long-term corticosteroids (108). Another study showed that human dental pulp cells were differentiated to odontoblast-like cells in patients treated with dexamethasone (109,110), which was more evident after the addition of 1,25-dihydroxyvitamin D₃ (109). Moreover, other studies showed the effect of ethylenediamine tetra-acetic acid (EDTA) in the exposure of the TGF-β1 from human dentin. Considerable small amounts of TGF-β1 were released after the dentin was treated with citric acid, mineral trioxide aggregate (MTA), sodium hypochlorite (NaOCL), and calcium hydroxide Ca(OH)₂ (111,112).

Finally, the causes of abrupt activation of stem cells in terms of different cellular events like proliferation, differentiation, migration, and matrix secretion after the pulp is

injured are still unclear. The molecular mechanism that controls the releasing of morphogens needs to be explained for therapeutic use in regenerative endodontics.

1.9.3 Stem Cells

These cells can be defined as clonogenic cells responsible for normal tissue renewal, healing and regeneration after injuries, and capable of self-renewal and multilineage differentiation (113). They are characterized by being undifferentiated and the maintenance of their phenotype by the environment or adjacent cell until they get exposed to the cellular signals, maintain their differentiation potential throughout life, and self-replicate for prolonged times (114). The difference between adult stem and progenitor cells is that progenitor cells retain the proliferation and differentiation property throughout life but lose their self-replication capacity (115).

Stem cells that are used in the regenerative medical field are mainly pluripotent stem cells that include multipotent stem cells like the adult and somatic stem cells, embryonic stem cells (ES), and induced pluripotent stem cells (iPS)(116). ES and iPS are associated with a high risk of tumorigenesis because they have the pluripotent capacity to differentiate into many type of cells(117). Contrarily, somatic stem cells, which include mesenchymal stem cells (MSCs), have the ability to differentiate into several types only and are not considered pluripotent, which decreases the risk of tumorigenesis (118). MSCs are widely used in the regenerative therapy (119,120).

The regulation of stem cell behavior is maintained by a stem cell niche environment, which is characterized by providing an anatomical space for the regulation

of stem cells in the form of the number of cells providing cellular instructions to maintain, differentiate, recruit, self-renew, and increase the long-term regenerative magnitude (121,122).

Dental pulp cells are a heterogenous population of mesenchymal cells and migrating neural crest cells(123). They are a group of precursor cells that have the capacity to differentiate into osteoblast-like or odontoblast-like cells and secrete type I collagen and various non-collagenous proteins like osteocalcin (OCN), alkaline phosphatase (ALP), bone sialoprotein (BSP), osteopontin (OPN), dentin matrix protein, and dentin sialo phosphoprotein, which are markers of differentiation(124). Major changes in the cytoskeleton of microtubules, actin filaments, and intermediate filaments can be seen in the differentiation process (125)(126).

The process of identification of differentiated odontoblasts is difficult because both of the osteoblasts and odontoblasts are similar in the mineralized nodules formation and in the expression of proteins(88). This makes cellular identification of a true odontoblast impossible to be concluded from one or two characteristics(88).

The differentiation into odontoblast-like cells has been reported in five different types of postnatal mesenchymal stem cells: dental pulp stem cells (DPSC)(127), stem cells of the apical papilla (SCAP)(128,129), stem cells of human exfoliated deciduous teeth (SHED)(130), dental follicle progenitor cells (DFPC)(131) and bone marrow derived mesenchymal stem cells (BMMSC) (132) .

Dental pulp mesenchymal stem cells (DPMSC) were first isolated from the pulp of human third molars and have been called (DPSC). Their location is reportedly in the

perivascular area and the cell rich zone (133,134). They express MSC surface markers such as CD44, 90, 105, and 146, and they have the ability to differentiate to neural cells, chondrocytes, adipocytes, and osteoblasts(127,135) and have been reported to be a source of odontoblasts replacement(133,134) and the formation of dentin/pulp complex-like structures (127) that make them ideal for regenerative endodontics (136).

1.9.4 Delivery systems

For the appropriate selection of a method to deliver these stem cells, scaffold and growth factors are considered the biggest challenges in tissue regeneration, which is needed to ensure that the regeneration process will happen in a way that prevents complete tissue calcification or cellular hypoxia. This is because almost all the cells in our body are within 0.1 mm to 1 mm of a blood vessel to ensure adequate diffusion of oxygen and nutrients through clinical procedures based on regenerative endodontics(137,138).

Clinical studies in the last 50 years have focused on revascularization techniques with minor components of tissue engineering. Most of these studies are either case reports or case series, even though they don't conclude with definitive evidence to support a treatment. Instead, they are considered higher evidence than in vitro and in vivo studies because they're done on humans, and there is lack of clinical trials that integrate the full concept of tissue engineering. The main difference between tissue engineering and revascularization is that the former is based on stem cells assembly in a scaffold that is supplied by growth factors, while the latter is based on triggering bleeding in the empty

canal, hoping that it will activate an effect that will resemble the blood clot wound healing mechanism in surgeries (139).

The breakthrough in gaining knowledge and new techniques and materials has led to a significant increase in the number of published studies regarding the treatment of necrotic immaturely developed permanent teeth (88). Many procedures were performed to treat immature formed roots; for example, apexogenesis is defined as “a vital pulp therapy procedure performed to encourage continued physiologic development and formation of the root end,” which is mainly indicated in vital teeth. Another term is apexification, which is defined as “a method to induce a calcified barrier in a root with an open apex or the continued development of an incompletely formed root in teeth with necrotic pulp tissue” (140), which is different than revascularization, which is defined as “the restoration of vascularity to a tissue or organ” (141).

1.10 Rationale and clinical significance for this research:

Many materials have been proposed for the vital pulp therapy procedures, which is used to protect and preserve the vitality of teeth. Most commonly, calcium hydroxide and bioceramic materials. These materials have limitations in the clinical setting, such as handling, setting time, or moisture-dependent setting.

Therefore, constant improvement of these materials is important to develop a material that will help to overcome these limitations. One of the main components in these materials is dicalcium silicate and tricalcium silicate, which consist of combination of silicon dioxide and calcium oxide. Some of the advantages of silica include its ability to be produced in different sizes and forms and its ability to allow surface modifications.

Biocompatibility is one of the main challenges when dealing with materials in the nanometer range. There was evidence of cytotoxicity in different cell line cultures when silica presented in nanometer sizes and in higher doses. This study investigated the effects of different sizes and doses of silica on the attachment efficiency, proliferation, cytotoxicity, and genotoxicity of the human dental pulp in vitro.

HYPOTHESIS

Chapter 2: HYPOTHESIS

It is hypothesized that silica particles at certain nano-levels will cause dose and size dependent cytotoxic or genotoxic effects on normal human dental pulp cell cultures.

The null hypothesis (H_0) was that there was no difference in the cytotoxicity and genotoxicity between the experimental sample group containing silica particles in different sizes and doses.

OBJECTIVES OF THE STUDY

Chapter 3: OBJECTIVES OF THE STUDY

Objective 1

To measure the cellular attachment efficiency of normal human dental pulp cells cultured on plastic tissue culture plates containing culture media with various sizes and doses of silica particles (12.5 µg/mL, 50 µg/mL, 100 µg/mL and 1000 µg/mL) at 16 hours and compare this to attachment efficiency of cells grown in media without particles (control).

Objective 2

To quantify cellular proliferation rates of normal human dental pulp cells grown in culture media that contain the same various sizes and doses of silica particles (12.5 µg/mL, 50 µg/mL, 100 µg/mL and 1000 µg/mL) at following time points 1, 7, and 14 days, and compare this to the proliferation rates of normal human dental pulp cells grown in media without particles (control) at the same time points.

Objective 3

To evaluate the cytotoxicity of normal human dental pulp cells grown in culture media that contains the same various sizes and doses of silica particles (12.5 µg/mL, 50 µg/mL, 100 µg/mL and 1000 µg/mL) at the following time points 1, 7, and 14 days, and compare this to the cytotoxicity of normal human dental pulp cells grown in media without particles (control) at the same time points.

Objective 4

To evaluate the genotoxicity of normal human dental pulp cells grown in culture media that contain the same various sizes and concentrations of silica particles (12.5 $\mu\text{g/mL}$, 50 $\mu\text{g/mL}$, 100 $\mu\text{g/mL}$ and 1000 $\mu\text{g/mL}$) at day 1, and compare this to the genotoxicity of normal human dental pulp cells grown in media without particles (control) at the same time point.

MATERIALS AND METHODS

Chapter 4: MATERIALS AND METHODS

2.1 Materials

2.1.1 Table 1 : List of materials

Material	Manufacturer	Catalog number
1.5 mL tubes	Fisher Scientific	05-408-129
15 ml centrifuge tubes	Fisher Scientific	14-959-70C
2 ml pipettes	Fisher Scientific	13-675-3C
10 ml pipettes	Fisher Scientific	13-678-11E
25 ml pipettes	Fisher Scientific	13-678-11
Aspirating pipettes	Fisher Scientific	13-675-16
Disposable masks	Kimberly-Clark	12978
Scalpel handles	Patterson Dental	089-4501
Manual pipette P20	Gilson, Pipetman	FA10003P
Manual pipette P100	Gilson, Pipetman	FA10004P

3x3 weighing paper	Fisher Scientific	NC9691607
50 mL centrifugation tubes	Fisher Scientific	14-432-22
Corning 12.5 cm ² Tissue culture flasks	Fisher Scientific	08-772-1F
Corning 225 cm ² Tissue culture flasks	Fisher Scientific	1482680
96 well plate flat clear bottom	Fisher Scientific	08-772-2C
Manual pipette P1000	Gilson, Pipetman	FA10006P
Multi tip pipette Transferpette 20-100 µL	Brinkman	10N3297
Multi tip pipette Transferpette 50-200 µL	Brinkman	07R2380
Pipette tips (blue) 200-1000 µL	Fisher Scientific	02-707-509
Pipette tips (yellow) 1-200 µL	Fisher Scientific	02-707-503
Surgical blades #11	Henry shein	100-5794

Pro-pette pipette aid (pipette controller)	MTC Bio	P6080
Weighing dish (small)	Fisher Scientific	02-202-100
Thermanox plastic coverslips, 15mm diameter	NUNC	174969
Timer	Fisher scientific	02-401-7
96-well clear bottom black plate	Fisher scientific	07-200-565
24 well tissue culture plates	celltreat	229123
330 high speed bur	midwest	386261
High speed hand piece	midwest	HP200
#7 bi bevel chisel	Hu-friedy	CC
Surgical dental mallet ML.01	Henry shein	100-5794
EMD Millipore stericup sterile vacuum filter units, 0.22 μ M	EMD Millipore	SCGVU02RE
SEM and TEM Grid	EMS	FCF300-Cu-SB

2.1.2 Table 2 : List of chemicals, enzymes, growth media and kits

Item	Manufacturer	product number
70 % Ethanol	Fisher Scientific	S25306A
10 % Formalin	Fisher Scientific	HT501128-4L
0.05% Trypsin-EDTA	Life Technologies	25300054
Cytotoxicity kit	Abcam	Ab112118
Crystal Violet, powder	Sigma	229288-100G
Basal medium eagle (500mL)	Fisher Scientific	21-010-046
Fetal bovine serum	Life Technologies	16000044
Fungizone (antifungal)	Fisher Scientific	15-290-018
Pen/Strep	Fisher Scientific	15-140-122

DPBS, case of 10	Fisher scientific	14-190-250
Silicon Dioxide 10-200 nm	SIGMA-ALDRICH	636238-50G
Silicon Dioxide 1-5 μm	SIGMA-ALDRICH	S5631-100G
Bovine serum albumin	Sigma	A8816-1G
Formaldehyde	Polysciences	18814-10
HCS DNA Damage kit	ThermoFisher	H10292

2.1.3 Table 3 : List of equipment used

Weight scale	OHAUS	TS400S
Weight scale	Denver Instruments	P-314
Table top Centrifuge	Beckman	TJ-6
Roto Mix shaker	Thermolyne	M51335
Ultrasonic Dismembrator	Fisher scientific	50 Sonic F50
PH meter with electrode	Corning	320
Microplate reader (spectrophotometer)	Tecan	Infinite 200 Pro
Microplate reader (spectrophotometer)	Tecan	Infinite 1000 Pro
Light microscope	Leica	LEITZ DM IL
Scanning electron microscope	Hitachi	SU6600
Transmission electron microscope	FEI	Tecnai Osiris

Wide field epifluorescence microscope	Nikon	Ti Eclipse Amber
Biological safety Cabinet	LABCONCO	3430809
Touch mixer tube shaker	Fisher scientific	231
Hemocytometer	Reichert	26715
Incubator	Thermo ELECTRON	3110
Dynamic light scattering	Brookhaven	NanoBrook Particle Size and Zeta Potential Analyzer
TEM plasma coating	PVA TePla America	M4L

2.2 Approvals and training

This study was approved by the Institutional Biosafety Committee at Boston University (IBC #16-661). All necessary human subject training was completed through the Collaborative Institutional Training Initiative (CITI). Online lab training was provided through the Office of Research at Boston University. Exempt review (IRB# H-33173) from the human subjects was granted from the Institutional Review Board to use biological waste material from human teeth. Patient identification for human waste extracted teeth is not possible.

2.3 Methods

2.3.1. Silica particles characterization

Silica nanoparticles and microparticles' sizes, shapes and behaviors in different solutions were characterized to confirm the manufacturer's specifications of those materials. To confirm the sizes, microparticles were analyzed through a scanning electron microscope, while nanoparticles' size was confirmed by using a transmission electron microscope. The behavior of nanoparticles was studied through dynamic light scattering to ensure the particles' stability against aggregation throughout the experiment.

2.3.1.1 SEM imaging

A scanning electron microscope (SEM) (Hitachi SU6600, Japan) was used to visualize the morphology and size of the SiO₂ particles. Prior to this analysis, different sizes of SiO₂ particles were dispersed in distilled water at a low concentration and dropped into copper grids and then mounted on aluminum stubs. Sputtering was accomplished with a thin layer of gold to finally acquire SEM images with an acceleration voltage of 5 kV at different magnifications.

2.3.1.2 Transmission electron microscope

The primary particle diameter and shape of Si-np were measured by transmission electron microscopy (TEM). Tecnai Osiris instrument was operated at 200 kV and aqueous suspensions of the nanoparticles were spread on a copper grid and allowed to air dry overnight.

2.3.1.3 Dynamic light scattering

The mean particle sizes in suspension (hydrodynamic diameter) and agglomeration states of nanoparticles were determined using a dynamic light scattering device (Brookhaven Instrument Corporation, Holtsville, NY, USA) equipped with a 657-nm laser (15 mW) at a detection angle of 90 degrees. The nanoparticles' suspensions were prepared in culture medium at 100 µg/mL concentrations and analyzed twice immediately after sonication (0 h) and 72 h of incubation.

2.3.2 Growth media preparation

Growth medium consisted of 10% fetal bovine serum (FBS, Atlanta Biologicals), 1X Penicillin antibiotic (100 U/mL), 1X Streptomycin (100 µg /mL), and Amphotericin B anti-fungal (0.25 µg/ml) in Eagle's Basal Medium (BME).

2.3.3 Cell culture preparation

2.3.3.1. Isolation of progenitor cells from the human dental pulp

The procedure to obtain human dental pulp cells was based on a previously published protocol (142) in which human dental pulp explants were obtained from freshly extracted third molars through the oral surgery department at Boston University School of Dental Medicine. Healthy patients with an age range of 20 to 35 years were screened to rule out the possibility of any metabolic or systemic disease or acute infections, including any steroid drugs that were taken in the six months preceding the surgery. Informed consent was obtained from the patients who met the inclusion criteria for sample collection. Exclusion criteria included caries, restorations, trauma, non-vital teeth or teeth associated with pathologic conditions. After the teeth were extracted, they were stored immediately in a centrifuge tube containing 1X PBS solution (Gibco) and then transported in a lid sealed icebox within one hour.

First, sagittal indentation was made with a high-speed handpiece and fissure bur using a coolant without exposing the pulp. Then the teeth were fixed on extraction forceps and the handle was secured with rubber bands. Sectioning was carried out using a #7 Chandler bi-bevel bone chisel (Hu-Friedy) and a hammer until the tooth was sectioned and the pulp exposed. The pulp tissue located in the pulp chamber was removed using sterile cotton pliers and placed in petri dishes containing sterile PBS. The samples were transported for tissue isolation and maintenance procedures, which were done entirely in a class II biological safety cabinet in order to ensure sterile conditions. Afterwards, the pulp tissue was divided into small pieces using sterile micro-dissecting scissors and a #11

surgical blade. One or two pieces of pulp tissue explants were placed in 12.5 cm² flasks containing 10 mL culture media and labeled with the sample ID and date. The amount of culture media was modified to ensure that the whole tissues were covered. The culture flasks were maintained in an incubator at 37° C with 5% CO₂ and saturated humidity. Photo (1) is showing Steps of human dental pulp cells extraction.



Photo 1 : Steps of human dental pulp cells extraction.

Note: The photo reveals the steps of extracting HDPCs from the extracted teeth.

2.3.3.2. Primary tissue culture maintenance and expansion

The primary cell culture in the 12.5 cm² flasks grew for about six to eight weeks until they reached 70%–80% confluence. Photo (2) is Displaying primary cell culture in 12.5cm² flask after 3 weeks. The growth medium was changed every two days in the first 10 days followed by a media change every 72 hours. The method of media changing was as follows. First, the old medium was aspirated, then 3 mL of 1X PBS were added to wash the tissue and then it was aspirated. Second, a 10 mL growth medium was added. In the first 10 days, pulp pieces were kept in the flask to allow cell migration and attachment. Then those pieces were removed to provide more space for the cells to grow and to reduce the chance of microbial contamination.

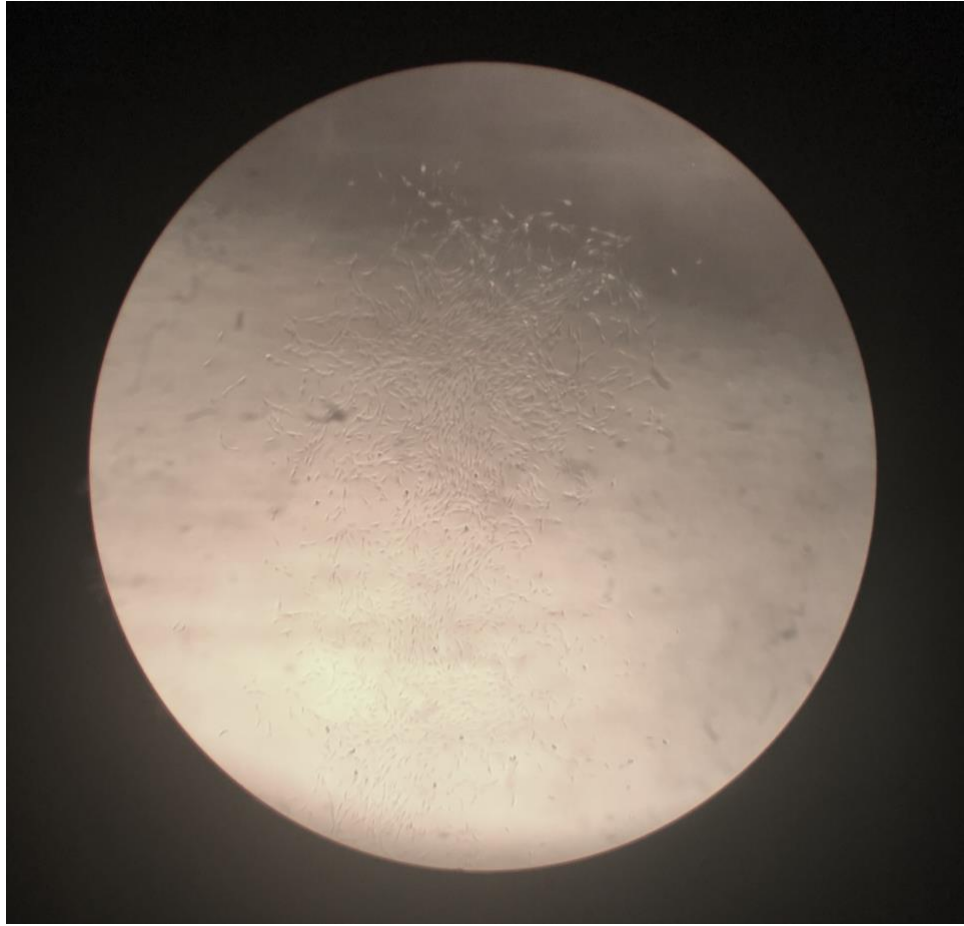


Photo 2 : Display of primary cell culture in 12.5cm² flask

The optimal time for primary cell culture expansion is when the primary culture reaches 70%–80% confluence after six to eight weeks. Photo (3) is displaying secondary cell culture 70-80% confluence. The process of media expansion is as follows. The medium was aspirated, followed by rinsing with 1X PBS and then aspirated. Then trypsinization was carried out using 1 mL of 0.05% trypsin EDTA for six to eight minutes in the incubator, thus allowing them to completely detach, which was confirmed using a light microscope. Then 10 mL of growth media were applied to block the trypsinization reaction, and cells in the growth media suspension were collected in 50mL sterile disposable tubes for centrifugation (five minutes with 1000 rpm at Room Temperature). When the cell pellet in the bottom of the tube was formed after centrifugation, the solution above the pellet containing the trypsin was carefully aspirated. Finally, cells were re-suspended in 10 mL fresh growth media and were then transferred in a new 225 cm² flask containing 60 mL of fresh growth media. The flask was labelled with sample ID and date.

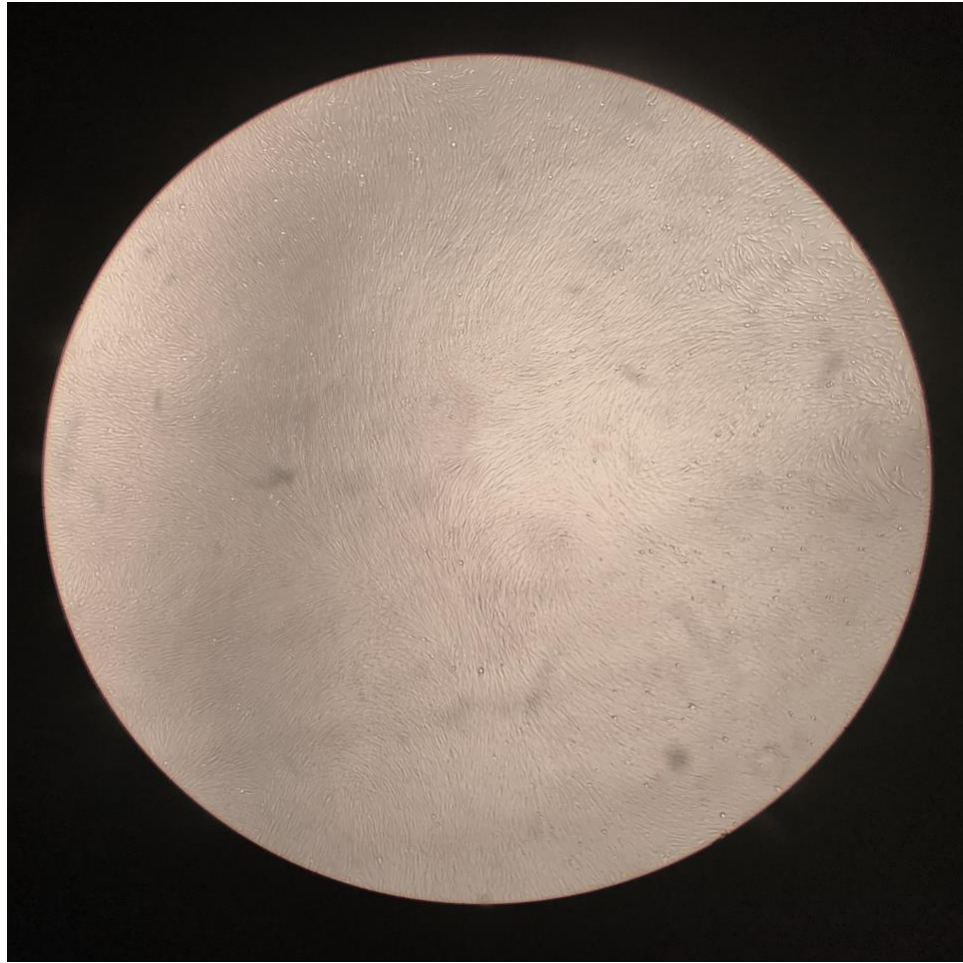


Photo 3 : Secondary cell culture showing 70-80% confluence.

2.3.3.3. Secondary tissue culture maintenance and processing

The secondary cell cultures in the 225 cm² flasks grew for about 7 to 10 days until they reached 70%–80% confluence. The growth medium was changed every 72 hours. The total amount needed for the flask was 60 mL and the flask were washed with 10 mL warm PBS during every media change.

The optimal time for secondary cell culture processing is when the secondary culture reaches 70%–80% confluence, which is after 7 to 10 days. The method of processing was as follows. The medium was aspirated, followed by rinsing with 10 mL 1X PBS and aspirated. Then trypsinization was carried out using 3 mL of 0.05% trypsin EDTA for six to eight minutes in the incubator, allowing cells to completely detach from the flask, which was confirmed using a light microscope. Then 30 mL of growth medium was applied to block the trypsinization reaction. Cells in the growth media suspension were collected in 50mL sterile disposable tubes for centrifugation (five minutes at 1000 rpm at room temperature). Consequently, a cell pellet was formed at the bottom of the tubes. The supernatant above the pellet was carefully aspirated and 10 mL of the fresh growth medium was added to resuspend the cellular pellet. Cell density was counted by using a hemocytometer (Reichert-Jung). The procedure for cell counting is as follows. First, a glass coverslip was attached to the hemocytometer and 20 μ L cell suspension was added slowly to the edge of the hemocytometer to avoid bubbles. Cell suspension was then drawn into the chamber via capillary action. A light microscope with 20X magnification was used to count each cell numbers in the four big squares, and the resulting total cell number was divided by four and then multiplied by 10⁴, which represents the cell number in 1 mL of

the suspension. Dilutions can be made accordingly to reach the desired number of cells for each experiment.

2.3.4 Determination of the optimal cell seeding concentration

A pilot experiment was done to determine the ideal cell seeding concentration for normal human dental pulp cells in a 96-well plate for 14 days. This is important to ensure that cells do not reach their full confluence and do not eventually die before 14 days, which otherwise might undermine the experiment's outcome. This was determined by testing different cell seeding concentrations on 96-well plates in triplicates. Light microscope was used daily to monitor the cells. After 1, 7, 14, days, the cells were fixed and stained by crystal violet dye and the absorbance was measured by a microplate reader to confirm the cell attachment. It was then concluded that the optimal cell seeding concentration for the proliferation and cytotoxicity experiments to reach 14 days is 800 cells per well.

2.3.5 Silica particles preparation

Before starting each experiment, silica particle stock solutions for the nanoparticles and microparticles were made at a concentration of 1 mg/mL by dissolving the material in BME (Gibco, Invitrogen, NY, USA) and diluted to the working concentrations of 12.5 µg/mL, 50 µg/mL, 100 µg/mL, and 1000 µg/mL. Suspensions of SiO₂ nanoparticles were dispersed by a probe sonicator (Fisher Scientific, Pittsburgh, PA, USA) at 20% amplitude for 5 minutes, and then immediately applied to the HDPCs.

2.3.6 Groups of materials: as shown in (Photo 4)

1. CM with Si-µp1000
2. CM with Si-µp100
3. CM with Si-µp50
4. CM with Si-µp12.5
5. CM with Si-np1000
6. CM with Si-np100
7. CM with Si-np50
8. CM with Si-np12.5
9. Control (CM only).

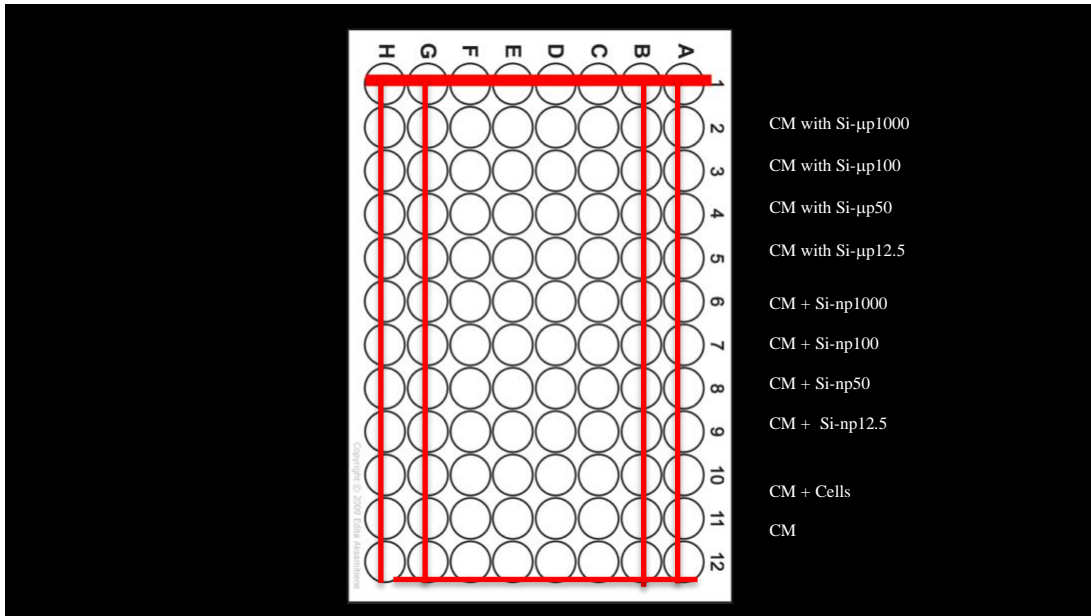


Photo 4 : 96 well plates design representing each experimental group (n=4)

2.3.7 Attachment efficiency assay

According to a previously published study, attachment efficiency was calculated to establish a baseline (at 16 hours) on normal behavior of human dental pulp cells in second passage of cell culture (146).

This experiment involved measuring the attachment efficiency of human dental pulp cells after seeding 800 cells per well in 96-well plates after being treated with various sizes and doses of silica particles in comparison to the control at 16 hours, the attached cells in the plates were fixed with 10% neutral buffered formalin solution for 1 hour at room temperature and stained with 0.2% (w/v) crystal violet dye for 1 hour at room temperature. Unbound stain was removed by rinsing plates thoroughly with deionized water until clear. The absorbance was measured in the spectrophotometer at 590 nm and recorded. As the absorbance of crystal violet is directly proportional to attached cell numbers, optical density was converted to cell numbers.

2.3.8 Proliferation rates with crystal violet staining assay

Crystal violet assay is a quick, reliable screening method to test the effect of different chemical compounds on cell proliferation. During cell death, adherent cells become detached from the well plates. This feature can be used to assess the differences in proliferation upon application of cytotoxic agents. The crystal violet dye stains the attached cell through binding with DNA. The optical density of the crystal violet dye that is absorbed by the monolayer of cells is quantified using a spectrophotometer. The dye is prepared by dissolving 0.2g of crystal violet in 100 mL deionized water, with a subsequent concentration of 0.2% (w/v).

At the beginning, 800 cells were seeded in clear-wall, flat-bottom, 96-well plates containing 200 μ L growth media for 16 hours until attachment, followed by aspiration then adding the culture medium or culture media with different sizes and doses of silica particles. Each condition was replicated four times. The growth medium, with or without the silica particles, were changed every 72 hours. The well plates were placed in the incubator at 37°C with 5% CO₂ and saturated humidity. The cells proliferation rates were determined at the following time points: 1 day, 7 days, and 14 days.

At 16h and each time point, the well plates were taken to the chemical hood, where the rest of the procedure was carried out. First, at each time point, culture medium was removed and cells were fixed with 10% neutral buffered formalin (Sigma) for one hour at RT. Fixation solution was then aspirated, plates were washed twice with 1x PBS. Later, plates were stained with 100 μ L of 0.2% (w/v) crystal violet stain (Sigma Aldrich) for one hour at RT. Unbound stain was aspirated by rinsing plates thoroughly with deionized water

until clear, then finally aspirated. The optical density of crystal violet dye was measured in the spectrophotometer (TECAN, infinite M200Pro) at a 590 nm wavelength.

The per cell optical density (O.D.) was calculated by subtracting the O.D. of cells at 16 hours by the O.D. of the background of plastic plates and then dividing that number by the initial seeding number (considering full cell attachment at 16 hours' time point). This gave us an estimation of the dye that was absorbed by a single cell (per cell) and then the per cell O.D. was used as a standard throughout the experiment to convert the optical density of different conditions to cell numbers.

$$\text{Per cell O.D.} = \frac{\text{O.D. cells at 16 hours} - \text{O.D. background}}{\text{initial seeding number}}$$

$$\text{Cell number} = \frac{\text{O.D. reading of each condition} - \text{O.D. background}}{\text{per cell O.D.}}$$

2.3.9 Cytotoxicity Assay

Measuring cell cytotoxicity is one of the most essential tasks for studying cell functions. The Abcam AB112118 kit utilizes a water-soluble dye that changes its absorption spectrum upon cellular reduction. The absorption ratio is directly proportional to the number of living cells.

Briefly, HDPCs were seeded at the concentration of 800 cells per well in 96-well plates and were incubated for 16 hours until fully attachment. Then, the media was replaced with 200µl of fresh media containing the designated test groups. After 1, 7, and 14 days of incubation, the Abcam cytotoxicity kit was used in accordance with the manufacturer protocol. 40µl of the assay solution was added to each well, and the samples were incubated for one hour. Finally, a spectrophotometer was used to measure the absorbance at 570 nm (OD570) and 605 nm(OD605).

The cell viability was calculated according to the following equation:

Cell viability (%) = $(R_{\text{Sample}} - R_o) / (R_{\text{Control}} - R_o) \times 100$ where,

R_{Sample} is the absorbance ratio (OD570/OD605) of samples cultured with silica particles.

R_{Control} is the absorbance ratio (OD570/OD605) for the samples cultured in normal culture media.

R_o is the average of the absorbance ratio of the control.

2.3.10 Genotoxicity Assay

Genotoxicity is defined as a double strand break (DSB) in DNA that is a harmful lesion in mammalian cells. One of the common responses to DSB formation is phosphorylation of H2A histones. Genotoxic agents promote phosphorylation of histone variant H2AX that forms micronuclei at the site of DNA DSB. Phosphorylated H2AX aids in the assembly of proteins that are essential for DSB repair. An HCS DNA Damage Kit (Invitrogen) was used to detect and measure genotoxicity through specific antibody-based detection of phosphorylated H2AX. Phosphorylated H2AX in the nucleus is used for measuring DNA damage, which is accomplished by using pH2AX monoclonal antibody.

Briefly, HDPCs were seeded at the concentration of 800 cells per well in 96-well plates and were incubated for 16 hours until fully attachment. Then, the media were replaced with 200 μ L of fresh media containing the designated test groups. After 1 day of incubation, HCS DNA Damage Kit (Invitrogen) was used as recommended in the manufacturer protocol.

The stock solutions were prepared freshly on the day of the assay. Component A was prepared by adding 1.8 μ L of Image-iT[®] Dead Green viability stain to 6 mL of culture medium. The fixative solution was prepared by adding 1.5mL 16% aqueous paraformaldehyde solution to 4.5 mL PBS. The permeabilization solution was prepared by adding 15 μ L of Triton[®] X-100 to 6 mL PBS. The blocking buffer was prepared by dissolving 0.25 g BSA in 25 mL PBS. The primary antibody solution was prepared by adding 6 μ L pH2AX antibody to 6 mL of blocking buffer. The secondary

antibody/counterstain solution was prepared by adding 3 μ L of Alexa Fluor®555 goat anti-mouse IgG and 1 μ L of Hoechst 33342 to 6 mL blocking buffer.

The process of labeling cells for imaging started by adding 50 μ L of component A to each well that contained 100 μ L of the tested medium, then incubated for 30 minutes at 37°. The medium was then aspirated, after which 100 μ L fixative solution was added to the plates and incubated at room temperature for 15 minutes. Fixative solution was once again aspirated, then the plates were washed once with PBS. Subsequently, permeabilization solution was added and incubated at room temperature for 15 minutes and then the plates were rinsed once with PBS. Following that, 100 μ L of the blocking solution was added, incubated for 60 minutes at room temperature then aspirated. Next, 50 μ L of the primary antibody solution was added and incubated for 60 minutes at room temperature. Then the solution in the plates was removed and rinsed three times with PBS. Finally, 50 μ L of the secondary antibody/counterstain solution was added and incubated for 60 minutes at room temperature, protected from light. After final incubation, the solution was aspirated and then washed three times with PBS. To be prepared for imaging, the plates were added by 100 μ L PBS.

Plates were scanned in a spectrophotometer equipped with a filter appropriate for TRITC. DNA damage was quantified by the increase of pH2AX signal in the TRITC channel (Alexa Flour 555 goat anti-mouse IgG: 555/565nm).

STATISTICAL ANALYSIS

2.4 STATISTICAL ANALYSIS

Data are presented in means and standard deviations (SD). The means and SDs of human dental pulp cell attachment and proliferation at 16 hours and 1, 7, and 14 days were calculated. Cytotoxicity assay (viability percentage) was calculated at 1, 7, and 14 days, and a genotoxicity assay was presented by the pH2AX mean average intensity at 24 hours. All experiments were performed in quadruplicate(n=4).

Statistical analysis was performed using software IBM SPSS (version 26) in One-way variance statistical analysis with a Tukey multiple comparison post hoc test to detect the statistical differences between the groups. Differences at $p \leq 0.05$ were considered statistically significant.

RESULTS

Chapter 5: RESULTS

3.1 Characterization of silica particles

3.1.1 SEM, TEM

Photo 5 shows scanning electron microscopy (SEM) images of Silica microparticles with diameters in the range of 1 μm - 5 μm , indicating that the particles are rounded and well-defined. The TEM analysis was performed to investigate the rounded shaped morphology. TEM and SEM measurements conducted on the micro and nanoparticles used in the study verified the size measurements provided by the suppliers (Photos 6 – 10).

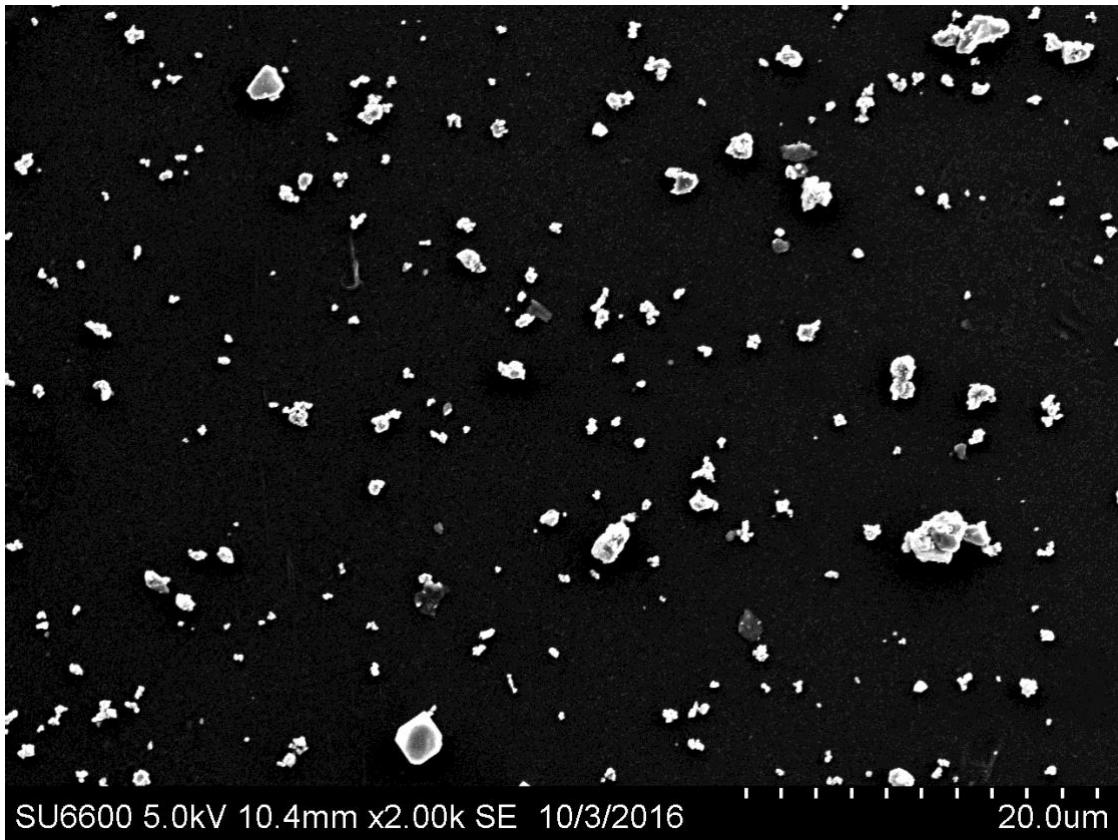


Photo 5 : SEM images of SiO₂ microparticles (1 - 5 μm) dispersed in DI water were analyzed to verify their morphology and size taken at lower magnification x2.00k.

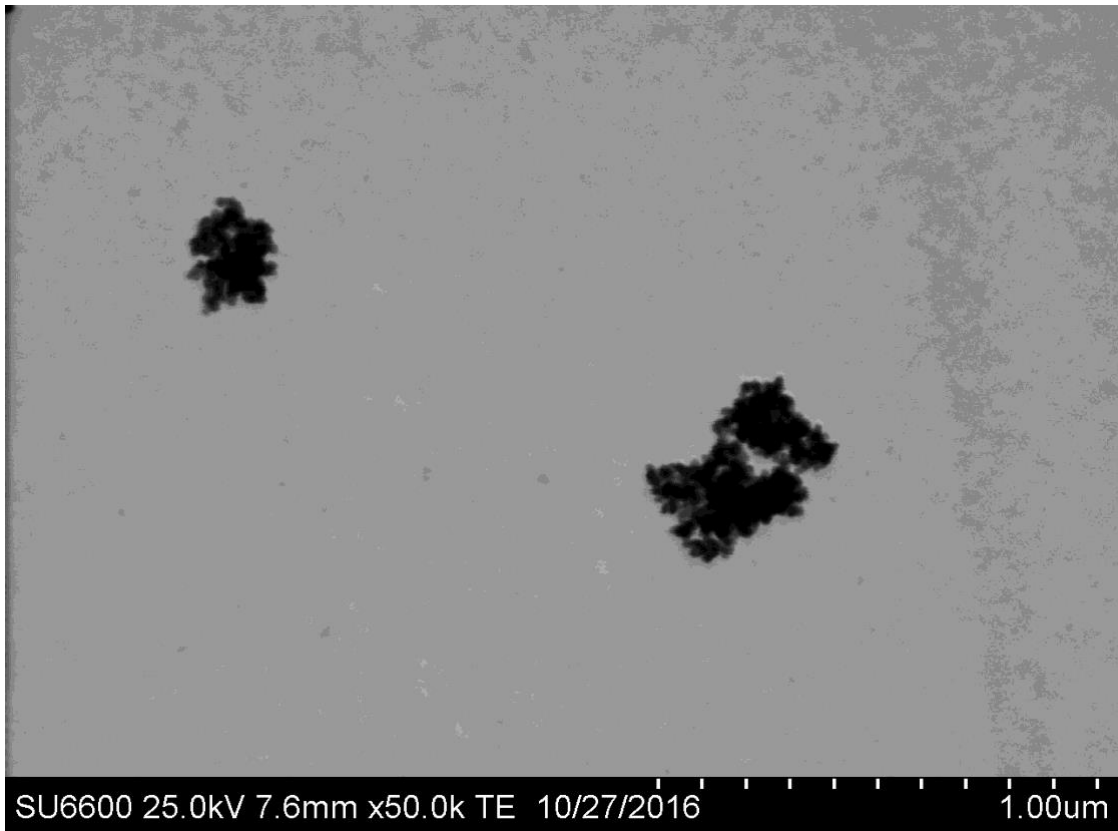


Photo 6 : SEM images of aggregated Si-np (70-225 nm) dispersed in DI water prior to particles sonication treatment.

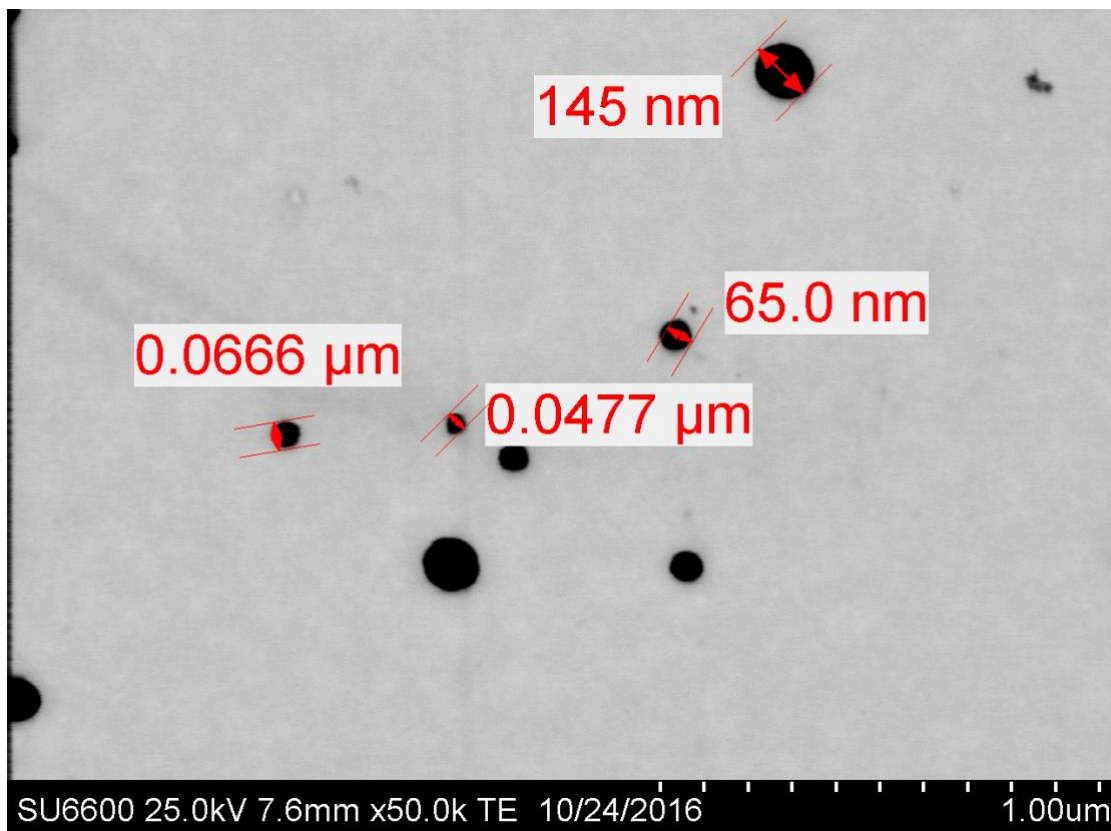


Photo 7 : SEM images of SiO₂ nanoparticles (70-225 nm) dispersed in DI water were analyzed to verify their morphology and size.

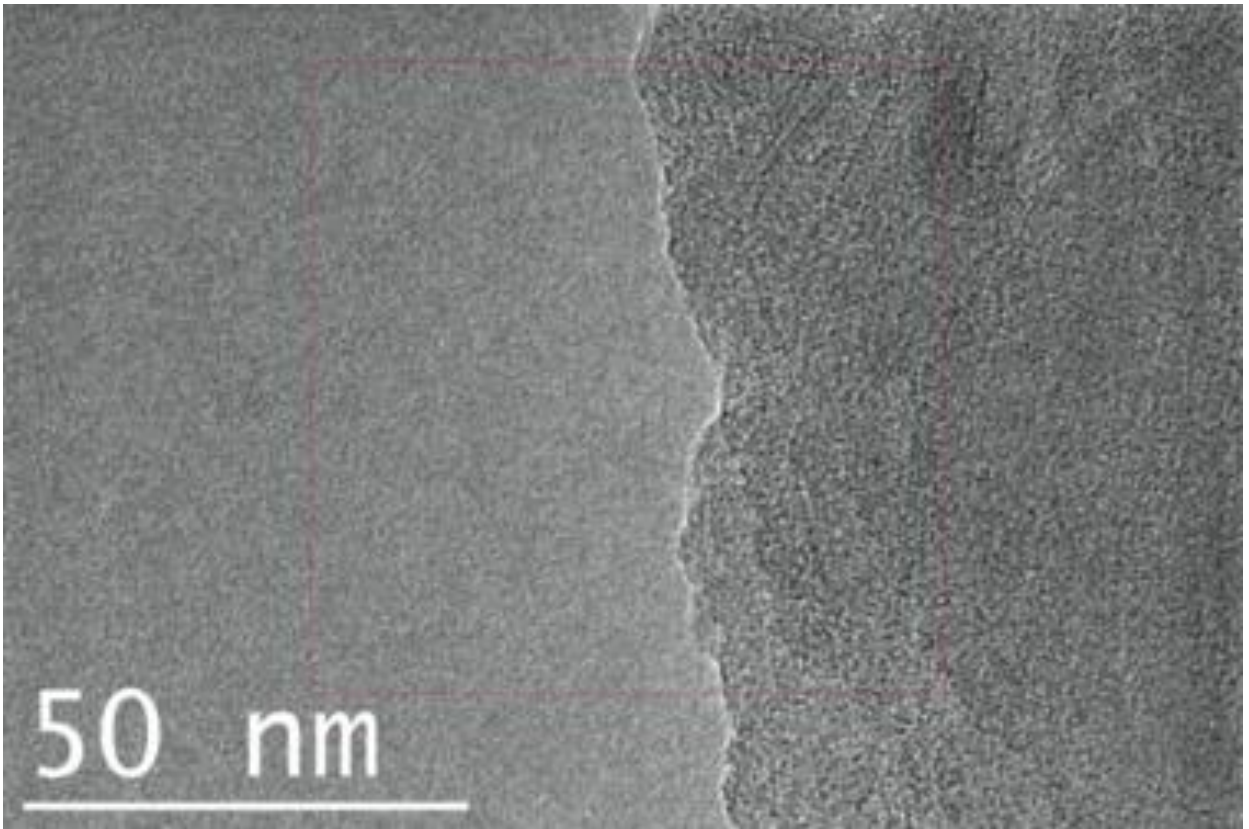


Photo 8 : TEM images of SiO₂ NPs (70-225 nm) to verify their size and shape

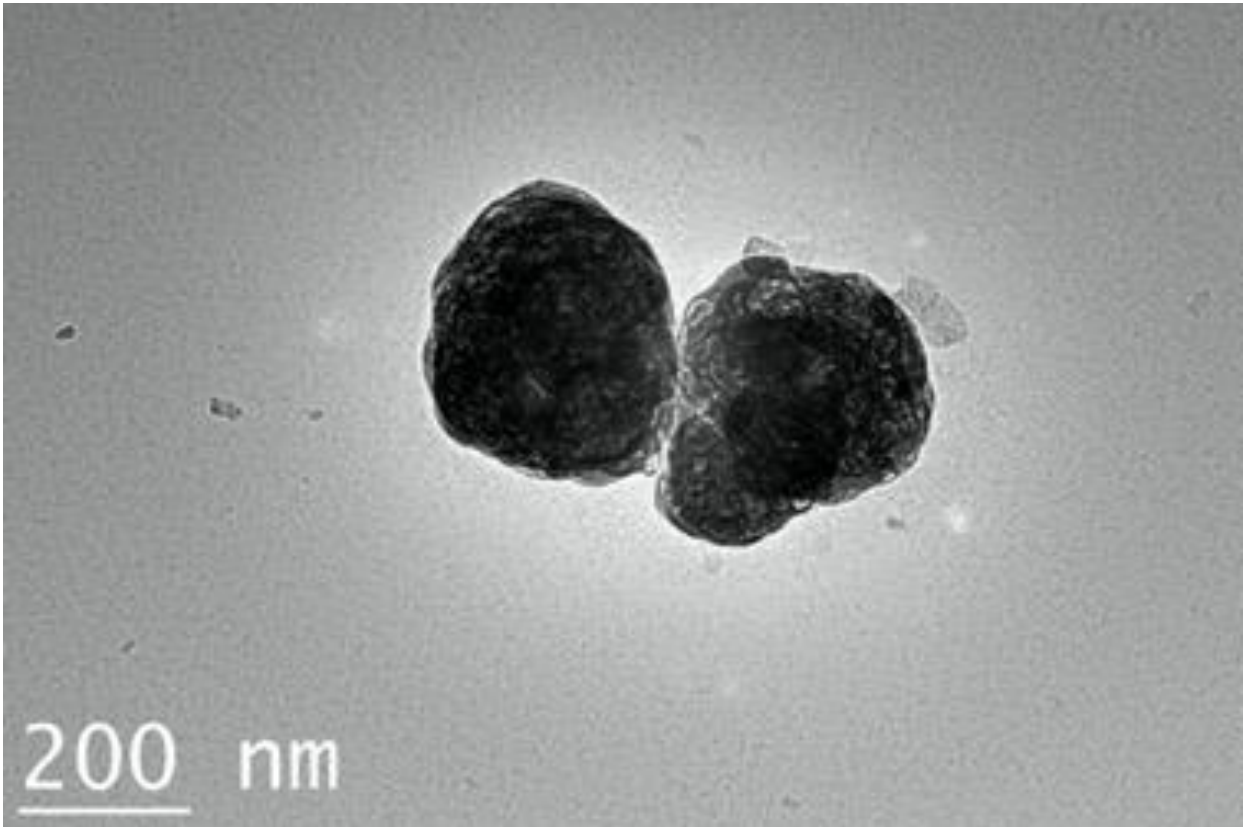


Photo 9 : TEM images of SiO₂ NPs (70-225 nm) to verify their size and shape.

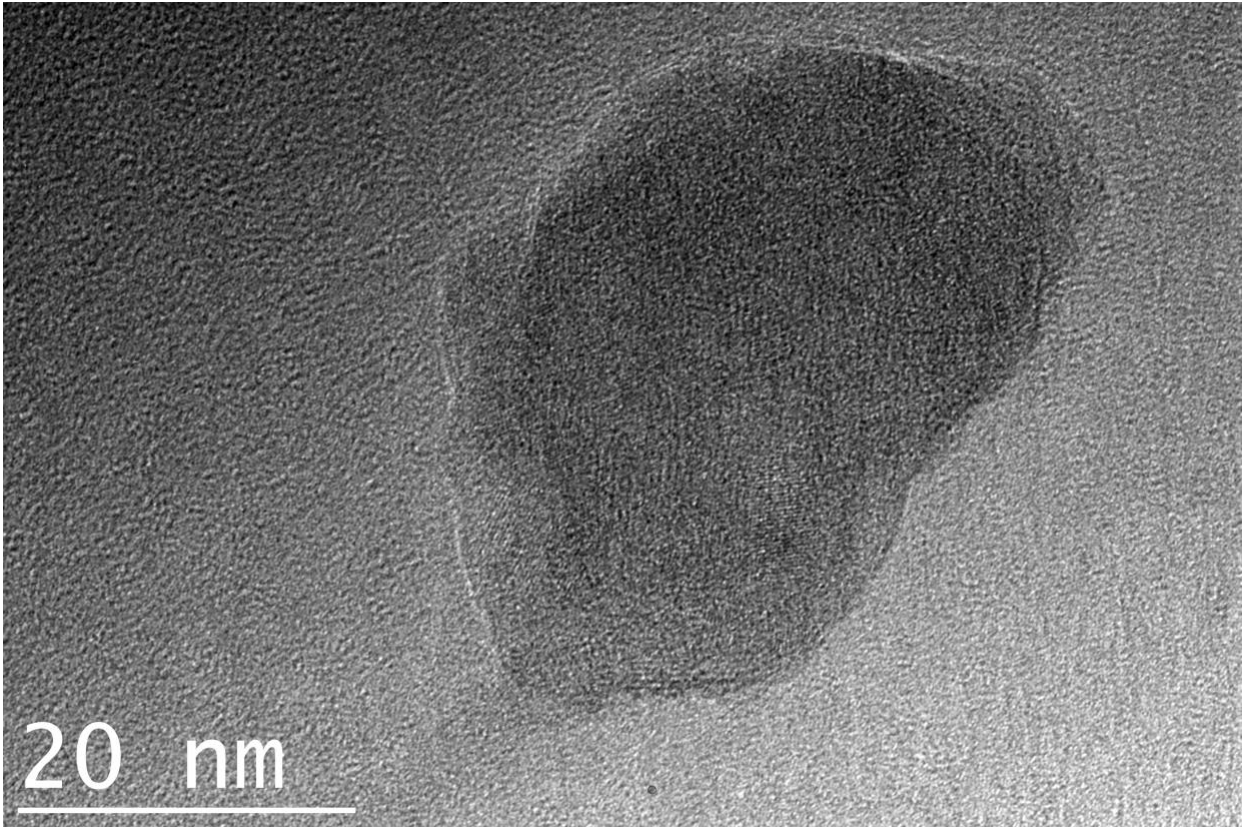


Photo 10 : TEM images of SiO₂ NPs (70-225 nm) to verify their size and shape.

3.1.2 DLS

The hydrodynamic size of silica nanoparticles was measured to reflect their dispersion throughout the experiments. The particles size distribution was 14 nm–70 nm with a mean of 32 nm at day 0 (Figure 1) and 38 nm–225 nm with a mean of 92 nm at day 3 (Figure 2). Because of the Van der Waals force and hydrophobic reaction with surrounding media, silica nanoparticles had the larger hydrodynamic size in dispersion media than their original size. There was no significant agglomeration detected in either group.

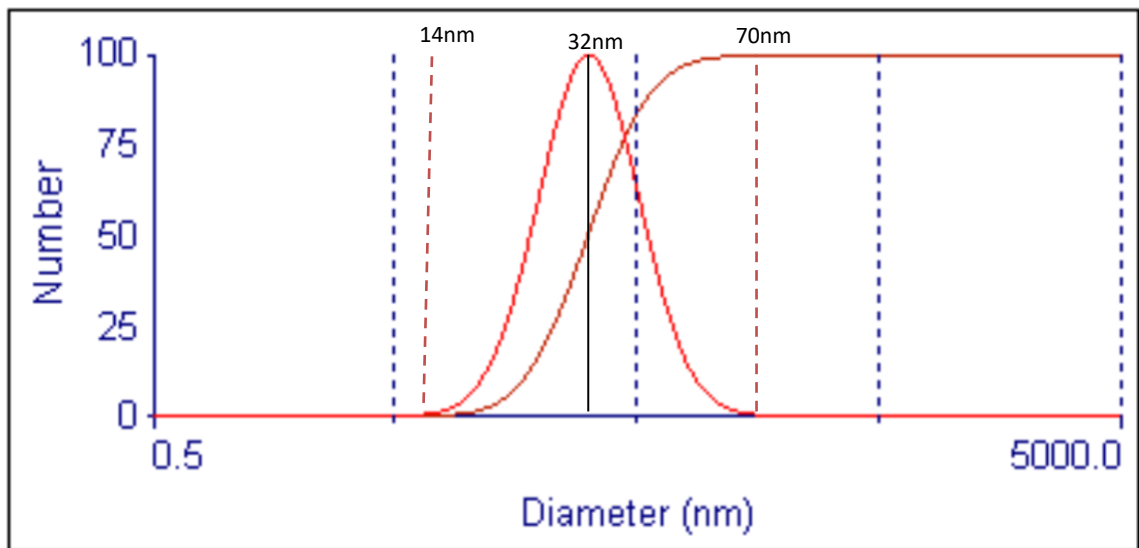


Figure 1 : The size distribution of the nanoparticles group, immediately after sonication in culture medium, ranging from 14 nm to 70 nm with a mean of 32 nm

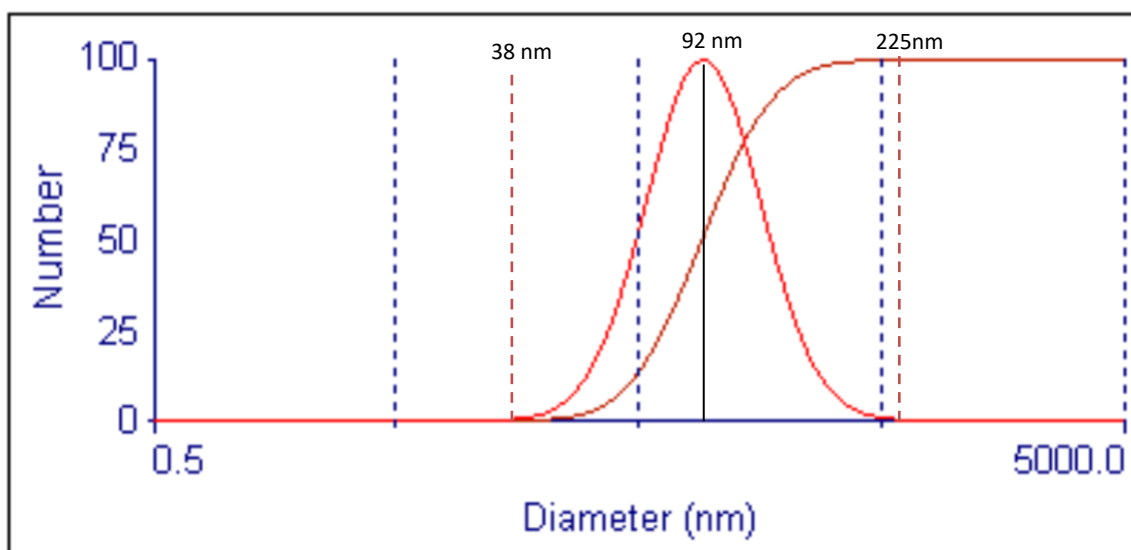


Figure 2 : The size distribution of the nanoparticles group, after 3 days, ranging from 38 nm to 225 nm with a mean of 92 nm.

3.2 Attachment efficiency

3.2.1 Attachment efficiency of normal human dental pulp cells affected by different doses of silica nanoparticles at 16 hours

In order to examine if the addition of different doses of silica nanoparticles in a culture medium was affecting cell attachment, 800 normal human dental pulp cells were cultured in 96-well plates containing culture media supplemented with different doses of silica nanoparticles, ranging from 12.5 $\mu\text{g/mL}$ to 1000 $\mu\text{g/mL}$, for 16 hours. The attached cells in the plates were fixed with 10% neutral buffered formalin solution for 1 hour at room temperature and stained with 0.2% (w/v) crystal violet dye for 1 hour at room temperature. Unbound stain was removed by rinsing plates thoroughly with deionized water until clear. The absorbance was measured in the spectrophotometer at 590 nm and the absorbance was recorded. As the absorbance of crystal violet is directly proportional to attached cell numbers, optical density was converted to cell numbers.

It was noted that at 16 hours, when comparing different doses of silica nanoparticles, there was a significant increase in the attachment efficiency in the 50 $\mu\text{g/mL}$ and 100 $\mu\text{g/mL}$ doses compared to the rest of the groups, where lower concentrations showed higher attachment efficiency ($p < 0.05$). A significant decrease in the attachment efficiency was also noticed in the 1000 $\mu\text{g/mL}$ group compared to the rest of the groups ($p < 0.05$) (Figure 3).

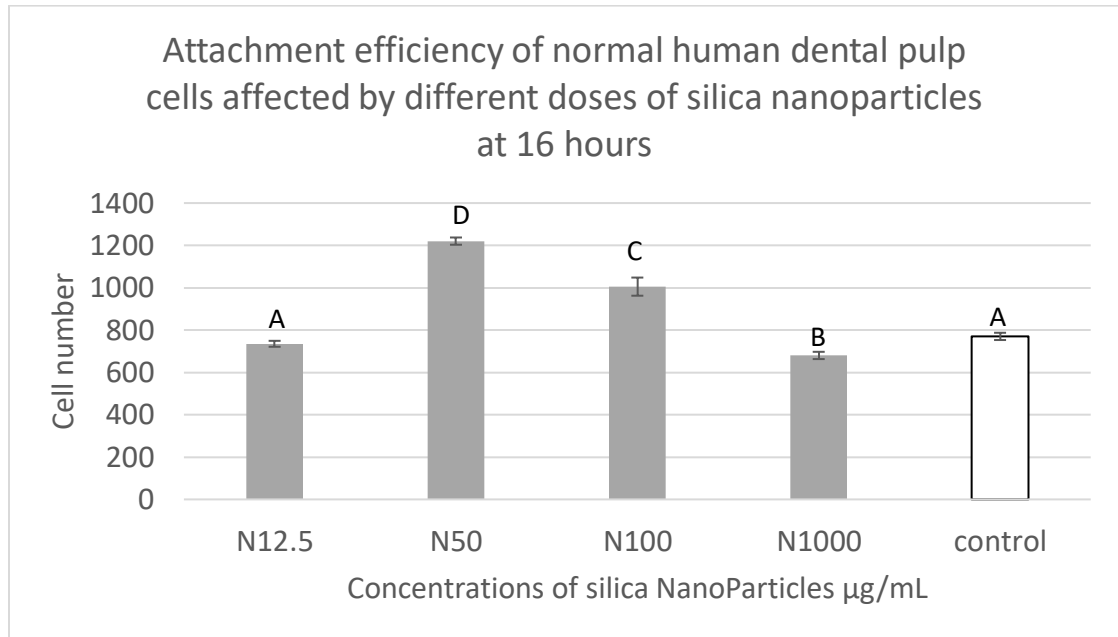


Figure 3 : Attachment efficiency of normal human dental pulp cells exposed to different doses of Silica Nanoparticles at 16 hours:

Normal human dental pulp cells were cultured for 16 hours with media containing silica nanoparticles ranging 12.5 µg/mL to 1000 µg/mL.

The control group was treated with growth media without supplemental silica particles. Error bars indicate the standard deviations of four replicates.

3.2.2 Attachment efficiency of normal human dental pulp cells affected by different doses of silica microparticles at 16 hours

When comparing different doses of silica microparticles, there was a significant increase in the attachment efficiency at 12.5 $\mu\text{g/mL}$, 50 $\mu\text{g/mL}$ and 100 $\mu\text{g/mL}$ compared to the rest of the groups where the 50 $\mu\text{g/mL}$ showed higher attachment efficiency ($p < 0.05$). No statistically significant difference was noted between the control and the 1000 $\mu\text{g/mL}$ group ($p > 0.05$) (Figure 4).

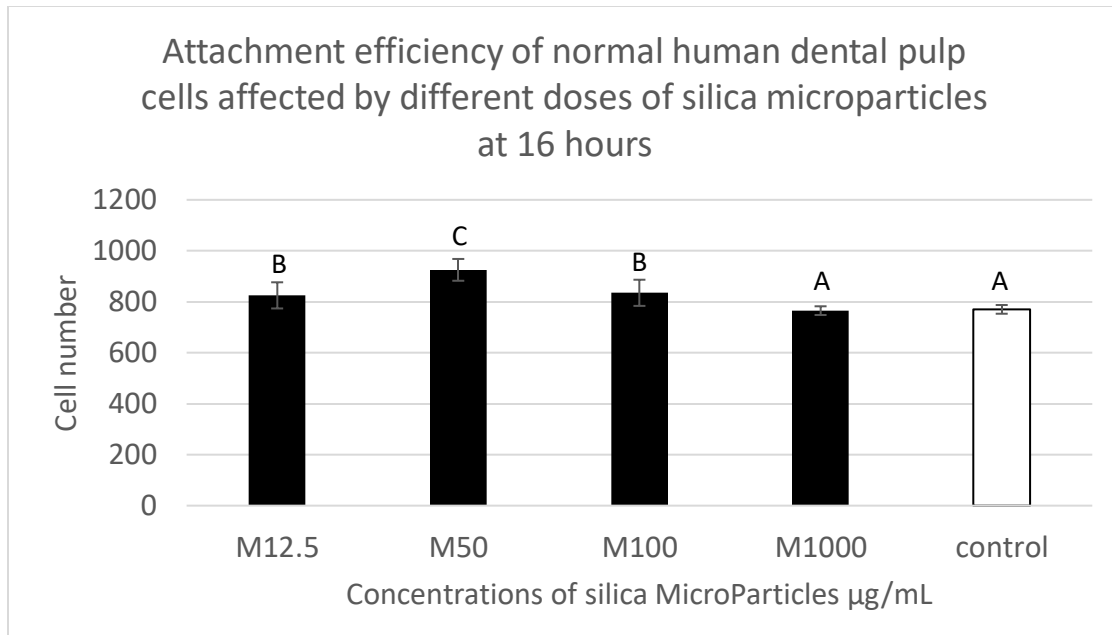


Figure 4 : Attachment efficiency of normal human dental pulp cells affected by different doses of silica microparticles at 16 hours

Normal human dental pulp cells were cultured for 16 hours with media containing silica Microparticles ranging 12.5 µg/mL to 1000 µg/mL.

The control group was treated with growth media without supplemental silica particles. Error bars indicate the standard deviations of four replicates

3.2.3 Attachment efficiency of normal human dental pulp cells affected by different sizes of silica particles at 16 hours

In the smaller dose at 12.5 $\mu\text{g/mL}$, there was a significant increase in the cell attachment of the microparticles compared to the control and the nanoparticles group ($p < 0.05$). Moving to the higher dose of 50 $\mu\text{g/mL}$, both nanoparticles and microparticles showed statistically significant higher cell attachments compared to the control, and the nanoparticles group was higher compared to microparticles ($p < 0.05$). The 100 $\mu\text{g/mL}$ dose showed a similar pattern as the 50 $\mu\text{g/mL}$ as both sizes were statistically significant compared to the control and the nanoparticles showed a higher cell attachment compared to microparticles ($p < 0.05$). In the highest dose of 1000 $\mu\text{g/mL}$, there was a significant decrease in the cell attachment of nanoparticles compared to the control and to the microparticles ($p < 0.05$). No significant difference was noted between the control and microparticles ($p > 0.05$) (Figure 5).

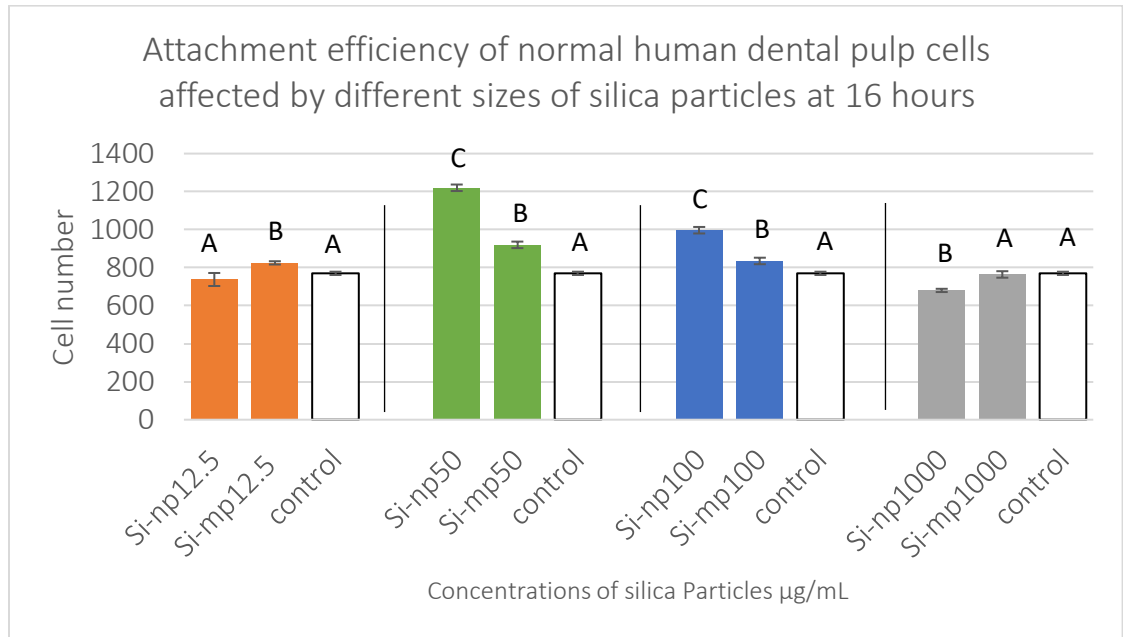


Figure 5 : Attachment efficiency of normal human dental pulp cells affected by different sizes of silica particles at 16 hours

Normal human dental pulp cells were cultured for 16 hours with media containing different sizes of silica particles ranging 12.5 µg/mL to 1000 µg/mL.

The control group was treated with growth media without supplemental silica particles. Error bars indicate the standard deviations of four replicates

Proliferation

3.3 Proliferation

3.3.1 Proliferation of normal human dental pulp cells affected by different doses of silica nanoparticles at different time intervals:

In order to examine if the addition of different doses of silica nanoparticles in a culture medium was affecting the proliferation, 800 normal human dental pulp cells were cultured in 96-well plates containing plain medium for 16 hours until full cell attachment. Then the plain media was replaced with culture media containing different doses of silica nanoparticles, ranging from 12.5 µg/mL to 1000 µg/mL, for 1, 7 and 14 days.

Initially, when human dental pulp cells proliferated at 24 hours (Figure 6), a significant increase in cell number was seen in the higher concentrations (1000 µg/mL and 100 µg/mL) compared to the control group and to each other. The two groups that represented smaller doses (12.5 µg/mL and 50 µg/mL) behaved similar to the control group that was grown on plain culture media without particles ($p > 0.05$).

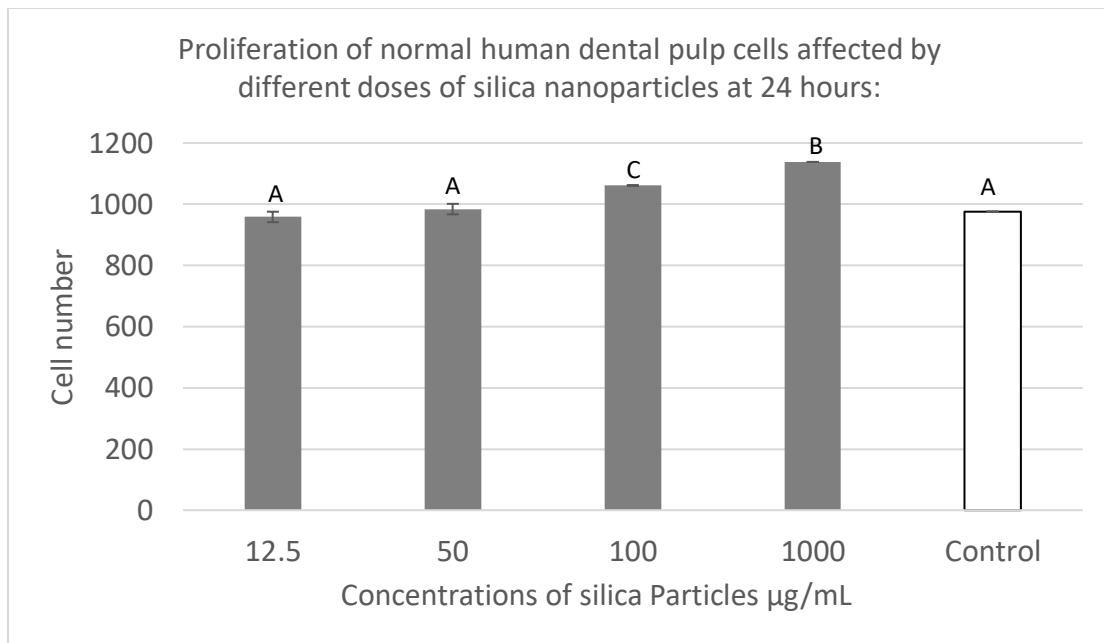


Figure 6 : Proliferation of normal human dental pulp cells affected by different doses of silica nanoparticles at 24 hours:

Proliferation of normal human dental pulp cells with media containing silica nanoparticles ranging 12.5 µg/mL to 1000 µg/mL for a time period of 24 hours. Cell number was calculated by using optical density measurement results dividing the constant number (per cell's optical density).

The control group was treated with growth media without supplemental silica particles. Groups with the same letters are not statistically significant ($P>0.05$). Error bars indicate the standard deviations of four replicates.

At seven days (Figure 7), no statistically significant difference was seen between the group containing 12.5 $\mu\text{g/mL}$ and 50 $\mu\text{g/mL}$ of silica nanoparticles and the control cells ($p < 0.05$). However, the two groups containing 100 $\mu\text{g/mL}$ and 1000 $\mu\text{g/mL}$ proliferated slower compared to the control group ($p < 0.05$). A statistically significant difference was seen when comparing both doses with each other's, which indicates that higher concentrations might limit the rate of human dental pulp cells' proliferation in a dose dependent manner.

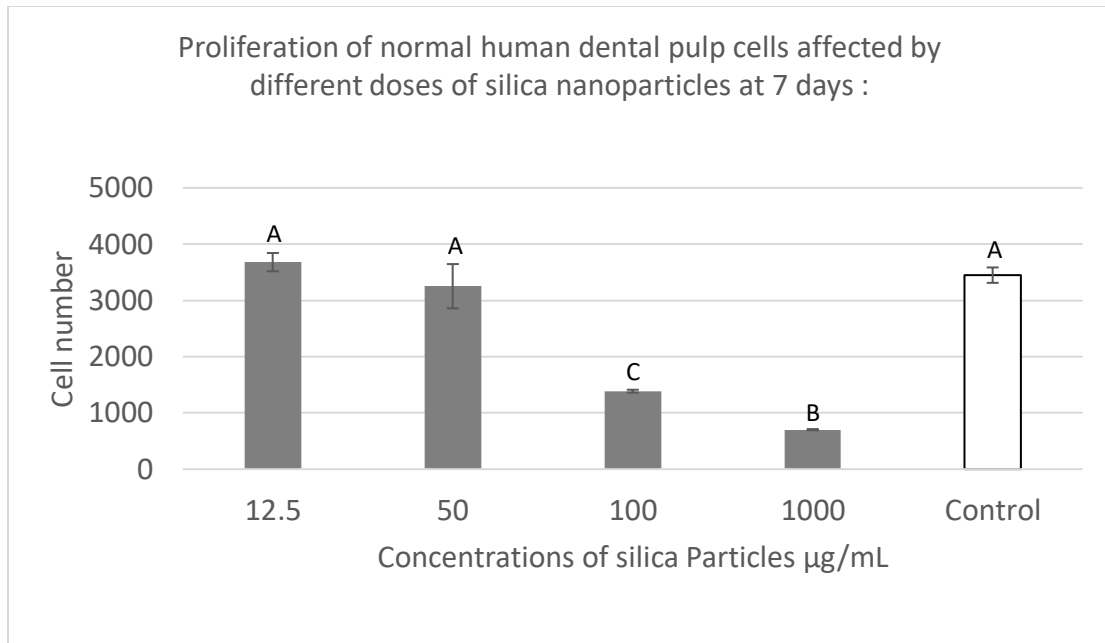


Figure 7 : Proliferation of normal human dental pulp cells affected by different doses of silica nanoparticles at 7 days:

Proliferation of normal human dental pulp cells with media containing silica nanoparticles ranging 12.5 µg/mL to 1000 µg/mL for a time period of 7 days. Cell number was calculated by using optical density measurement results dividing the constant number (per cell's optical density).

The control group was treated with growth media without supplemental silica particles. Groups with the same letters are not statistically significant ($P > 0.05$).

Error bars indicate the standard deviations of four replicates.

Surprisingly, on day 14, which was the last proliferation time point (Figure 8), the 12.5 $\mu\text{g}/\text{mL}$ and 50 $\mu\text{g}/\text{mL}$ groups containing silica nanoparticles showed a statistically significant reduction in cell proliferation compared to the control ($p < 0.05$). Interestingly, the 100 $\mu\text{g}/\text{mL}$ and 1000 $\mu\text{g}/\text{mL}$ groups had a significant loss of cell number compared to the control group ($p < 0.05$) and compared to the 12.5 $\mu\text{g}/\text{mL}$ and 50 $\mu\text{g}/\text{mL}$ groups ($p < 0.05$).

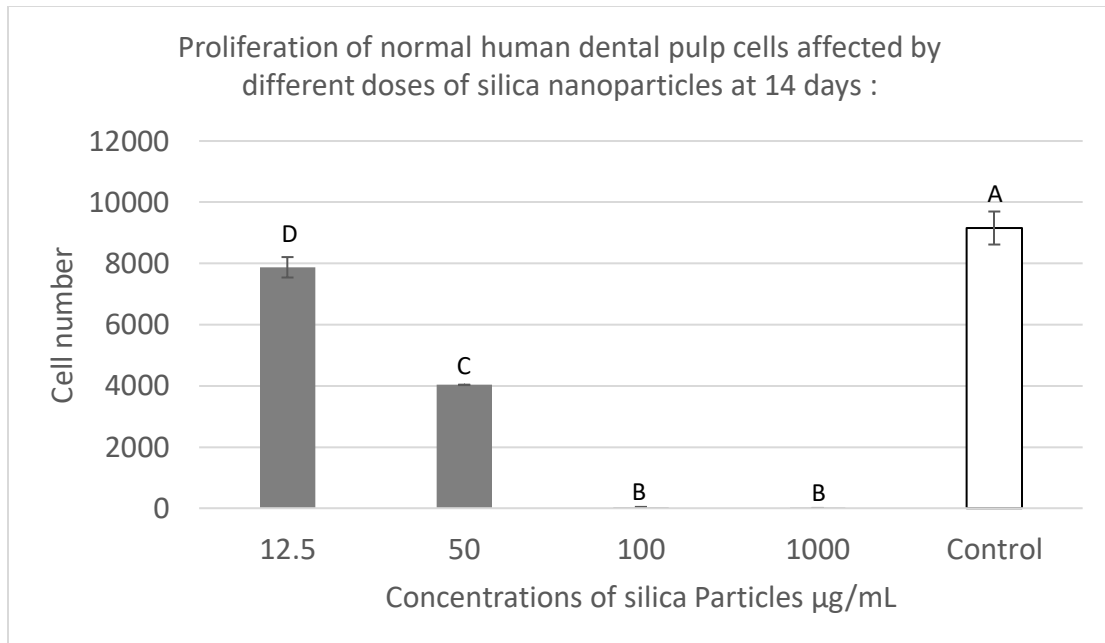


Figure 8 : Proliferation of normal human dental pulp cells affected by different doses of silica nanoparticles at 14 days:

Proliferation of normal human dental pulp cells with media containing silica nanoparticles ranging 12.5 µg/mL to 1000 µg/mL for a time period of 14 days. Cell number was calculated by using optical density measurement results dividing the constant number (per cell's optical density).

The control group was treated with growth media without supplemental silica particles. Groups with the same letters are not statistically significant ($P > 0.05$). Error bars indicate the standard deviations of four replicates.

3.3.2 Proliferation of normal human dental pulp cells affected by different doses of silica microparticles at different time intervals:

Initially, when human dental pulp cells proliferated at 24 hours (Figure 9), a significant increase in the cell number was seen in the highest concentration compared to the rest of the groups that had smaller doses ($p < 0.05$). Interestingly, no statistical significance was seen between the three lower concentrations of silica microparticles compared to the control and compared to each other ($p > 0.05$).

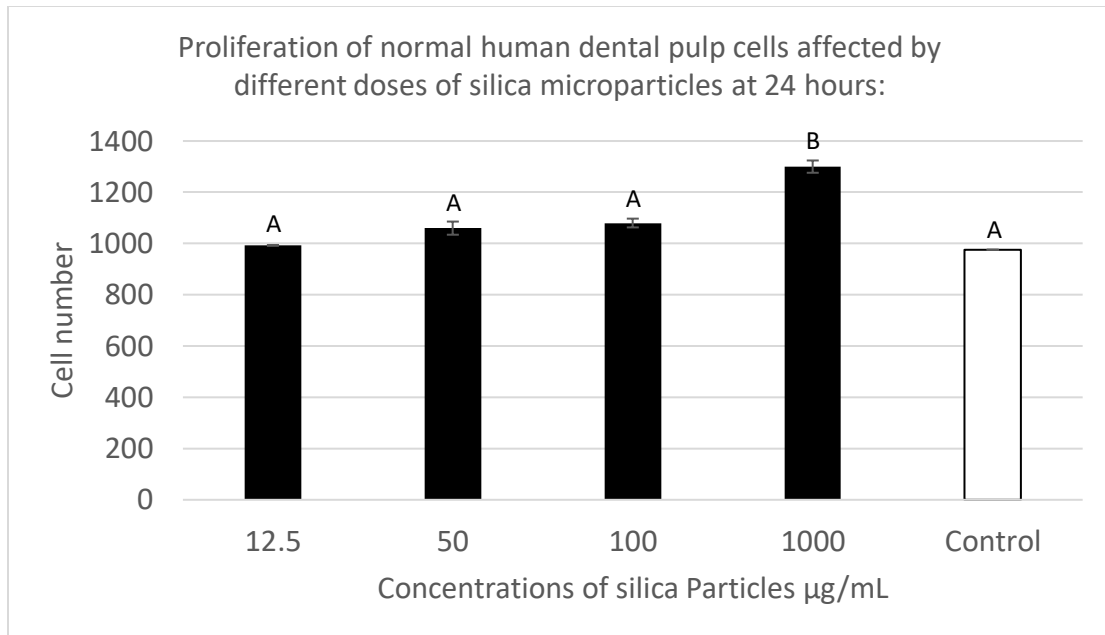


Figure 9 : Proliferation of normal human dental pulp cells affected by different doses of silica microparticles at 24 hours:

Proliferation of normal human dental pulp cells with media containing silica microparticles ranging 12.5 µg/mL to 1000 µg/mL for a time period of 24 hours. Cell number was calculated by using optical density measurement results dividing the constant number (per cell's optical density).

The control group was treated with growth media without supplemental silica particles. Groups with the same letters are not statistically significant ($P > 0.05$). Error bars indicate the standard deviations of four replicates.

At 7 days (Figure 10), the 12.5 $\mu\text{g/mL}$, 50 $\mu\text{g/mL}$ groups containing silica micro particles proliferated faster than the control cells ($p < 0.05$), and when comparing both groups with each other, it was higher in the 12.5 $\mu\text{g/mL}$ group. Statistically significant reductions in the proliferation can be noticed in the 100 $\mu\text{g/mL}$ and 1000 $\mu\text{g/mL}$ groups, compared to the other two groups and the control ($p < 0.05$).

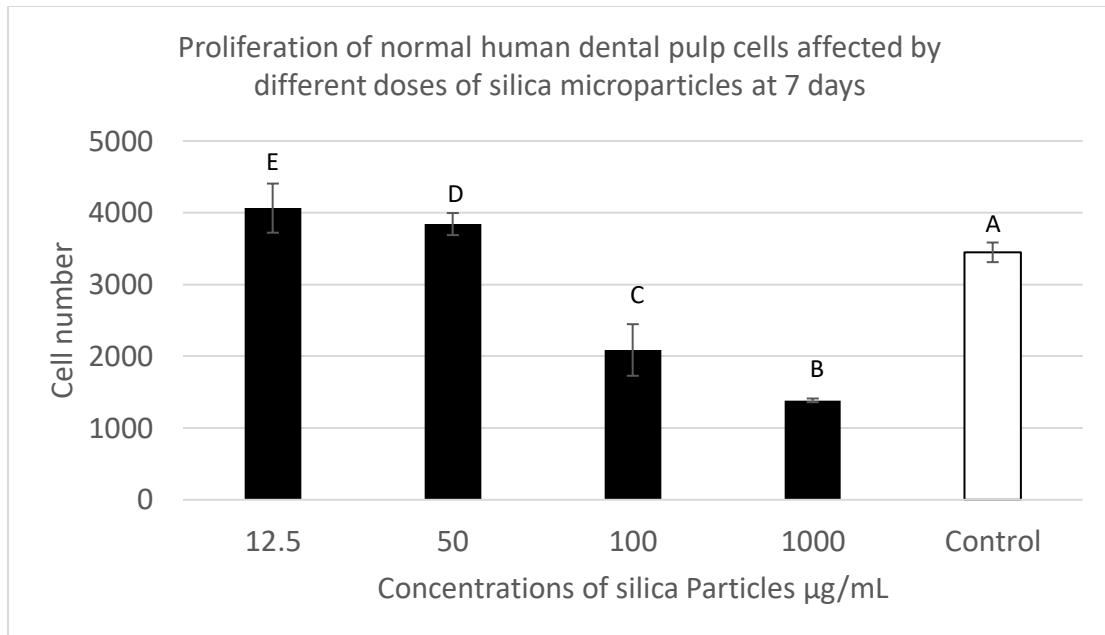


Figure 10 : Proliferation of normal human dental pulp cells affected by different doses of silica microparticles at 7 days

Proliferation of normal human dental pulp cells with media containing silica Microparticles ranging 12.5 µg/mL to 1000 µg/mL for a time period of 7 days. Cell number was calculated by using optical density measurement results dividing the constant number (per cell's optical density).

The control group was treated with growth media without supplemental silica particles. Groups with the same letters are not statistically significant ($P > 0.05$).

Error bars indicate the standard deviations of four replicates.

Finally, at day 14 (Figure 11), the 12.5 $\mu\text{g}/\text{mL}$ group had the same level of proliferation compared to the control ($P>0.05$). A statistically significance decrease in the proliferation was seen when comparing the 50 $\mu\text{g}/\text{mL}$ group with the control ($p < 0.05$). The 100 $\mu\text{g}/\text{mL}$ and 1000 $\mu\text{g}/\text{mL}$ groups showed reductions in the proliferation ($p < 0.05$) compared to the control group and the other two groups. There was a dose-dependent decrease in the proliferation rate when comparing all the different doses with each other ($p > 0.05$).

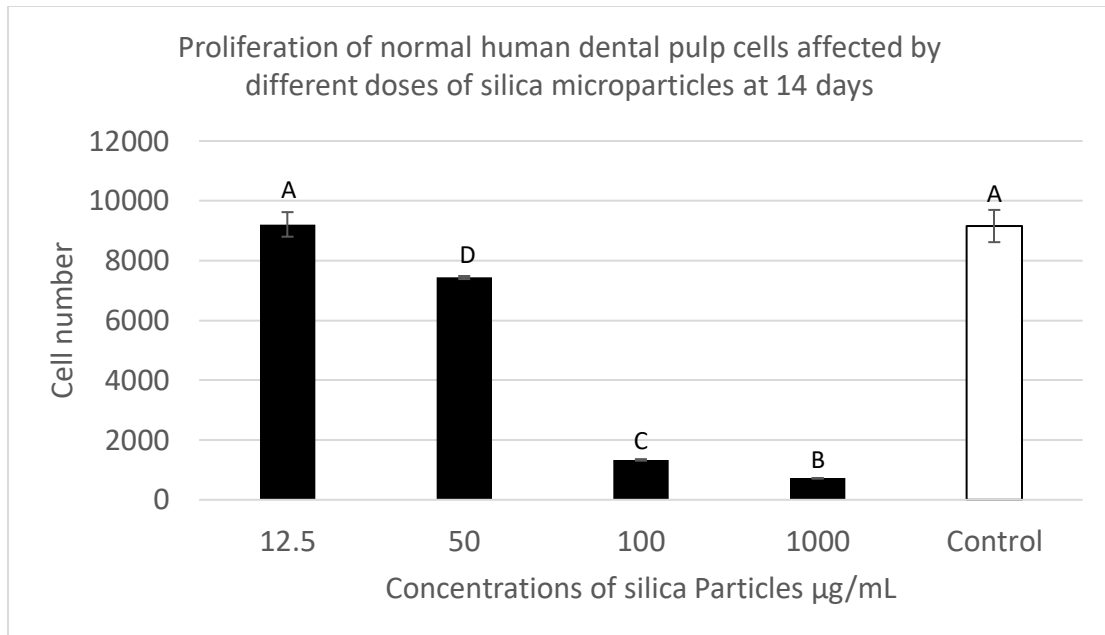


Figure 11 : Proliferation of normal human dental pulp cells affected by different doses of silica microparticles at 14 days

Proliferation of normal human dental pulp cells with media containing silica Microparticles ranging 12.5 µg/mL to 1000 µg/mL for a time period of 14 days. Cell number was calculated by using optical density measurement results dividing the constant number (per cell's optical density).

The control group was treated with growth media without supplemental silica particles Groups with the same letters are not statistically significant ($P>0.05$). Error bars indicate the standard deviations of four replicates.

3.3.3 Proliferation of normal human dental pulp cells affected by different sizes of silica particles at different time intervals:

Initially when human dental pulp cells proliferated at 24 hours (Figure 12), the 12.5 $\mu\text{g/mL}$ and 100 $\mu\text{g/mL}$ groups showed higher proliferation in the microparticles compared to nanoparticles although it was not statistically significant ($p > 0.05$). Statistically significant differences were seen in the 1000 $\mu\text{g/mL}$ group where both sizes proliferated faster than the control, and a higher proliferation was seen in the microparticles when comparing both sizes with each other ($p < 0.05$).

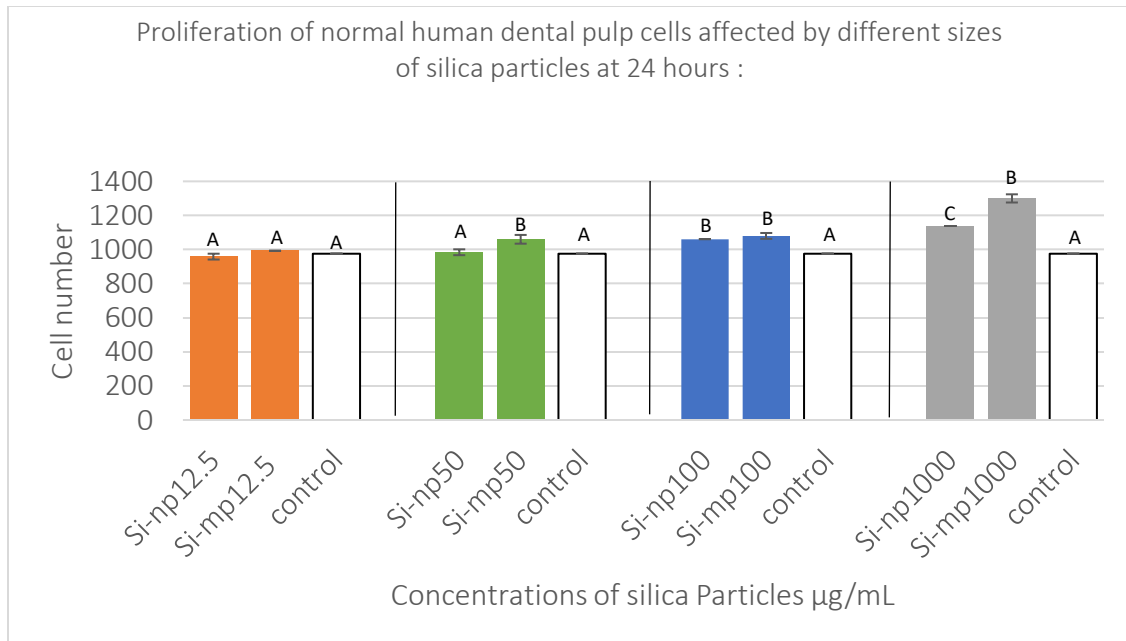


Figure 12 : Proliferation of normal human dental pulp cells affected by different sizes of silica particles at 24 hours:

Proliferation of normal human dental pulp cells with media containing different sizes of silica particles ranging 12.5 µg/mL to 1000 µg/mL for a time period of 24 hours. Cell number was calculated by using optical density measurement results dividing the constant number (per cell's optical density).

The control group was treated with growth media without supplemental silica particles. Groups with the same letters are not statistically significant ($P>0.05$). Error bars indicate the standard deviations of four replicates.

At Day 7 (Figure 13), the 12.5 $\mu\text{g/mL}$ group microparticles showed statistically significant increases in the proliferation compared to the control ($p < 0.05$), no statistically significant difference was seen when comparing control to nanoparticles ($p > 0.05$). However, in the 50 $\mu\text{g/mL}$, statistically significant difference was seen when comparing microparticles to nanoparticles ($p < 0.05$), where microparticles had higher proliferation compared to nanoparticles.

In the 100 $\mu\text{g/mL}$ group and 1000 $\mu\text{g/mL}$ group, there was a statistically significant decrease in proliferation on both sizes compared to the control ($p < 0.05$). There was also a statistically significant decrease in the proliferation of nanoparticles compared to microparticles ($p < 0.05$).

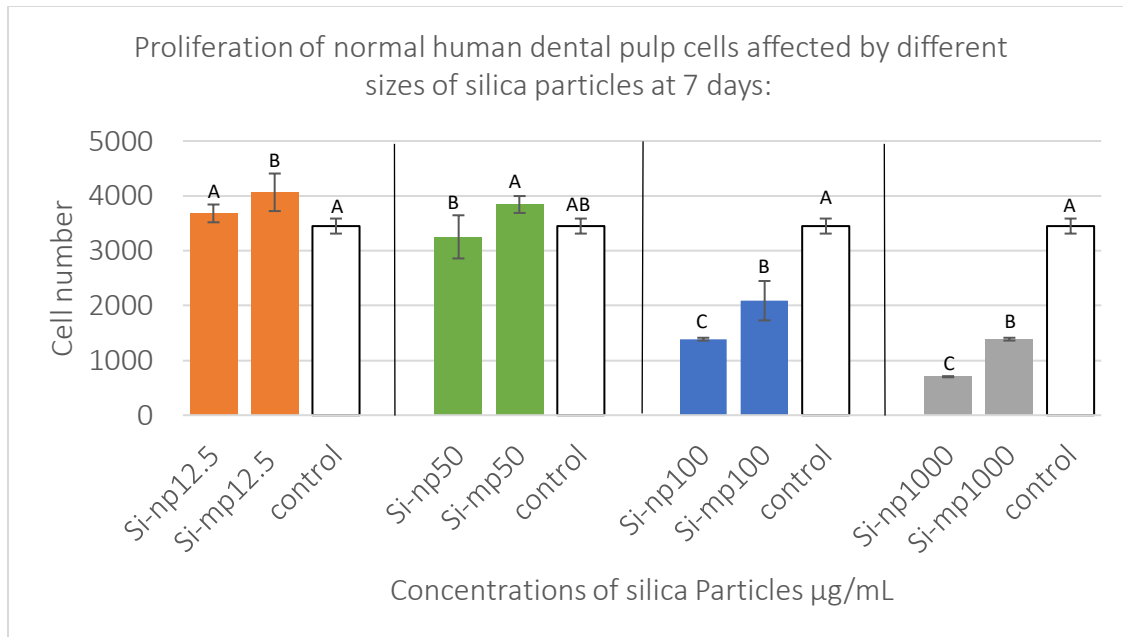


Figure 13 : Proliferation of normal human dental pulp cells affected by different sizes of silica particles at 7 days:

Proliferation of normal human dental pulp cells with media containing different sizes of silica particles ranging 12.5 µg/mL to 1000 µg/mL for a time period of 7 days. Cell number was calculated by using optical density measurement results dividing the constant number (per cell's optical density).

The control group was treated with growth media without supplemental silica particles. Groups with the same letters are not statistically significant ($P > 0.05$). Error bars indicate the standard deviations of four replicates.

Finally, at day 14 (Figure 14), in the 12.5 $\mu\text{g/mL}$ group, higher proliferation in the microparticles was noted compared with nanoparticles ($p < 0.05$). In the 50 $\mu\text{g/mL}$, 100 $\mu\text{g/mL}$, and 1000 $\mu\text{g/mL}$ groups, there was a statistically significant decrease of proliferation in both microparticles and nanoparticles groups compared to in the control group. However, in the 100 $\mu\text{g/mL}$ group and 1000 $\mu\text{g/mL}$ groups, microparticles showed some minor proliferation compared to nanoparticles that showed significant decrease in proliferation, which might indicate that silica nanoparticles might limit the proliferation of human dental pulp cells at 14 days.

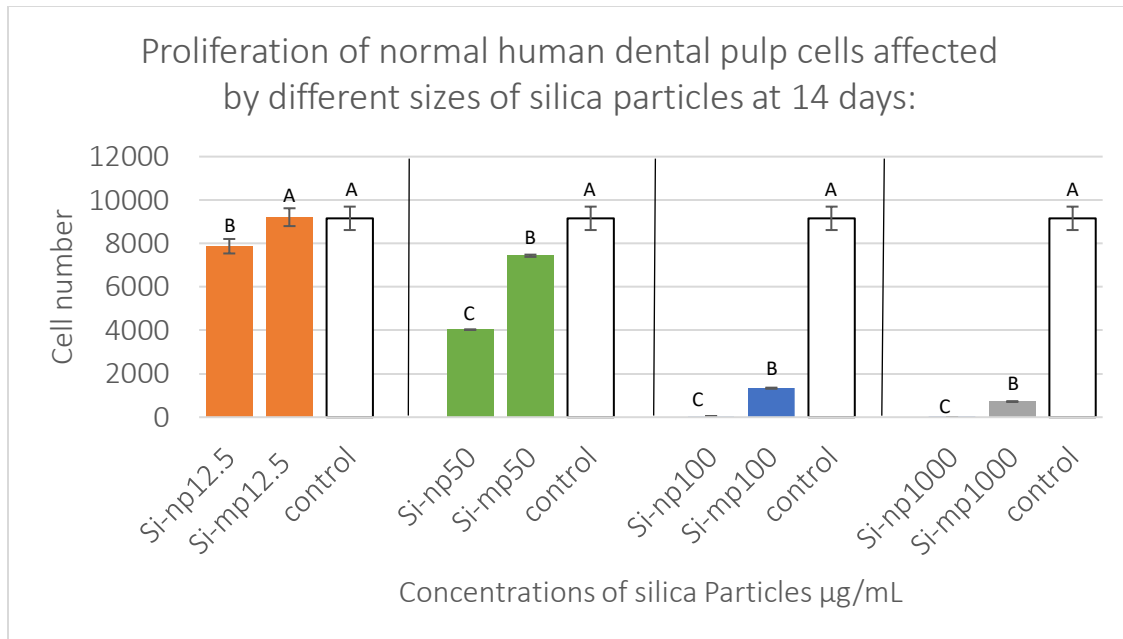


Figure 14 : Proliferation of normal human dental pulp cells affected by different sizes of silica particles at 14 days:

Proliferation of normal human dental pulp cells with media containing different sizes of silica particles ranging 12.5 µg/mL to 1000 µg/mL for a time period of 14 days. Cell number was calculated by using optical density measurement results dividing the constant number (per cell's optical density).

The control group was treated with growth media without supplemental silica particles. Groups with the same letters are not statistically significant ($P > 0.05$). Error bars indicate the standard deviations of four replicates.

Cytotoxicity

3.4 Cytotoxicity

3.4.1 Cytotoxicity of normal human dental pulp cells affected by different doses of silica nanoparticles at different time intervals:

In order to examine if the addition of different doses of silica nanoparticles in a culture medium was affecting the cytotoxicity, 800 normal human dental pulp cells were cultured in 96-well plates containing plain medium for 16 hours until full cell attachment. Then the plain media was replaced with culture media containing different doses of silica nanoparticles, ranging from 12.5 $\mu\text{g/mL}$ to 1000 $\mu\text{g/mL}$, for 1, 7 and 14 days.

Initially, when human dental pulp cells were exposed to silica Nano particles at 24 hours (Figure 15), no statistically significant difference in the viability percentage was seen between all the groups and the control ($p > 0.05$), which indicates that silica nanoparticles were not cytotoxic on human dental pulp cells at 24 hours.

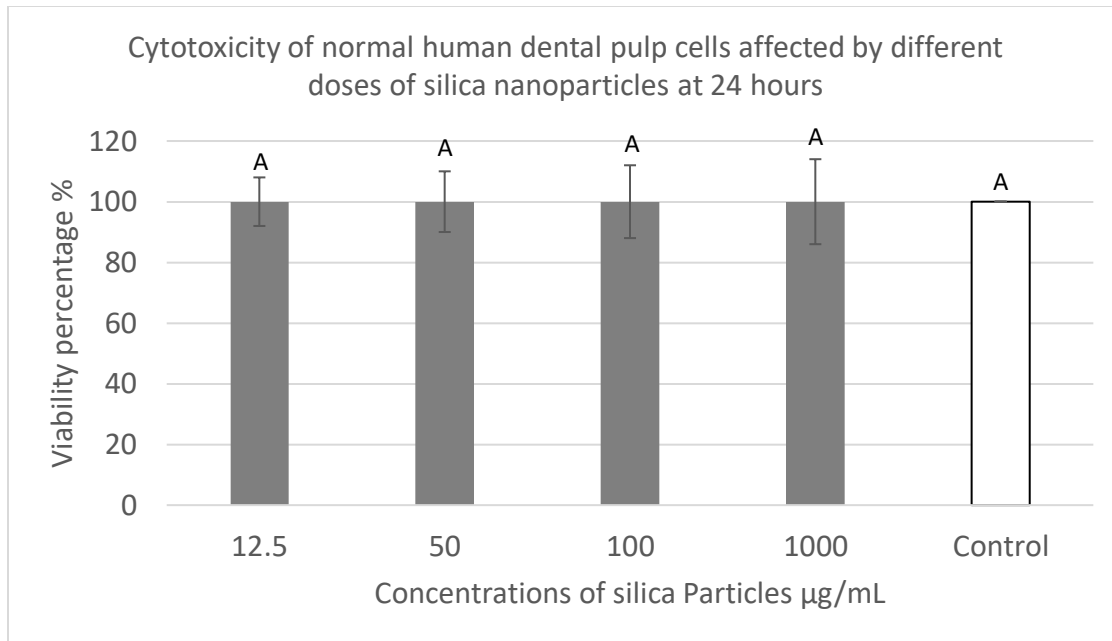


Figure 15 : Cytotoxicity of normal human dental pulp cells affected by different doses of silica nanoparticles at 24 hours

Cytotoxicity of normal human dental pulp cells with media containing silica

Nanoparticles ranging 12.5 µg/mL to 1000 µg/mL for a time period of 24 hours. The cell viability was calculated according to the following equation:

$$\text{Cell viability (\%)} = (R_{\text{Sample}} - R_o) / (R_{\text{Control}} - R_o) \times 100$$

The control group was treated with growth media without supplemental silica particles. Groups with the same letters are not statistically significant ($P > 0.05$). Error bars indicate the standard deviations of four replicates.

At day 7 (Figure 16), the 12.5 $\mu\text{g}/\text{mL}$ group containing silica nanoparticles was the only concentration shown not to be cytotoxic compared to the control. The three higher concentrations containing silica nanoparticles showed a statistically significant difference in the viability percentage compared to the control ($p < 0.05$). There was statistically significant reduction in the viability percentage between the two higher concentrations groups when compared to each other and compared to the 50m $\mu\text{g}/\text{mL}$ group. This indicates that higher concentrations of silica nanoparticles are cytotoxic to human dental pulp cells at seven days ($p < 0.05$).

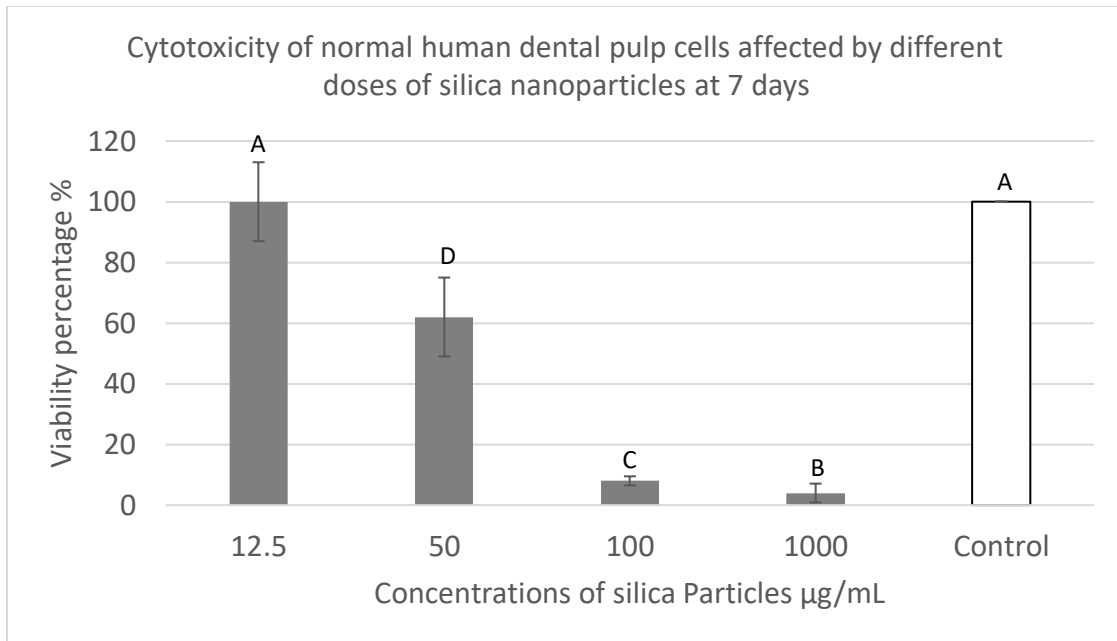


Figure 16 : Cytotoxicity of normal human dental pulp cells affected by different doses of silica nanoparticles at 7 days

Cytotoxicity of normal human dental pulp cells with media containing silica

Nanoparticles ranging 12.5 µg/mL to 1000 µg/mL for a time period of 7 days. The cell viability was calculated according to the following equation:

$$\text{Cell viability (\%)} = (R_{\text{Sample}} - R_0) / (R_{\text{Control}} - R_0) \times 100$$

The control group was treated with growth media without supplemental silica particles. Groups with the same letters are not statistically significant ($P > 0.05$). Error bars indicate the standard deviations of four replicates.

At Day 14 (Figure 17), all the groups showed statistically significant reductions in the viability percentage compared to the control ($p < 0.05$), there was a statistically significant difference between the lowest concentration and the three higher concentrations. No statistically significant difference was shown when comparing the two highest concentrations with each other ($p > 0.05$).

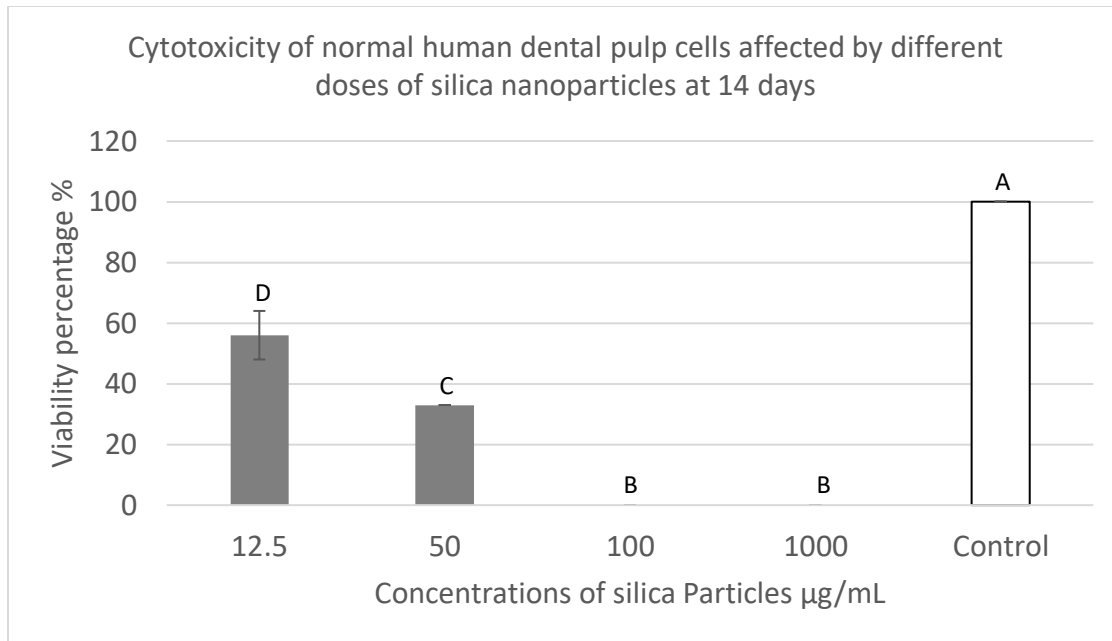


Figure 17 : Cytotoxicity of normal human dental pulp cells affected by different doses of silica nanoparticles at 14 days

Cytotoxicity of normal human dental pulp cells with media containing silica

Nanoparticles ranging 12.5 µg/mL to 1000 µg/mL for a time period of 14 days. The cell viability was calculated according to the following equation:

$$\text{Cell viability (\%)} = (R_{\text{Sample}} - R_o) / (R_{\text{Control}} - R_o) \times 100$$

The control group was treated with growth media without supplemental silica particles. Groups with the same letters are not statistically significant ($P > 0.05$). Error bars indicate the standard deviations of four replicates.

3.4.2 Cytotoxicity of normal human dental pulp cells affected by different doses of silica microparticles at different time intervals:

Initially, when human dental pulp cells were exposed to silica microparticles at Day 1 (Figure 18), no statistically significant differences in the viability percentage were noticed between the groups and the control, which represents plain media without particles. This shows that silica microparticles were not cytotoxic in each of the tested doses at Day 1 ($p > 0.05$).

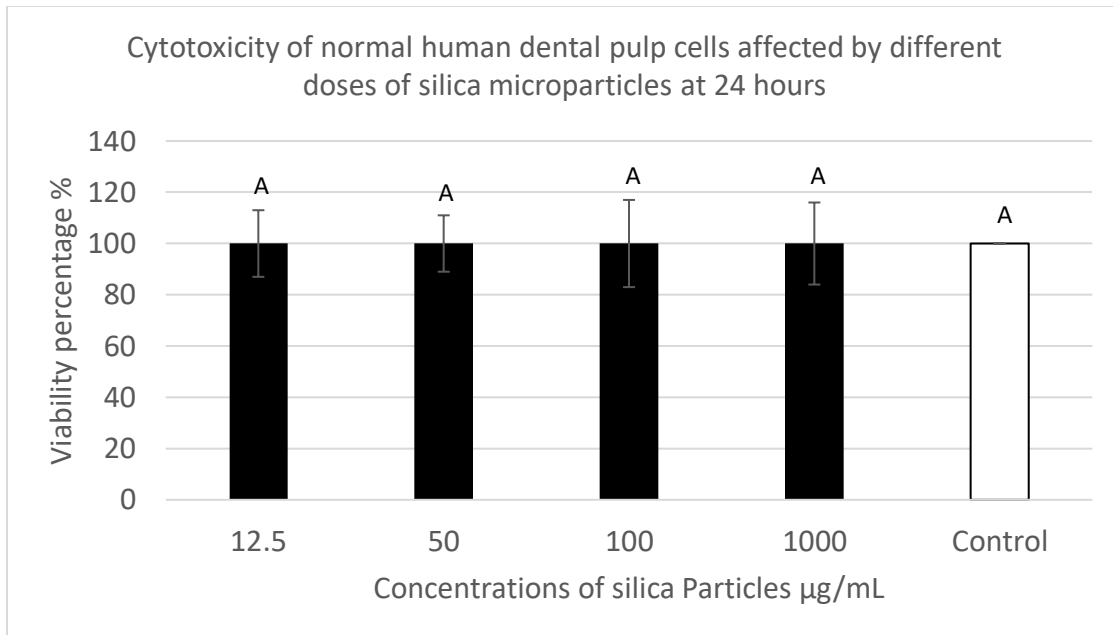


Figure 18 : Cytotoxicity of normal human dental pulp cells affected by different doses of silica microparticles at 24 hours

Cytotoxicity of normal human dental pulp cells with media containing silica

Microparticles ranging 12.5 $\mu\text{g/mL}$ to 1000 $\mu\text{g/mL}$ for a time period of 24 hours. The cell viability was calculated according to the following equation:

$$\text{Cell viability (\%)} = (R_{\text{Sample}} - R_o) / (R_{\text{Control}} - R_o) \times 100$$

The control group was treated with growth media without supplemental silica particles. Groups with the same letters are not statistically significant ($P > 0.05$). Error bars indicate the standard deviations of four replicates.

At Day 7 (Figure 19), no reduction in the viability percentage was seen in the 12.5 $\mu\text{g}/\text{mL}$ group and 50 $\mu\text{g}/\text{mL}$ group compared to the control. Cytotoxicity was noted in the 100 $\mu\text{g}/\text{mL}$ group and 1000 $\mu\text{g}/\text{mL}$ compared to the control and compared to the 12.5 $\mu\text{g}/\text{mL}$ group and 50 $\mu\text{g}/\text{mL}$ ($p < 0.05$).

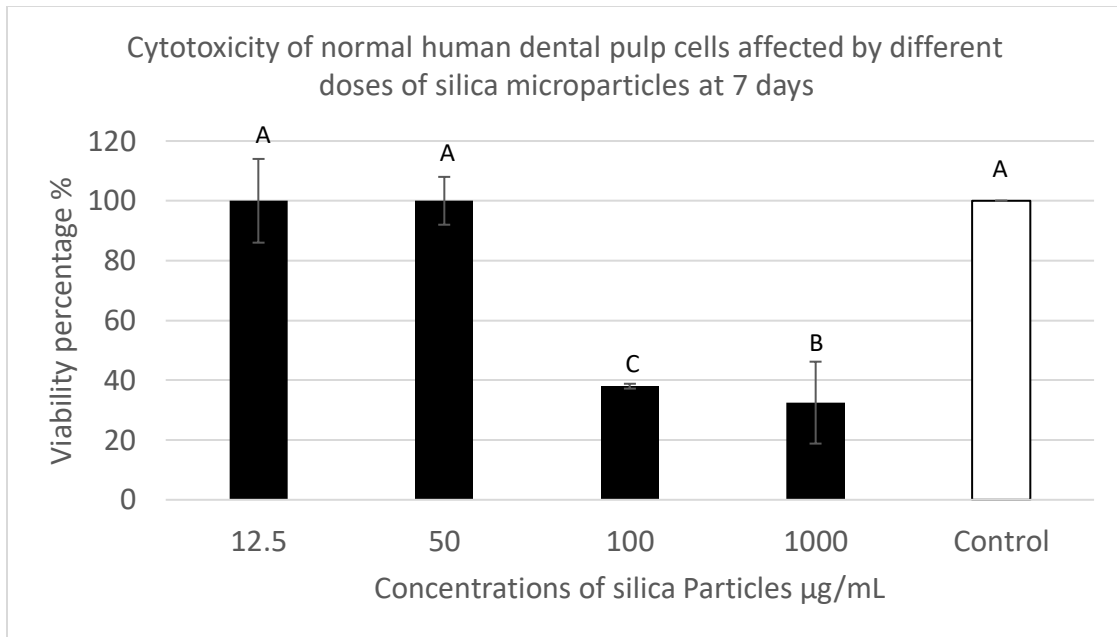


Figure 19 : Cytotoxicity of normal human dental pulp cells affected by different doses of silica microparticles at 7 days

Cytotoxicity of normal human dental pulp cells with media containing silica

Microparticles ranging 12.5 µg/mL to 1000 µg/mL for a time period of 7 days. The cell viability was calculated according to the following equation:

$$\text{Cell viability (\%)} = (R_{\text{Sample}} - R_o) / (R_{\text{Control}} - R_o) \times 100$$

The control group was treated with growth media without supplemental silica particles. Groups with the same letters are not statistically significant ($P > 0.05$). Error bars indicate the standard deviations of four replicates.

Finally, on Day 14 (Figure 20), no reduction in the viability was detected when comparing the 12.5 $\mu\text{g/mL}$ group to the control ($p > 0.05$). The 50 $\mu\text{g/mL}$, 100 $\mu\text{g/mL}$, and 1000 $\mu\text{g/mL}$ groups showed reductions in the viability percentage ($p < 0.05$), compared to the control group and when comparing between each other. This reduction seems to be in a dose-dependent manner, where the highest cytotoxicity can be seen in the 1000 $\mu\text{g/mL}$ group followed by 100 $\mu\text{g/mL}$ and 50 $\mu\text{g/mL}$.

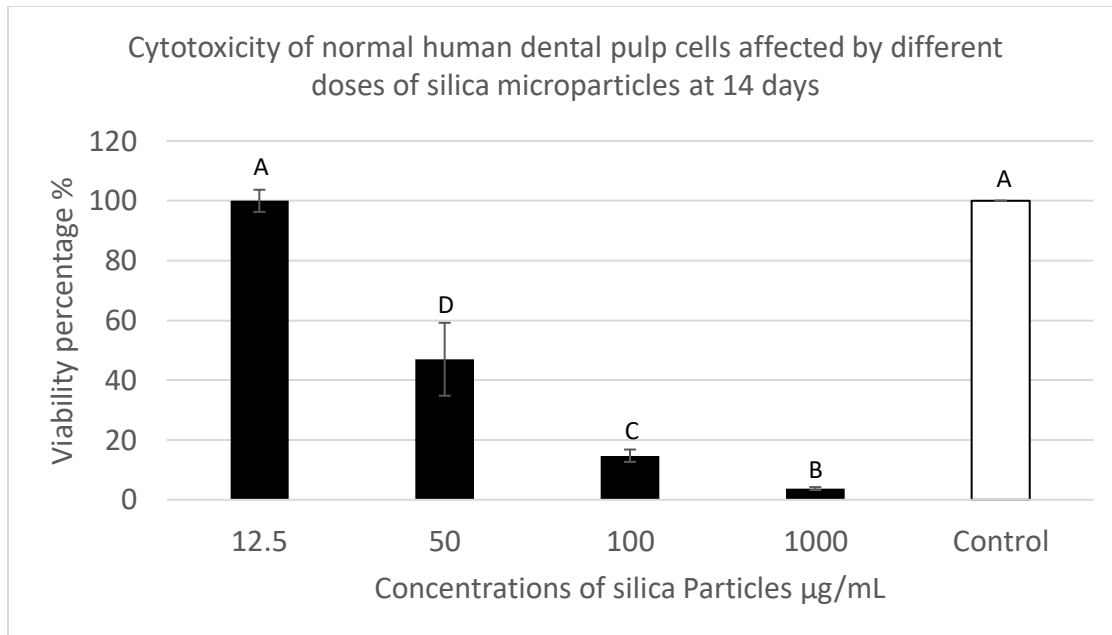


Figure 20 : Cytotoxicity of normal human dental pulp cells affected by different doses of silica microparticles at 14 days

Cytotoxicity of normal human dental pulp cells with media containing silica

Microparticles ranging 12.5 µg/mL to 1000 µg/mL for a time period of 14 hours The cell viability was calculated according to the following equation:

$$\text{Cell viability (\%)} = (R_{\text{Sample}} - R_o) / (R_{\text{Control}} - R_o) \times 100$$

The control group was treated with growth media without supplemental silica particles. Groups with the same letters are not statistically significant ($P > 0.05$). Error bars indicate the standard deviations of four replicates.

3.4.3 Cytotoxicity of normal human dental pulp cells affected by different sizes of silica particles at different time intervals :

Initially, when human dental pulp cells were exposed to different sizes of silica micro and nanoparticles (Figure 21), no statistically significant difference in the viability percentage was seen compared to the control, which represented plain culture media without particles in all the groups. This indicates that silica particles did not possess any significant size-related cytotoxic effect on Day 1 in vitro ($p > 0.05$).

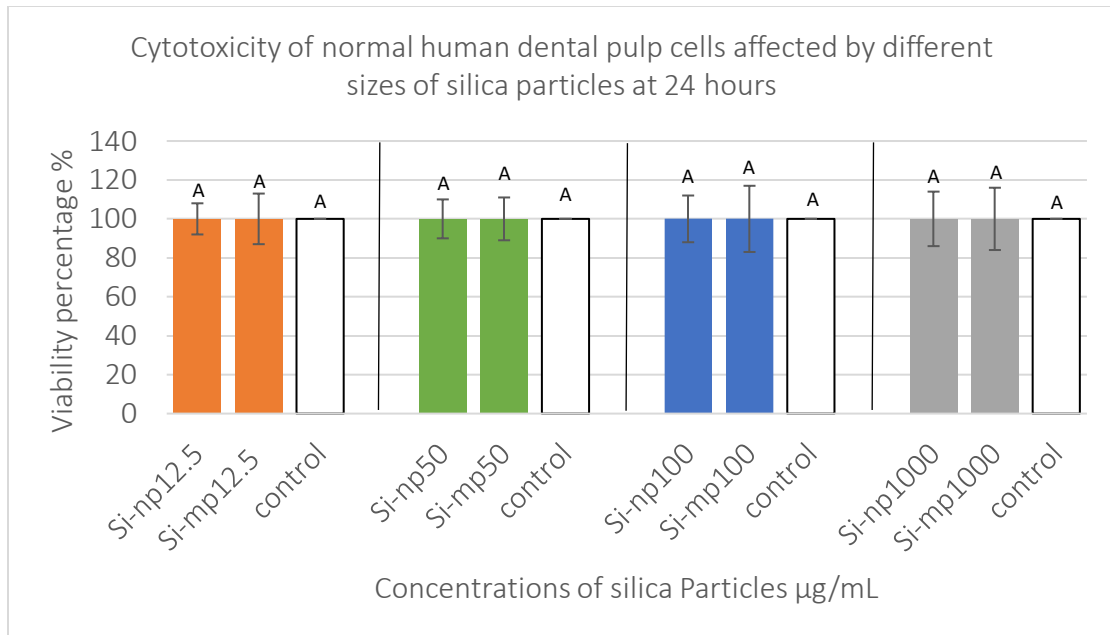


Figure 21 : Cytotoxicity of normal human dental pulp cells affected by different sizes of silica particles at 24 hours

Cytotoxicity of normal human dental pulp cells with media containing different sizes of silica particles ranging 12.5 µg/mL to 1000 µg/mL for a time period of 24 hours.

The cell viability was calculated according to the following equation:

$$\text{Cell viability (\%)} = \frac{(R_{\text{Sample}} - R_o)}{(R_{\text{Control}} - R_o)} \times 100$$

The control group was treated with growth media without supplemental silica particles. Groups with the same letters are not statistically significant ($P > 0.05$). Error bars indicate the standard deviations of four replicates.

At Day 7 (Figure 22), there was no significant difference in the 12.5 $\mu\text{g}/\text{mL}$ group compared to the control when both sizes were exposed to the human dental pulp cells ($p > 0.05$). A statistically significant decrease in the viability percentage in the 50 $\mu\text{g}/\text{mL}$ were where the nanoparticles showed a marked reduction compared to microparticles and the control. Significant size-dependent decreases in the viability percentages in the 100 $\mu\text{g}/\text{mL}$ and 1000 $\mu\text{g}/\text{mL}$ groups were where nanoparticles showed a decrease in the viability percentage compared to microparticles ($p < 0.05$), and both sizes showed statistically significant reductions in the viability percentage compared to the control ($p < 0.05$). This confirms that silica nanoparticles are cytotoxic when exposed to human dental pulp cells at Day 7.

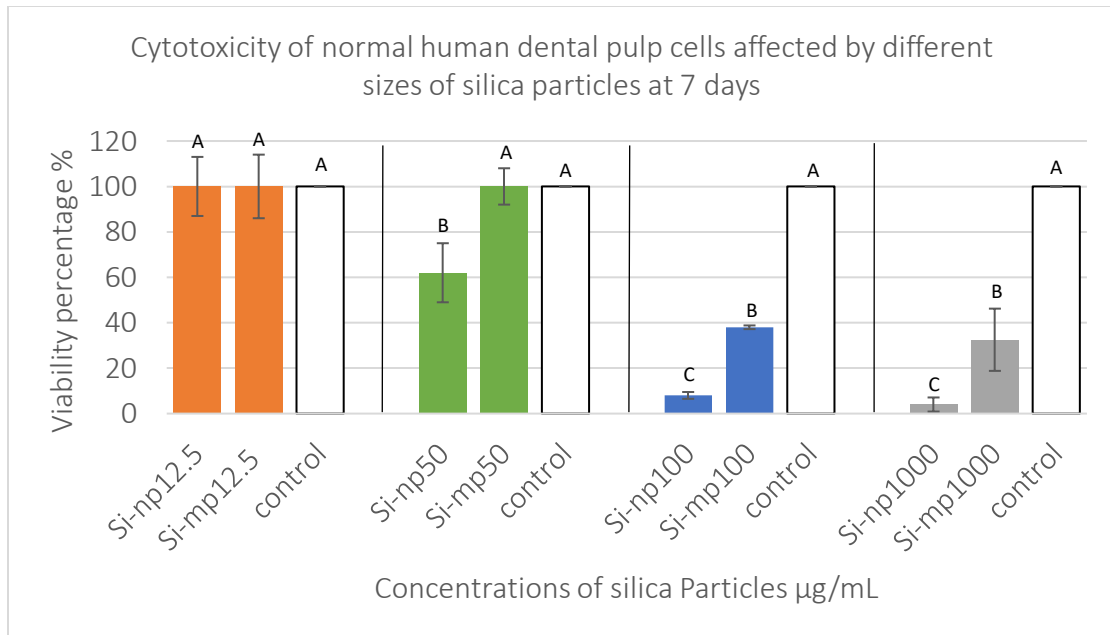


Figure 22 : Cytotoxicity of normal human dental pulp cells affected by different sizes of silica particles at 7 days

Cytotoxicity of normal human dental pulp cells with media containing different sizes of silica particles ranging 12.5 µg/mL to 1000 µg/mL for a time period of 7 days.

The cell viability was calculated according to the following equation:

$$\text{Cell viability (\%)} = \frac{(R_{\text{Sample}} - R_o)}{(R_{\text{Control}} - R_o)} \times 100$$

The control group was treated with growth media without supplemental silica particles. Groups with the same letters are not statistically significant ($P > 0.05$). Error bars indicate the standard deviations of four replicates.

Finally, on Day 14 (Figure 23), statistically significant difference was noted in the 12.5 $\mu\text{g/mL}$ group where nanoparticles showed reduction in the viability compared to both microparticles and control ($p < 0.05$), no statistically significant difference was seen between microparticles and control ($p > 0.05$). However, statistically significant decreases in the viability percentages in the 50 $\mu\text{g/mL}$, 100 $\mu\text{g/mL}$, and 1000 $\mu\text{g/mL}$ groups were where nanoparticles showed marked reductions in the viability compared to micro particles ($p < 0.05$). Both sizes showed statistically significant decreases in the viability percentages compared to the control, thus confirming the previous hypothesis that the decrease of cell numbers in those concentrations might be due to cytotoxic effect.

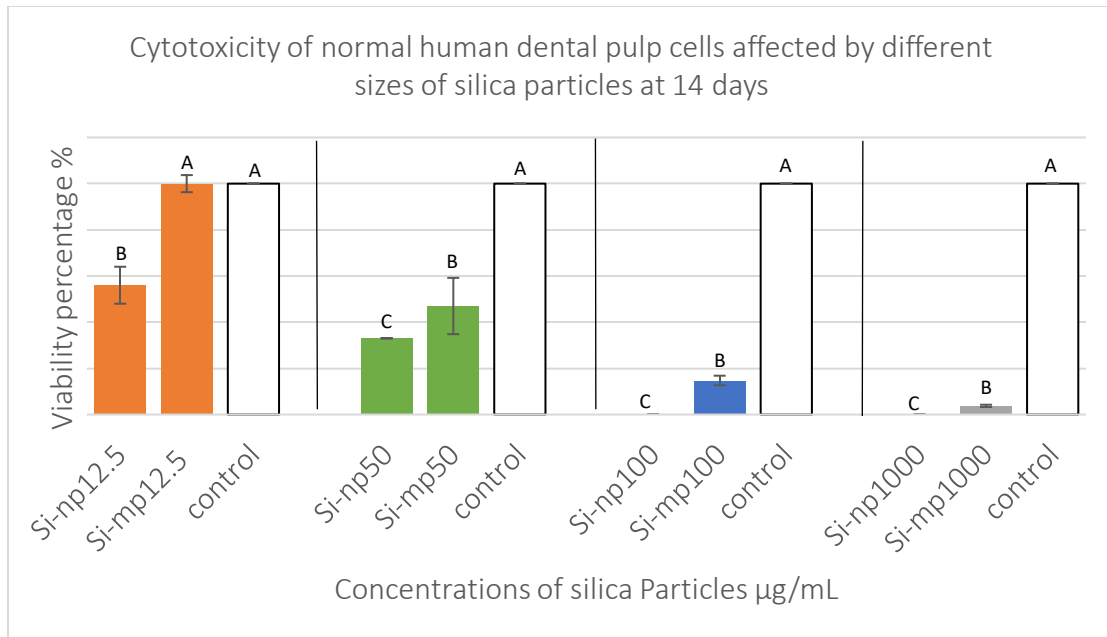


Figure 23 : Cytotoxicity of normal human dental pulp cells affected by different sizes of silica particles at 14 days

Cytotoxicity of normal human dental pulp cells with media containing different sizes of silica particles ranging 12.5 µg/mL to 1000 µg/mL for a time period of 14 days. The cell viability was calculated according to the following equation:

$$\text{Cell viability (\%)} = (R_{\text{Sample}} - R_0) / (R_{\text{Control}} - R_0) \times 100$$

The control group was treated with growth media without supplemental silica particles. Groups with the same letters are not statistically significant ($P > 0.05$). Error bars indicate the standard deviations of four replicates.

Genotoxicity

3.5 Genotoxicity

3.5.1 Genotoxicity of normal human dental pulp cells affected by different doses of silica nanoparticles at different time intervals:

In order to examine if the addition of different doses of silica nanoparticles in a culture medium was affecting the genotoxicity, 800 normal human dental pulp cells were cultured in 96-well plates containing plain medium for 16 hours until full cell attachment. Then the plain media was replaced with culture media containing different doses of silica nanoparticles, ranging from 12.5 µg/mL to 1000 µg/mL, for 24 hours.

Initially, when human dental pulp cells proliferated at 24 hours (Figure 24), a significant increase in the genotoxicity was seen in all concentrations of silica nanoparticles when compared to the control ($p < 0.05$). A statistically significant difference was found when comparing different doses of silica particles in a dose-dependent manner ($p < 0.05$).

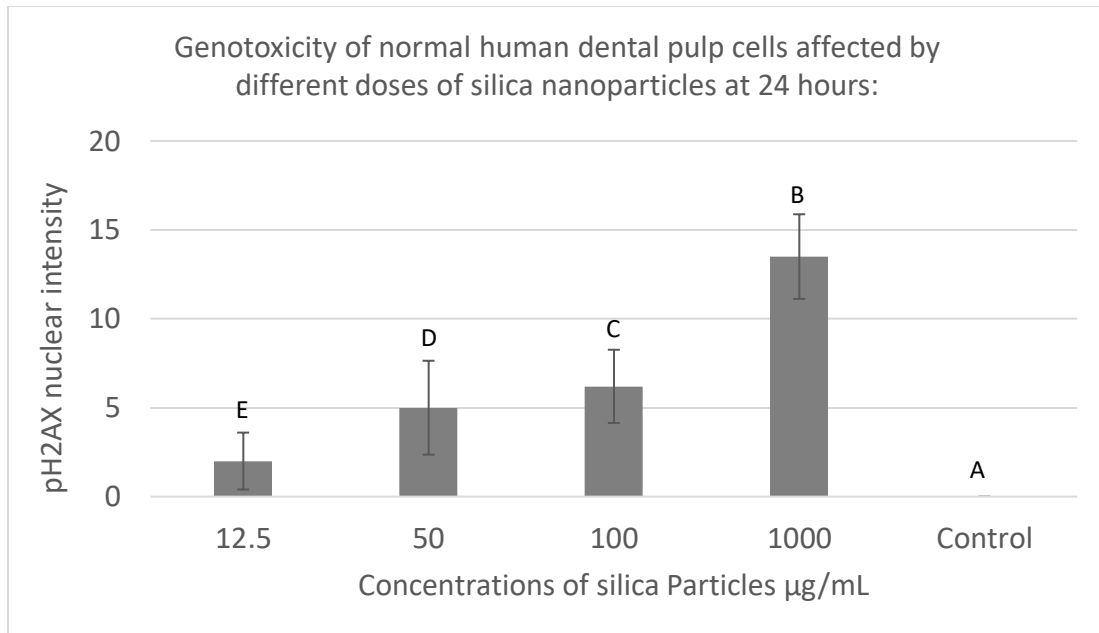


Figure 24 : Genotoxicity of normal human dental pulp cells affected by different doses of silica nanoparticles at 24 hours:

Genotoxicity of normal human dental pulp cells with media containing silica Nanoparticles ranging 12.5 µg/mL to 1000 µg/mL for a time period of 24 hours.

The control group was treated with growth media without supplemental silica particles. Groups with the same letters are not statistically significant ($P > 0.05$). Error bars indicate the standard deviations of four replicates.

3.5.2 Genotoxicity of normal human dental pulp cells affected by different doses of silica microparticles at different time intervals:

Initially, when human dental pulp cells proliferated at 24 hours (Figure 25), a significant increase in the genotoxicity was seen in all concentrations of silica microparticles when compared to the control ($p < 0.05$). A statistically significant difference was found when comparing genotoxicity between different doses of silica particles in a dose-dependent manner ($p < 0.05$).

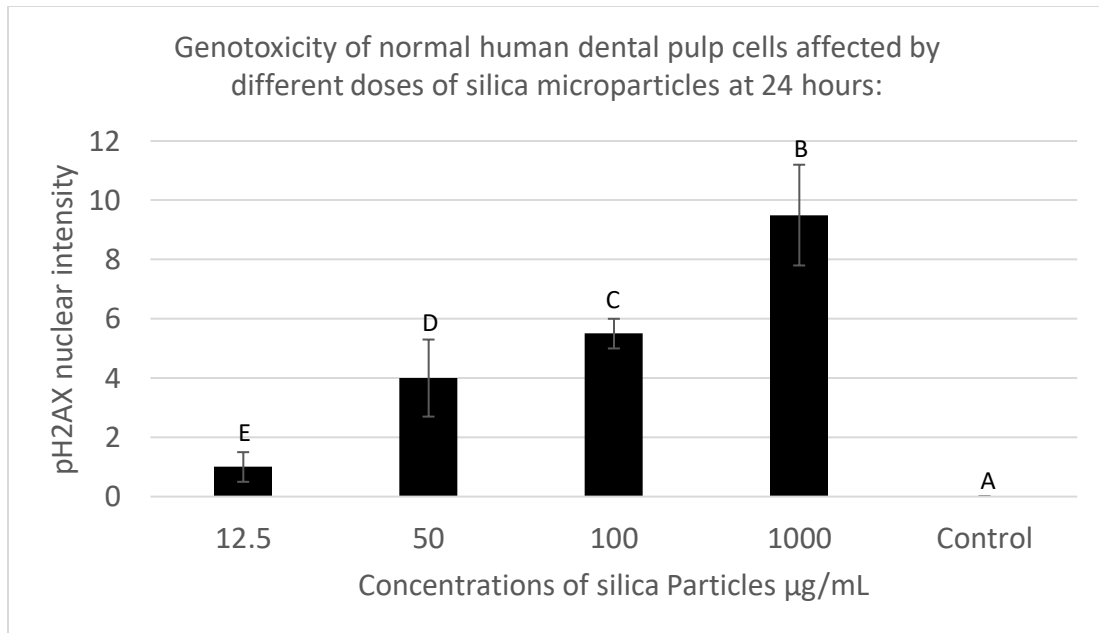


Figure 25 Genotoxicity of normal human dental pulp cells affected by different doses of silica microparticles at 24 hours:

Genotoxicity of normal human dental pulp cells with media containing silica Microparticles ranging 12.5 $\mu\text{g/mL}$ to 1000 $\mu\text{g/mL}$ for a time period of 24 hours.

The control group was treated with growth media without supplemental silica particles. Groups with the same letters are not statistically significant ($P > 0.05$). Error bars indicate the standard deviations of four replicates.

3.5.3 Genotoxicity of normal human dental pulp cells affected by different sizes of silica particles at different time intervals:

Initially, when human dental pulp cells proliferated at 24 hours (Figure 26), a significant increase in the genotoxicity was seen in all the doses of silica particles when compared to the control ($p < 0.05$). However, when comparing genotoxicity in different sizes of silica particles, silica nanoparticles showed higher levels of genotoxicity compared to microparticles in all the tested doses ($p < 0.05$).

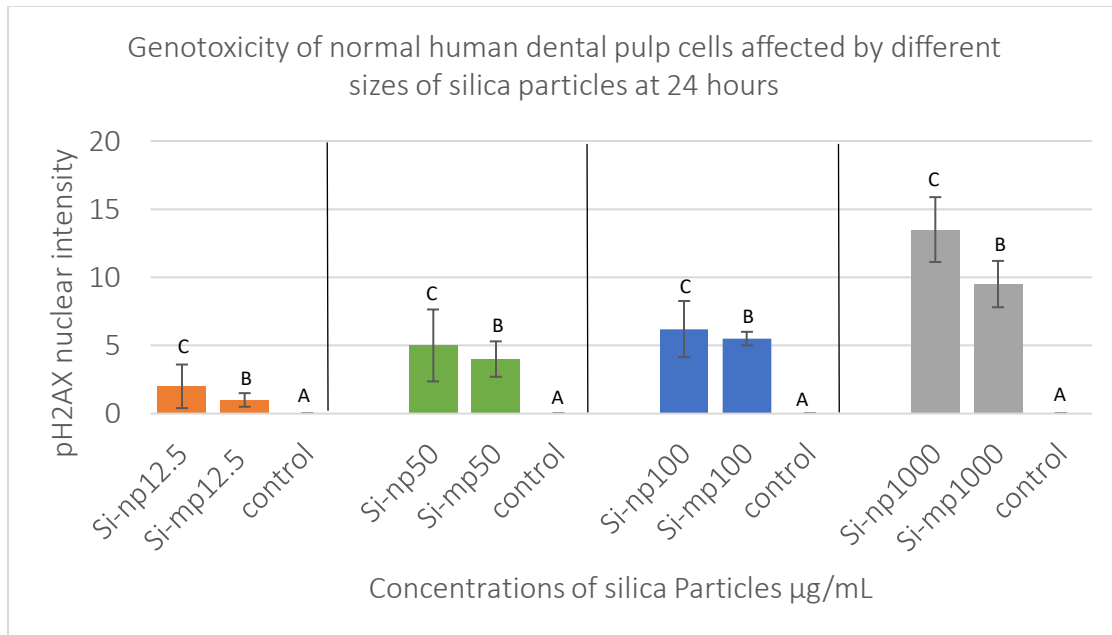


Figure 26 Genotoxicity of normal human dental pulp cells affected by different sizes of silica particles at 24 hours

Genotoxicity of normal human dental pulp cells with media containing different sizes of silica particles ranging 12.5 µg/mL to 1000 µg/mL for a time period of 24 hours.

The control group was treated with growth media without supplemental silica particles. Groups with the same letters are not statistically significant ($P > 0.05$). Error bars indicate the standard deviations of four replicates.

DISCUSSION

Chapter 6: DISCUSSION

The aim of the present study was to evaluate the attachment efficiency, proliferation, cytotoxic and genotoxic effects of a wide range of sizes and doses of silica particles on normal human dental pulp cell cultures. Most studies have revealed that silica particles possess a cytotoxic effect in different cell lines, in a dose and size dependent manner. The Findings in this study on normal human dental pulp cells were more clinically relevant compared to results from other studies, which used malignant cell lines or animal cells. With this advantage in clinical relevance, cell attachment, proliferation rate, cytotoxicity, and genotoxicity were investigated.

The dental pulp is found in the center of the tooth and is made of living cells, including odontoblasts, endothelial cells, immune system cells, neurons, and the extracellular matrix. It consists of a neural network which protects it against harmful stimuli, and blood vessels that deliver nutrients and clear waste products. Dendritic cells, macrophages, and T- lymphocytes provide protection from microorganisms and other foreign antigens. Pulp cells and odontoblasts play important roles in the regeneration of dentin damaged by tooth wear or dental procedures, as well as acting as a protective defense in the removal of external stimuli by deposition of tertiary dentin on the pulp chamber. Acute pain and tissue ischemia occur in the presence of inflammatory agents that occur when there is acute infection or increased internal pressure in the pulp chamber (143).

Human dental pulp stem cells (HDPSCs) are mesenchymal stem cells isolated from adult teeth that have the ability to differentiate into different cell lines like osteoblastic, chondrogenic, adipogenic, chondrogenic, and odontoblastic-like cells (144,145). These cells show immunosuppressive and immunomodulatory properties. They also secrete type I collagen and other noncollagenous proteins including osteopontin (OPN), osteocalcin (OCN), alkaline phosphatase (ALP), bone sialoprotein, dentin matrix protein 1, and dentin sialo phosphoprotein (146), therefore, making them a useful cell line for regenerative endodontics (136).

Vital pulp therapy includes different procedures like direct pulp capping, indirect pulp capping, partial or full pulpotomy (147). Direct pulp capping is a technique aimed to preserve exposed dental pulp with a protective material and inducing hard tissue repair. Indirect pulp capping is indicated when no vital pulp exposure occurs. Pulpotomy is different from pulp capping only in that a part of the coronal pulp is removed before the capping material is applied (148). The materials used in the those procedures should have adequate biocompatibility and bioactivity to induce dental pulp stem cells activity and pulp tissue healing in permanent and primary teeth (149).

Historically, Ca(OH)_2 has been used as a direct pulp capping material because it can induce the formation of a dentinal bridge. However, many disadvantages, such as the presence of tunnels and defects in the dentinal bridge, poor adherence to the tooth structure, and degradation after etching, have been reported with the use of calcium hydroxide. Consequently, calcium hydroxide is not considered an ideal pulp capping material (150). An alternative material, mineral trioxide aggregate (MTA) was developed in the late 1990s

(151). MTA produces a significantly larger frequency of dentinal bridge formation and less pulp irritation compared with calcium hydroxide. It has also been shown to facilitate the adhesion, migration, and attachment of undifferentiated cells to form a dentinal bridge (151). Because of its remarkable properties, MTA may represent the closest to ideal pulp capping material developed to date. Nevertheless, some concerns regarding MTA, including the potential release of hazardous substances, difficult handling, and long setting time have been raised (152).

Recently, a bioceramic material, EndoSequence Root Repair Material (RRM; Brasseler USA, Savannah, GA), was introduced to endodontics. The main constituents of RRM are calcium silicates, tantalum pentoxide, zirconium oxide, and monobasic calcium phosphate. Calcium silicate was shown to induce cell differentiation (153), have osteoconductive effects (154), and reduce inflammation of human dental pulp cells (HDPCs) (155,156). The clinical applications of RRM are similar to MTA. RRM is seen as a superior clinical alternative to MTA because of the differences in nanostructure and easier manipulation (157,158). Moreover, compared with gray and white MTA, RRM showed a reduced risk of tooth discoloration (159). However, one of the drawbacks of this material is that the setting time has been demonstrated to be longer than compared to what the manufacturer claims (160).

Silica is found in the earth's crust and is widely used for many purposes. There are two forms of silica that essentially differ in their biological activity yet have the same molecular formula: crystalline and non-crystalline (amorphous) silica (161). The recent advances in nanotechnology enable us to produce different types nanoparticles with unique physical and chemical characteristics.

Silica (SiO_2) nanoparticles have extensive industrial applications and are additives to cosmetics, drugs, varnishes, and food. Recently, the use of SiO_2 nanoparticles has been extended to biomedical and biotechnological fields, such as, in biomarkers for leukemia cell identification using optical imaging (162), biosensors for simultaneous assay of glucose, lactate, L-glutamate, and hypoxanthine levels in rat striatum (97), DNA delivery (163), drug delivery (164), enzyme immobilization (165), and cancer therapy (36).

The increasing use of these nanoparticles in industrial and consumer products has given rise to concerns about their biological activity and environmental impact. It is therefore important to address the potential effects of nanoparticles on human health and environment (166).

In regards to in vitro nanotoxicity studies, the careful and accurate characterizations of particle size, morphology, composition surface area, and surface chemistry are crucial. Recent studies have focused on the importance of accurate physicochemical characterization of nanoparticles before undertaking in vitro toxicity experiments. Most of the reported toxicity studies relied on the characteristics of the particles, although the physicochemical characteristics of nanoparticles are likely to change under in vitro conditions (167,168).

The cell attachment efficiency assay is essential because it is well known that a biomaterial's surface characteristics can change cell behavior at many levels, such as differentiation, proliferation, and apoptosis. These are determined by cell shape and cytoskeletal organization directly, which in turn, affect cell/surface interaction (169)(170). The cellular interaction with a material surface depends on both chemistry and surface texture (topography) (171). These surface characteristics have been a subject of interest because they can alter protein absorption and regulate cell adhesion, proliferation, differentiation, and bony formation (172–176). The external membrane of a typical cell is covered by at least six different receptor systems that can be activated by interactions with neighboring cells, ligands in the surrounding (ECM), and signaling molecules (177).

The definite mechanisms by which surface characteristics affect cellular attachment and growth are not yet known. The cell microenvironment is a tortuous array of chemical and topographical processes and recent studies have showed that surface profile size on the nanometer scale can affect protein adsorption (178–180).

In a study that examined the effects of changing the Si/Ca ratio of a calcium silicate material on in vitro cell attachment, Alamar Blue was used for measuring cell attachment and proliferation. Si and Ca ion concentrations of the culture medium, in addition to three different calcium silicate materials seeded with MG63 cells, were quantified, and researchers found that the higher the Si content in the material, the more cells attached at all time points. Both proliferation and differentiation increased significantly ($p < 0.05$) with an increase in the Si content of the calcium silicate materials. The researchers also found

that the Si ion concentration of the culture medium increased significantly ($p < 0.05$) with increasing Si content and culture time (153).

Another study investigated the role of integrin in the proliferation and differentiation of HDPCs cultured with calcium silicate (CS) cement and b-tricalcium phosphate (TCP) cement. Si ions were released from CS, and their concentration in DMEM increased and this, in turn, continued in proportion to culture time (181).

We were surprised to notice that the cell attachment efficiency results from this study did not confirm the previous findings. In this study, higher attachment efficiency levels were seen when human dental pulp cells were exposed to nanoparticles in the 50 $\mu\text{g/mL}$ and 100 $\mu\text{g/mL}$ groups compared to the control and other groups. When comparing both doses with each other, higher level of attachment was seen in the 50 $\mu\text{g/mL}$ group compared to 100 $\mu\text{g/mL}$ group. Significant decrease in the attachment was seen in the 1000 $\mu\text{g/mL}$ group compared to the control and other groups.

Yet another study tested the effects of SiO_2 particles on cell adhesion, fibroblasts were exposed to 100 mg/mL SiO_2 particles for 10 hours, detached, and then allowed to adhere for another 8 to 24 hours. The morphologies, attachment, and spreading behavior of the particle-treated cells were different from the control group. The percentages of the 24 hour attached cells decreased significantly to 80% and 57% after the cells were incubated with the 80 nm and 500 nm SiO_2 particles, respectively. They concluded that particles with larger sizes caused less adhesion and spreading of the fibroblasts (14).

Similarly, this study indicated that higher levels of cell attachment were seen in the nanoparticles compared to microparticles in the 50 $\mu\text{g/mL}$ and 100 $\mu\text{g/mL}$ groups. This is where larger particles caused less cell attachment compared to smaller particles. Different patterns were seen in the 12.5 $\mu\text{g/mL}$ and 1000 $\mu\text{g/mL}$, where nanoparticles treated group showed less cell attachment compared to microparticles treated group.

The rate of cell growth is an essential indicator of overall cell health and of the possibility for nanoparticles to interfere with proliferative processes. The proliferation assay aims to detect changes in the number of cells and is considered a direct contact cytotoxicity method.

In this study, we used a crystal violet assay which is a quick, reliable screening method to test the effects of different sizes and doses of silica particles on cell proliferation. During cell death, adherent cells become detached from the well plates, and this feature is used to assess the differences in proliferation upon the application of cytotoxic agents. The crystal violet dye stains the attached cells by binding with DNA.

Another cytotoxicity assay used was the elution assay, which is the standard protocol of ISO 10993 for evaluating the biocompatibility of medical devices. It determines the effect of ions or other components released from the biomaterials on cell growth/viability.

In the past, many groups used different cell lines to elaborate their findings. For example, human bronchoalveolar carcinoma-derived cells were utilized to evaluate cytotoxicity of SiO₂ nanoparticles. Two sizes of silica nanoparticles were employed for that study (15 nm and 46 nm). Decreased cell viability after exposure to 15-nm or 46-nm SiO₂ nanoparticles for 48 hours at dosage levels between 10 µg/ml and 100 µg/ml in a dose-dependent manner was noticed. However, the cytotoxicity of different sizes (15-nm and 46-nm) of silica nanoparticles were not significantly different. The 15-nm SiO₂ nanoparticles were used to assess time-dependent cytotoxicity. Cell viability decreased significantly as a function of both nanoparticle dosage and exposure (44).

At day 14, the proliferation assay in this study demonstrated decreased cell number in a dose-dependent manner in both silica nanoparticles and microparticles. Decrease cell number was also observed in a size-dependent manner when comparing silica nanoparticles to silica microparticles in all doses.

Similar to the findings in this study, another study investigated the cytotoxic effects of 20 nm and 50 nm silica nanoparticles on cultured human embryonic kidney cells (HEK293), and they found that exposure to SiO₂ nanoparticles at dosages between 20 µg/ml and 100 µg/ml decreased cell viability in a dose-dependent manner(50).

Similar findings were seen in a study when human lung fibroblasts (HFL-Is) were exposed to two different sizes of SiO₂ nanoparticles. The effects of both size and concentration on cell responses were studied by analyzing the cell viability, the ratio of apoptosis, and the pathway of cell injury. They concluded that the size and dose-dependent toxicity of HFL-Is was induced by SiO₂ NPs. Meanwhile, the expression of ROS in HFL-

I was significantly increased. This effect was accompanied by the release of cytochrome C from chondriosomes, upregulation of p53 expression, and activation of Bax and caspase 9 for the inhibition of Bcl2. Apoptosis was induced by SiO₂ nanoparticles by stimulating ROS release and subsequently causing the activation of the p53 pathway(51).

At day 14, the cytotoxicity assay in this study demonstrated decreased cell viability in a dose-dependent manner in both silica nanoparticles and microparticles; furthermore, complete cell death was noted in the Sinp100 and Sinp1000 groups. Decreased cell viability was also observed in a size-dependent manner when comparing silica nanoparticles to silica microparticles in all doses.

However, in a study that evaluated the systemic toxicity after applying 20 nm colloidal silica nanoparticles on rat skin for 90 days, unlike the inhalation route or GI route, the application of silica nanoparticles through skin did not result in any toxicity or any change in organs up to a dose of 2,000 mg/kg(182).

A genotoxicity test is an ideal assessment of safety at the molecular level for nanomaterials. This is a very sensitive assay for DSBs based on the fact that a cellular response to these breaks is the phosphorylation of one of the nucleosomal histones, H2AX. The phosphorylated form is known as pH2AX, and the concentration of DSB is sufficient to form a focus that is visible by immunohistochemistry using a fluorescence-tagged antibody to the phosphorylated form. Alternatively, -H2AX can be measured by flow cytometry (183,184).

Amorphous silica particles of different nano-sizes have been shown to cause genotoxic effects in a variety of in vitro assays, but the results were not consistent. For example, one study investigated the mechanisms of genetic and cellular toxicity induced by silica nanoparticles (SiNPs) to determine if such an effect is influenced by nanoparticles' size, amorphous SiNPs (12 nm, 5 nm–10 nm, and 10 nm–15 nm), and micrometer size (SiP2 μm). Mouse lung epithelial (FE1) cells were exposed to various concentrations (12.5, 25, 50, 100 $\mu\text{g}/\text{mL}$) of SiNPs and SiP2 μm . Cellular viability, micronucleus formation, and mutation frequency were measured at different time points. A size-dependent increase in micronucleus formation was observed for SiNPs, which suggests that SiNPs induce cellular and genetic toxicity in a size-dependent manner (40).

Similarly, our studies on normal human dental pulp revealed the same pattern of genotoxic effect, where nanoparticles resulted in a significant higher genotoxic effect compared to microparticles at 24 hours, and in a dose-dependent manner, where higher doses showed higher levels of genotoxicity compared to lower doses.

Other study investigated the effects of nanoparticles in an in vivo comet/micronucleus combination assay and in an in vitro MN assay performed with human blood. Amorphous silica nanoparticles (15 nm and 55 nm) were studied. DNA damage in livers, lung and blood cells, and micronuclei in circulating reticulocytes were measured in Wistar rats. No genotoxic effects were observed (185).

Other authors concluded that genotoxicity may be cell type-dependent and not a concentration- or size-dependent, and that different cell lines should be examined. For

example, brain (A-172) and liver (Huh-7) cells have responded more quickly than stomach (MKN-1) and lung (A549) cells to SiO₂ nanoparticles (186).

Contrary to the findings in this study, no significant genotoxicity was observed in testing of colloidal silica nanoparticles (4 µg/mL and 40 µg/mL) on 3T3-L1 fibroblasts at 3, 6, and 24 hour incubations using the Comet assay (39).

Genotoxicity was reported in other studies using different materials. In a study that evaluated the genotoxicity of silver nanoparticle hydrogel, a significant increase in the micronucleation frequency of HeLa cells was induced by silver nanoparticle hydrogel exposure at concentrations of 20, 40, and 60mg/ml (in medium), compared to the negative control, suggesting that silver nanoparticle hydrogel has high risk of genotoxicity (187).

This is the first report to demonstrate the influence of size and dose of silica nanoparticles on the attachment efficiency, proliferation, cytotoxicity and genotoxicity of normal human dental pulp cells. These results will lead to a better understanding of the biocompatibility of this material when it comes into contact with human dental pulp tissue.

CONCLUSIONS AND CLINICAL CONSIDERATIONS

Chapter 7: CONCLUSIONS

It was concluded that smaller sizes and higher doses of silica particles significantly decrease the proliferation and produce cytotoxic and genotoxic effects on normal human dental pulp culture in a dose-dependent and size-dependent manner.

This is the first report to demonstrate the influence of size and dose of silica nanoparticles on the attachment efficiency, proliferation, cytotoxicity and genotoxicity of normal human dental pulp cells. These results will lead to a better understanding of the biocompatibility of this material when it comes into contact with human dental pulp tissue.

Clinical Considerations

Vital pulp therapy procedures, such as direct pulp capping and pulpotomy, are used to protect and preserve the vitality of teeth. Many materials have been proposed for this clinical application, most commonly, calcium hydroxide, mineral trioxide aggregate, and bioceramic materials. These materials have limitations in the clinical setting, such as handling, setting time, or moisture-dependent setting. Therefore, constant improvement of these materials is essential to develop a material that will help to overcome these limitations. One of the main components in these materials is silica in the form of dicalcium silicate and tricalcium silicate. Some of the advantages of silica include its ability to be produced in different sizes and forms and its ability to allow surface modifications.

One of the main issues when dealing with materials in the nanometer range is biocompatibility. There was evidence of cytotoxicity in different cell line cultures when silica presented in nanometer sizes and in higher doses. This study investigated the effects of different sizes and doses of silica on the attachment efficiency, proliferation, cytotoxicity, and genotoxicity of the human dental pulp in vitro.

The observed significant decrease in cell number and increase in cytotoxic and genotoxic effects in a size and dose dependent manner may aid in the understanding of the cellular behavior that would arise from the use of silica particles. These data can be used to develop better materials with better handling, better tissue healing, and long-term survival of vital pulp therapy procedures.

Future Studies

This in vitro study showed that amorphous silica nanoparticles down-regulated proliferation, induced cytotoxic and genotoxic effects in a size-, dose-, and time-dependent manner on normal human dental pulp cells. This study dealt with a narrow range of doses. Further in vitro studies should be conducted on a broader range of doses to evaluate their effects on pulp tissue cells, mechanism of cell death at a molecular level, and cell cycle analysis. Also, different forms of silica, like mesoporous particles, can be evaluated for their effects on human dental pulp, especially since they are being evaluated for their properties as drug carriers.

This study demonstrated the effects of different sizes and doses of silica on normal human dental pulp cells. Additional studies are required for evaluating their effect on other cell models like cancer cell lines in order to evaluate if they can produce an anticancer effect. Additionally, it can be evaluated on different bacterial cultures to test their antibacterial effects. Further studies are essential to determine the degradation rate of silica containing biomaterials to achieve the optimal in vivo concentrations of released silica for such silica-induced effects.

Animal studies will also be essential to obtain the necessary data that may lead to future biocompatibility studies of those biomaterials in order to expand and improve the clinical applications of dental materials containing silica nanoparticles.

REFERENCES

1. EUR. Potocnik J. Commission recommendation of 18 October 2011 on the definition of nanomaterial. The Official Journal of the European Union 2011;275:38-40.
2. Peppas NA, Hilt JZ, Khademhosseini A, Langer R. Hydrogels in Biology and Medicine: From Molecular Principles to Bionanotechnology. *Advanced Materials*. 2006 Jun 6;18(11):1345–60.
3. Curtis A, Wilkinson C. Nantotechniques and approaches in biotechnology. *Trends in Biotechnology*. 2001 Mar;19(3):97–101.
4. Gaharwar AK, Peppas NA, Khademhosseini A. Nanocomposite hydrogels for biomedical applications. *Biotechnology & Bioengineering*. 2014 Mar;111(3):441–53.
5. Venugopal J, Prabhakaran M, Low S, Choon A, Zhang Y, Deepika G, et al. Nanotechnology for Nanomedicine and Delivery of Drugs. *Current Pharmaceutical Design*. 2008 Aug 1;14(22):2184–200.
6. Carrow JK, Gaharwar AK. Bioinspired Polymeric Nanocomposites for Regenerative Medicine. *Macromolecular Chemistry and Physics*. 2015 Feb;216(3):248–64.
7. Langer R, Vacanti J. Tissue engineering. *Science*. 1993 May 14;260(5110):920–6.
8. Schexnailder P, Schmidt G. Nanocomposite polymer hydrogels. *Colloid and Polymer Science*. 2009 Jan;287(1):1–11.
9. thomas. Thomas JB, Peppas NA, Sato M, Webster TJ. 22 *Nanotechnology and Biomaterials*.
10. Goenka S, Sant V, Sant S. Graphene-based nanomaterials for drug delivery and tissue engineering. *Journal of Controlled Release*. 2014 Jan;173:75–88.
11. Roduner E. Size matters: why nanomaterials are different. *Chemical Society Reviews*. 2006;35(7):583.
12. Buzea C, Pacheco II, Robbie K. Nanomaterials and nanoparticles: Sources and toxicity. *Biointerphases*. 2007 Dec;2(4):MR17–71.
13. Hall JB, Dobrovolskaia MA, Patri AK, McNeil SE. Characterization of nanoparticles for therapeutics. *Nanomedicine*. 2007 Dec;2(6):789–803.

14. Zhang Y, Hu L, Yu D, Gao C. Influence of silica particle internalization on adhesion and migration of human dermal fibroblasts. *Biomaterials*. 2010 Nov;31(32):8465–74.
15. Xavier JR, Desai P, Varanasi VG, Al-Hashimi I, Gaharwar AK. Advanced Nanomaterials: Promises for Improved Dental Tissue Regeneration. In: Kishen A, editor. *Nanotechnology in Endodontics*.
16. Shubayev VI, Pisanic TR, Jin S. Magnetic nanoparticles for theragnostics. *Advanced Drug Delivery Reviews*. 2009 Jun;61(6):467–77.
17. Moghimi SM, Hunter AC, Murray JC. Long-circulating and target-specific nanoparticles: theory to practice. *Pharmacological Reviews*. 2001 Jun;53(2):283–318.
18. Veisheh O, Gunn JW, Zhang M. Design and fabrication of magnetic nanoparticles for targeted drug delivery and imaging. *Advanced Drug Delivery Reviews*. 2010 Mar;62(3):284–304.
19. Cho EJ, Holback H, Liu KC, Abouelmagd SA, Park J, Yeo Y. Nanoparticle Characterization: State of the Art, Challenges, and Emerging Technologies. *Molecular Pharmaceutics*. 2013 Jun 3;10(6):2093–110.
20. Wiogo HTR, Lim M, Bulmus V, Yun J, Amal R. Stabilization of Magnetic Iron Oxide Nanoparticles in Biological Media by Fetal Bovine Serum (FBS). *Langmuir Journal*. 2011 Jan 18;27(2):843–50.
21. Lazzari S, Moscatelli D, Codari F, Salmona M, Morbidelli M, Diomede L. Colloidal stability of polymeric nanoparticles in biological fluids. *Journal of Nanoparticle Research*. 2012 Jun;14(6):920.
22. Lim JK, Majetich SA, Tilton RD. Stabilization of Superparamagnetic Iron Oxide Core–Gold Shell Nanoparticles in High Ionic Strength Media. *Langmuir Journal*. 2009 Dec;25(23):13384–93.
23. Schwarz K. A bound form of silicon in glycosaminoglycans and polyuronides. *Proceedings of the National Academy of Sciences U S A*. 1973 May;70(5):1608–12.
24. Carlisle EM. The Nutritional Essentiality of Silicon. *Nutrition Reviews*. 2009 Apr 27;40(7):193–8.
25. Simpson TL, Volcani BE. *Silicon and siliceous structures in biological systems*. New York, NY: Springer-Verlag; 2011.

26. Lyu K. Effect of silicon on the osteogenesis of human osteoblasts. 1999
27. Keeting PE, Oursler MJ, Wiegand KE, Bonde SK, Spelsberg TC, Riggs BL. Zeolite a increases proliferation, differentiation, and transforming growth factor β production in normal adult human osteoblast-like cells in vitro. *Journal of Bone and Mineral Research*. 2009 Dec 3;7(11):1281–9.
28. Wilson J, Low SB. Bioactive ceramics for periodontal treatment: Comparative studies in the patas monkey. *Journal of Applied Biomaterials*. 1992;3(2):123–9.
29. De La Rocha C, Conley DJ. *Silica Stories*. Cham: Springer International Publishing Imprint : Springer; 2017 [cited 2020 Mar 22]. Available from: <https://doi.org/10.1007/978-3-319-54054-2>.
30. Uboldi C, Giudetti G, Broggi F, Gilliland D, Ponti J, Rossi F. Amorphous silica nanoparticles do not induce cytotoxicity, cell transformation or genotoxicity in Balb/3T3 mouse fibroblasts. *Mutation Research - Genetic Toxicology and Environmental Mutagenesis*. 2012 Jun;745(1–2):11–20.
31. Lu J, Liong M, Zink JJ, Tamanoi F. Mesoporous Silica Nanoparticles as a Delivery System for Hydrophobic Anticancer Drugs. *Small*. 2007 Aug 3;3(8):1341–6.
32. Xia T, Kovochich M, Liong M, Meng H, Kabehie S, George S, et al. Polyethyleneimine Coating Enhances the Cellular Uptake of Mesoporous Silica Nanoparticles and Allows Safe Delivery of siRNA and DNA Constructs. *American Chemical Society Nano*. 2009 Oct 27;3(10):3273–86.
33. Dekkers S, Krystek P, Peters RJB, Lankveld DPK, Bokkers BGH, van Hoven-Arentzen PH, et al. Presence and risks of nanosilica in food products. *Nanotoxicology*. 2011 Sep;5(3):393–405.
34. Huang D, Hung Y, Ko B, Hsu S, Chen W, Chien C, et al. Highly efficient cellular labeling of mesoporous nanoparticles in human mesenchymal stem cells: implication for stem cell tracking. *Federation of American Society of Experimental Biology Journal*. 2005 Dec;19(14):2014–6.
35. Shi H, He X, Yuan Y, Wang K, Liu D. Nanoparticle-Based Biocompatible and Long-Life Marker for Lysosome Labeling and Tracking. *Analytical Chemistry*. 2010 Mar 15;82(6):2213–20.
36. Hirsch LR, Stafford RJ, Bankson JA, Sershen SR, Rivera B, Price RE, et al. Nanoshell-mediated near-infrared thermal therapy of tumors under magnetic resonance guidance. *Proceedings of the National Academy of Sciences. U S A*. 2003 Nov 11;100(23):13549–54.

37. Moghimi SM, Hunter AC, Murray JC. Nanomedicine: current status and future prospects. *Federation of American Society of Experimental Biology journal*. 2005 Mar;19(3):311–30.
38. Park MVDZ, Verharen HW, Zwart E, Hernandez LG, van Benthem J, Elsaesser A, et al. Genotoxicity evaluation of amorphous silica nanoparticles of different sizes using the micronucleus and the plasmid *lacZ* gene mutation assay. *Nanotoxicology*. 2011 Jun;5(2):168–81.
39. Barnes CA, Elsaesser A, Arkusz J, Smok A, Palus J, Leśniak A, et al. Reproducible Comet Assay of Amorphous Silica Nanoparticles Detects No Genotoxicity. *Nano Letters*. 2008 Sep 10;8(9):3069–74.
40. Decan N, Wu D, Williams A, Bernatchez S, Johnston M, Hill M, et al. Characterization of in vitro genotoxic, cytotoxic and transcriptomic responses following exposures to amorphous silica of different sizes. *Mutation Research - Genetic Toxicology and Environmental Mutagenesis*. 2016 Jan;796:8–22.
41. Choi S-J, Oh J-M, Choy J-H. Toxicological effects of inorganic nanoparticles on human lung cancer A549 cells. *Journal of inorganic Biochemistry* . 2009 Mar;103(3):463–71.
42. Napierska D, Thomassen LCJ, Rabolli V, Lison D, Gonzalez L, Kirsch-Volders M, et al. Size-Dependent Cytotoxicity of Monodisperse Silica Nanoparticles in Human Endothelial Cells. *Small*. 2009 Apr 6;5(7):846–53.
43. Ye Y, Liu J, Xu J, Sun L, Chen M, Lan M. Nano-SiO₂ induces apoptosis via activation of p53 and Bax mediated by oxidative stress in human hepatic cell line. *Toxicology In Vitro*. 2010 Apr;24(3):751–8.
44. Lin W, Huang Y, Zhou X-D, Ma Y. In vitro toxicity of silica nanoparticles in human lung cancer cells. *Toxicology and Applied Pharmacology*. 2006 Dec;217(3):252–9.
45. Yang X, Liu J, He H, Zhou L, Gong C, Wang X, et al. SiO₂ nanoparticles induce cytotoxicity and protein expression alteration in HaCaT cells. *Particle and Fibre Toxicology*. 2010;7(1):1.
46. Eom H-J, Choi J. Oxidative stress of silica nanoparticles in human bronchial epithelial cell, Beas-2B. *Toxicology In Vitro*. 2009 Oct;23(7):1326–32.
47. Choi J, Zheng Q, Katz HE, Guilarte TR. Silica-Based Nanoparticle Uptake and Cellular Response by Primary Microglia. *Environmental Health Perspectives*. 2010 May;118(5):589–95.

48. Dutta D, Sundaram SK, Teeguarden JG, Riley BJ, Fifield LS, Jacobs JM, et al. Adsorbed Proteins Influence the Biological Activity and Molecular Targeting of Nanomaterials. *Toxicological Sciences*. 2007 Nov;100(1):303–15.
49. Park E-J, Park K. Oxidative stress and pro-inflammatory responses induced by silica nanoparticles in vivo and in vitro. *Toxicology Letters*. 2009 Jan;184(1):18–25.
50. Wang F, Gao F, Lan M, Yuan H, Huang Y, Liu J. Oxidative stress contributes to silica nanoparticle-induced cytotoxicity in human embryonic kidney cells. *Toxicology In Vitro*. 2009 Aug;23(5):808–15.
51. Xu Z, Chou L, Sun J. Effects of SiO₂ nanoparticles on HFL-I activating ROS-mediated apoptosis via p53 pathway: Effects of SiO₂ nanoparticles on HFL-I. *Journal of Applied Toxicology*. 2012 May;32(5):358–64.
52. Oberdörster G. TOXICOLOGY OF ULTRAFINE PARTICLES: *IN VIVO* STUDIES. In: *Ultrafine Particles in the Atmosphere* [Internet]. PUBLISHED BY IMPERIAL COLLEGE PRESS AND DISTRIBUTED BY WORLD SCIENTIFIC PUBLISHING CO.; 2003 [cited 2020 Mar 22]. p. 203–30.
53. Brown DM, Wilson MR, MacNee W, Stone V, Donaldson K. Size-Dependent Proinflammatory Effects of Ultrafine Polystyrene Particles: A Role for Surface Area and Oxidative Stress in the Enhanced Activity of Ultrafines. *Toxicology and Applied Pharmacology*. 2001 Sep;175(3):191–9.
54. Bernick S, Nedelman C. Effect of aging on the human pulp. *Journal of Endodontics*. 1975 Mar;1(3):88–94.
55. Goldberg M, Lasfargues J-J. Pulpo-dentinal complex revisited. *Journal of Dentistry*. 1995 Feb;23(1):15–20.
56. Pashley. Potential treatment modalities for dentin hypersensitivity—in office products. In Addy M, Orchardson R, editors: *Tooth wear and sensitivity*, L.
57. Nanci A, Ten Cate AR. Ten Cate's oral histology: development, structure, and function. [Internet]. 2013 [cited 2020 Mar 22]. Available from: <http://public.ebookcentral.proquest.com/choice/publicfullrecord.aspx?p=2072432>
58. Engström C, Linde A, Persliden B. Acid hydrolases in the odontoblast-predentin region of dentinogenically active teeth. *European Journal of Oral Sciences*. 1976 Apr;84(2):76–81.

59. Butler WT, D'Souza RN, Bronckers AL, Happonen RP, Somerman MJ. Recent investigations on dentin specific proteins. *Proceedings of the Finnish Dental Society*. 1992;88 Suppl 1:369–76.
60. Lesot H, Osman M, Ruch JV. Immunofluorescent localization of collagens, fibronectin, and laminin during terminal differentiation of odontoblasts. *Developmental Biology* 1981 Mar;82(2):371–81.
61. Linde A. Session II: Cells and Extracellular Matrices of the Dental Pulp — C.T. Hanks, Chairman: The Extracellular Matrix of the Dental Pulp and Dentin. *Journal Dental Research*. 1985 Apr;64(4):523–9.
62. Breschi L, Lopes M, Gobbi P, Mazzotti G, Falconi M, Perdigão J. Dentin proteoglycans: An immunocytochemical FEISEM study: Proteoglycans in Human Dentin. *Journal of Biomedical Materials Research*. 2002 Jul;61(1):40–6.
63. Embery G. Glycosaminoglycans of human dental pulp. *Journal of Biology Buccale*. 1976 Sep;4(3):229–36.
64. Goldberg M, Takagi M. Dentine proteoglycans: composition, ultrastructure and functions. *Journal of Histochemistry*. 1993 Nov;25(11):781–806.
65. Ngassapa D, Närhi M, Hirvonen T. Effect of serotonin (5-HT) and calcitonin gene-related peptide (CGRP) on the function of intradental nerves in the dog. *Proceedings of the Finnish Dental Society*. 1992;88 Suppl 1:143–8.
66. Zhang J. The existence of CD11c+ sentinel and F4/80+ interstitial dendritic cells in dental pulp and their dynamics and functional properties. *International Immunology*. 2006 Jul 14;18(9):1375–84.
67. Hahn C-L, Falkler WA, Siegel MA. A study of T and B cells in pulpal pathosis. *Journal of Endodontics*. 1989 Jan;15(1):20–6.
68. Sakurai K, Okiji T, Suda H. Co-increase of Nerve Fibers and HLA-DR and/or Factor-XIIIa-expressing Dendritic Cells in Dentinal Caries-affected Regions of the Human Dental Pulp: An Immunohistochemical Study. *Journal of Dental Research*. 1999 Oct;78(10):1596–608.
69. Mangkornkarn C, Steiner JC. In vivo and in vitro glycosaminoglycans from human dental pulp. *Journal of Endodontics*. 1992 Jul;18(7):327–31.
70. Ikeda H, Tokita Y, Suda H. Capsaicin-sensitive A δ Fibers in Cat Tooth Pulp. *Journal of Dental Research*. 1997 Jul;76(7):1341–9.

71. Haug SR, Heyeraas KJ. Modulation of Dental Inflammation by the Sympathetic Nervous System. *Journal of Dental Research*. 2006 Jun;85(6):488–95.
72. Johnsen DC, Harshbarger J, Rymer HD. Quantitative assessment of neural development in human premolars. *The anatomical Record*. 1983 Apr;205(4):421–9.
73. Johnsen D, Johns S. Quantitation of nerve fibres in the primary and permanent canine and incisor teeth in man. *Archives of Oral Biology*. 1978;23(9):825–9.
74. Matthews B, Vongsavan N. Interactions between neural and hydrodynamic mechanisms in dentine and pulp. *Archives of Oral Biology*. 1994;39:S87–95.
75. Närhi M, Virtanen A, Kuhta J, Huopaniemi T. Electrical stimulation of teeth with a pulp tester in the cat. *European Journal of Oral Sciences*. 1979 Feb;87(1):32–8.
76. Aars H, Gazelius B, Edwall L, Olgart L. Effects of autonomic reflexes on tooth pulp blood flow in man. *Acta Physiologica*. 1992 Dec;146(4):423–9.
77. Berggreen E, Heyeraas KJ. The Role of Sensory Neuropeptides and Nitric Oxide on Pulpal Blood Flow and Tissue Pressure in the Ferret. *Journal of Dental Research*. 1999 Sep;78(9):1535–43.
78. Kim S, Dörscher-Kim JE, Liu M. Microcirculation of the dental pulp and its autonomic control. *Proceedings of the Finnish Dental Society*. 1989;85(4–5):279–87.
79. Olgart LM, Edwall B, Gazelius B. Neurogenic mediators in control of pulpal blood flow. *Journal of Endodontics*. 1989 Sep;15(9):409–12.
80. Heyeraas Tønder K, Naess G. Nervous control of blood flow in the dental pulp in dogs. *Acta Physiologica*. 1978 Sep;104(1):13–23.
81. uoa. The distribution of blood vessels in the human dental pulp. In Finn SB, editor: *Biology of the dental pulp Organ*, Birmingham, 1968, University of Alabama Press, p 361.
82. Takahashi K, Kishi Y, Kim S. A scanning electron microscope study of the blood vessels of dog pulp using corrosion resin casts. *Journal of Endodontics*. 1982 Mar;8(3):131–5.
83. Hirakawa S, Detmar M. New insights into the biology and pathology of the cutaneous lymphatic system. *Journal of Dermatological Science*. 2004 Jun;35(1):1–8.

84. Ryan TJ, Mortimer PS, Jones RL. Lymphatics of the Skin.: Neglected but Important. *The International Journal of Dermatology*. 1986 Sep;25(7):411–9.
85. Rotstein I, Ingle JI, editors. *Ingle's endodontics 7*. Raleigh, North Carolina: PMPH USA; 2019.
86. Murray PE, Garcia-Godoy F, Hargreaves KM. Regenerative Endodontics: A Review of Current Status and a Call for Action. *Journal of Endodontics*. 2007 Apr;33(4):377–90.
87. Kvinnsland I, Heyeraas KJ. Dentin and osteodentin matrix formation in apicoectomized replanted incisors in cats. *Acta Odontologica Scandinavica*. 1989 Jan;47(1):41–52.
88. Berman LH, Hargreaves KM, Cohen SR. *Cohen's Pathways of the Pulp Expert Consult*. London: Elsevier Health Sciences; 2010
89. Nakahara T. A Review of New Developments in Tissue Engineering Therapy for Periodontitis. *Dental Clinics of North America*. 2006 Apr;50(2):265–76.
90. Nakashima M, Reddi AH. The application of bone morphogenetic proteins to dental tissue engineering. *Nature Biotechnology*. 2003 Sep;21(9):1025–32.
91. Sharma B, Elisseeff JH. Engineering Structurally Organized Cartilage and Bone Tissues. *Annals of Biomedical Engineering*. 2004 Jan;32(1):148–59.
92. Bi Y, Ehrchiou D, Kilts TM, Inkson CA, Embree MC, Sonoyama W, et al. Identification of tendon stem/progenitor cells and the role of the extracellular matrix in their niche. *Nature Medicine*. 2007 Oct;13(10):1219–27.
93. Yamamura T. Differentiation of Pulpal Cells and Inductive Influences of Various Matrices with Reference to Pulpal Wound Healing. *Journal of Dental Research*. 1985 Apr;64(4):530–40.
94. Vacatello M, D'Auria G, Falcigno L, Dettin M, Gambaretto R, Di Bello C, et al. Conformational analysis of heparin binding peptides. *Biomaterials*. 2005 Jun;26(16):3207–14.
95. Yang X, van der Kraan PM, Bian Z, Fan M, Walboomers XF, Jansen JA. Mineralized Tissue Formation by BMP2-transfected Pulp Stem Cells. *Journal of Dental research*. 2009 Nov;88(11):1020–5.
96. Ando Y, Honda MJ, Ohshima H, Tonomura A, Ohara T, Itaya T, et al. The induction of dentin bridge-like structures by constructs of subcultured dental pulp-

- derived cells and porous HA/TCP in porcine teeth. *Nagoya Journal of Medical Sciences*. 2009 Feb;71(1–2):51–62.
97. Zhang F-F, Wan Q, Li C-X, Wang X-L, Zhu Z-Q, Xian Y-Z, et al. Simultaneous assay of glucose, lactate, L-glutamate and hypoxanthine levels in a rat striatum using enzyme electrodes based on neutral red-doped silica nanoparticles. *analytical chemistry journal*. 2004 Oct;380(4):637–42.
 98. Yang X, Yang F, Walboomers XF, Bian Z, Fan M, Jansen JA. The performance of dental pulp stem cells on nanofibrous PCL/gelatin/nHA scaffolds. *Journal of Biomedical Materials Research*. 2009;9999A:NA-NA.
 99. Dobie K, Smith G, Sloan AJ, Smith AJ. Effects of Alginate Hydrogels and TGF- β 1 on Human Dental Pulp Repair In Vitro. *Connective Tissue Research*. 2002 Jan;43(2–3):387–90.
 100. Fujiwara S, Kumabe S, Iwai Y. Isolated Rat Dental Pulp Cell Culture and Transplantation with an Alginate Scaffold. *Okajimas Folia Anatomica Japonica* 2006;83(1):15–24.
 101. Anneroth G, Bang G. The effect of allogeneic demineralized dentin as a pulp capping agent in Java monkeys. *Odontologisk revy*. 1972;23(3):315–28.
 102. Guo W, He Y, Zhang X, Lu W, Wang C, Yu H, et al. The use of dentin matrix scaffold and dental follicle cells for dentin regeneration. *Biomaterials*. 2009 Dec;30(35):6708–23.
 103. Huang GT-J, Sonoyama W, Chen J, Park SH. In vitro characterization of human dental pulp cells: various isolation methods and culturing environments. *Cell and Tissue Research*. 2006 May;324(2):225–36.
 104. Nakashima M. Induction of dentine in amputated pulp of dogs by recombinant human bone morphogenetic proteins-2 and -4 with collagen matrix. *Archives of Oral Biology*. 1994 Dec;39(12):1085–9.
 105. Tziafas D, Kolokuris I, Alvanou A, Kaidoglou K. Short-term dentinogenic response of dog dental pulp tissue after its induction by demineralized or native dentine, or predentine. *Archives of Oral Biology*. 1992 Feb;37(2):119–28.
 106. Anitua E, Sánchez M, Nurden AT, Nurden P, Orive G, Andía I. New insights into and novel applications for platelet-rich fibrin therapies. *Trends in Biotechnology*. 2006 May;24(5):227–34.

107. Anitua E, Andia I, Ardanza B, Nurden P, Nurden A. Autologous platelets as a source of proteins for healing and tissue regeneration. *Thrombosis and Hemostasis* 2004;91(01):4–15.
108. Näsström K, Forsberg B, Petersson A, Westesson P-L. Narrowing of the dental pulp chamber in patients with renal diseases. *Oral Surgery, Oral Medicine, Oral Pathology* 1985 Mar;59(3):242–6.
109. Huang GT-J, Shagramanova K, Chan SW. Formation of Odontoblast-Like Cells from Cultured Human Dental Pulp Cells on Dentin In Vitro. *Journal of Endodontics*. 2006 Nov;32(11):1066–73.
110. Wei X, Ling J, Wu L, Liu L, Xiao Y. Expression of Mineralization Markers in Dental Pulp Cells. *Journal of Endodontics*. 2007 Jun;33(6):703–8.
111. Graham L, Cooper PR, Cassidy N, Nor JE, Sloan AJ, Smith AJ. The effect of calcium hydroxide on solubilisation of bio-active dentine matrix components. *Biomaterials*. 2006 May;27(14):2865–73.
112. Tomson PL, Grover LM, Lumley PJ, Sloan AJ, Smith AJ, Cooper PR. Dissolution of bio-active dentine matrix components by mineral trioxide aggregate. *Journal of Dentistry* 2007 Aug;35(8):636–42.
113. van der Kooy D. Why Stem Cells? *Science*. 2000 Feb 25;287(5457):1439–41.
114. Barry FP. Biology and clinical applications of mesenchymal stem cells. *Birth Defects Research Part C - Embryo Today Reviews*. 2003 Aug;69(3):250–6.
115. Nakashima M, Akamine A. The Application of Tissue Engineering to Regeneration of Pulp and Dentin in Endodontics. *Journal of Endodontics*. 2005 Oct;31(10):711–8.
116. Kawashima N, Noda S, Yamamoto M, Okiji T. Properties of Dental Pulp-derived Mesenchymal Stem Cells and the Effects of Culture Conditions. *Journal of Endodontics*. 2017 Sep;43(9):S31–4.
117. Bilic J, Belmonte JCI. Concise Review: Induced Pluripotent Stem Cells Versus Embryonic Stem Cells: Close Enough or Yet Too Far Apart? *STEM CELLS*. 2012 Jan;30(1):33–41.
118. Knoepfler PS. Deconstructing Stem Cell Tumorigenicity: A Roadmap to Safe Regenerative Medicine. *Stem Cells*. 2009 May;27(5):1050–6.
119. Squillaro T, Peluso G, Galderisi U. Clinical Trials with Mesenchymal Stem Cells: An Update. *Cell Transplant*. 2016 May;25(5):829–48.

120. Giordano A, Galderisi U, Marino IR. From the laboratory bench to the patient's bedside: An update on clinical trials with mesenchymal stem cells. *Journal of Cellular Physiology*. 2007 Apr;211(1):27–35.
121. Albuquerque MTP, Ryan SJ, Münchow EA, Kamocka MM, Gregory RL, Valera MC, et al. Antimicrobial Effects of Novel Triple Antibiotic Paste–Mimic Scaffolds on *Actinomyces naeslundii* Biofilm. *Journal of Endodontics*. 2015 Aug;41(8):1337–43.
122. Torabinejad M, Milan M, Shabahang S, Wright KR, Faras H. Histologic Examination of Teeth with Necrotic Pulp and Periapical Lesions Treated with 2 Scaffolds: An Animal Investigation. *Journal of Endodontics*. 2015 Jun;41(6):846–52.
123. Chai Y, Jiang X, Ito Y, Bringas P, Han J, Rowitch DH, et al. Fate of the mammalian cranial neural crest during tooth and mandibular morphogenesis. *Development*, Cambridge England. 2000 Apr;127(8):1671–9.
124. Hwang Y-C, Hwang I-N, Oh W-M, Park J-C, Lee D-S, Son H-H. Influence of TGF- β 1 on the expression of BSP, DSP, TGF- β 1 receptor I and Smad proteins during reparative dentinogenesis. *The Journal of Molecular Histology*. 2008 Apr;39(2):153–60.
125. Nishikawa S, Kitamura H. Microtubules, intermediate filaments, and actin filaments in the odontoblast of rat incisor. *The anatomical Record*. 1987 Oct;219(2):144–51.
126. Diekwisch T. Localization of microfilaments and microtubules during dental development in the rat. *Acta histochemica*. 1989;37:209–12.
127. Gronthos S, Brahim J, Li W, Fisher LW, Cherman N, Boyde A, et al. Stem Cell Properties of Human Dental Pulp Stem Cells. *Journal of Dental Research*. 2002 Aug;81(8):531–5.
128. Sonoyama W, Liu Y, Fang D, Yamaza T, Seo B-M, Zhang C, et al. Mesenchymal Stem Cell-Mediated Functional Tooth Regeneration in Swine. Csete M, editor. *PLOS ONE*. 2006 Dec 20;1(1):e79.
129. Sonoyama W, Liu Y, Yamaza T, Tuan RS, Wang S, Shi S, et al. Characterization of the Apical Papilla and Its Residing Stem Cells from Human Immature Permanent Teeth: A Pilot Study. *Journal of Endodontics*. 2008 Feb;34(2):166–71.

130. Miura M, Gronthos S, Zhao M, Lu B, Fisher LW, Robey PG, et al. SHED: Stem cells from human exfoliated deciduous teeth. *Proceedings of the National Academy of Sciences*. 2003 May 13;100(10):5807–12.
131. Morsczeck C, Götz W, Schierholz J, Zeilhofer F, Kühn U, Möhl C, et al. Isolation of precursor cells (PCs) from human dental follicle of wisdom teeth. *Matrix Biology*. 2005 Apr;24(2):155–65.
132. Baksh D, Song L, Tuan RS. Adult mesenchymal stem cells: characterization, differentiation, and application in cell and gene therapy. *Journal of Cellular and Molecular Medicine*. 2004 Jul;8(3):301–16.
133. Fitzgerald M, Chiego DJ, Heys DR. Autoradiographic analysis of odontoblast replacement following pulp exposure in primate teeth. *Archives of Oral Biology*. 1990;35(9):707–15.
134. Shi S, Gronthos S. Perivascular Niche of Postnatal Mesenchymal Stem Cells in Human Bone Marrow and Dental Pulp. *Journal of Bone and Mineral Research*. 2003 Apr 1;18(4):696–704.
135. Huang GT-J, Gronthos S, Shi S. Mesenchymal Stem Cells Derived from Dental Tissues vs . Those from Other Sources: Their Biology and Role in Regenerative Medicine. *Journal of Dental Research*. 2009 Sep;88(9):792–806.
136. Chen Y-J, Zhao Y-H, Zhao Y-J, Liu N-X, Lv X, Li Q, et al. Potential dental pulp revascularization and odonto-/osteogenic capacity of a novel transplant combined with dental pulp stem cells and platelet-rich fibrin. *Cell and Tissue Research*. 2015 Aug;361(2):439–55.
137. Gould TRL. Ultrastructural Characteristics of Progenitor Cell Populations in the Periodontal Ligament. *Journal of Dental Research*. 1983 Aug;62(8):873–6.
138. Helmlinger G, Yuan F, Dellian M, Jain RK. Interstitial pH and pO₂ gradients in solid tumors in vivo: High-resolution measurements reveal a lack of correlation. *Nature Medicine*. 1997 Feb;3(2):177–82.
139. Ostby BN. The role of the blood clot in endodontic therapy. An experimental histologic study. *Acta Odontologica Scandinavica*. 1961 Dec;19:324–53.
140. American Association of Endodontists: Glossary of Endodontic Terms, ed 7, Chicago, IL, 2003, American Association of Endodontists.
141. Amler MH. The age factor in human extraction wound healing. *Journal of oral surgery* 1965. 1977 Mar;35(3):193–7.

142. Alsenan F , Jomana. Silicon, calcium and phosphate effect on human dental pulp cell cultures . OpenBU; 2019. Available from:
<https://open.bu.edu/handle/2144/37027>
143. Hargreaves KM, editor. Seltzer and Bender's dental pulp. Rev. ed. Chicago: Quintessence Publ. Co; 2002. 500 p.
144. Rodríguez-Lozano FJ, Bueno C, Insausti CL, Meseguer L, Ramírez MC, Blanquer M, et al. Mesenchymal stem cells derived from dental tissues: Dental stem cells. *International Endodontic Journal*. 2011 Sep;44(9):800–6.
145. Gronthos S, Mankani M, Brahim J, Robey PG, Shi S. Postnatal human dental pulp stem cells (DPSCs) in vitro and in vivo. *Proceedings of the National Academy of Sciences U S A*. 2000 Dec 5;97(25):13625–30.
146. Sloan A, Smith A. Stem cells and the dental pulp: potential roles in dentine regeneration and repair. *Oral Disease*. 2007 Mar;13(2):151–7.
147. Saghiri MA, Asatourian A, Garcia-Godoy F, Sheibani N. Effect of biomaterials on angiogenesis during vital pulp therapy. *Dental Materials Journal*. 2016;35(5):701–9.
148. Miyashita H, Worthington HV, Qualtrough A, Plasschaert A. Pulp management for caries in adults: maintaining pulp vitality. In: *The Cochrane Collaboration, editor. Cochrane Database of Systematic Reviews* . Chichester, UK: John Wiley & Sons, Ltd; 2007
149. Gandolfi MG, Spagnuolo G, Siboni F, Procino A, Riviaccio V, Pelliccioni GA, et al. Calcium silicate/calcium phosphate biphasic cements for vital pulp therapy: chemical-physical properties and human pulp cells response. *Clinical Oral Investigations*. 2015 Nov;19(8):2075–89.
150. Sangwan P, Sangwan A, Duhan J, Rohilla A. Tertiary dentinogenesis with calcium hydroxide: A review of proposed mechanisms. *International Endodontic Journal*. 2013 Jan;46(1):3–19.
151. Camilleri J, Pitt Ford TR. Mineral trioxide aggregate: a review of the constituents and biological properties of the material. *International Endodontic Journal*. 2006 Oct;39(10):747–54.
152. Parirokh M, Torabinejad M. Mineral Trioxide Aggregate: A Comprehensive Literature Review—Part III: Clinical Applications, Drawbacks, and Mechanism of Action. *Journal of Endodontics*. 2010 Mar;36(3):400–13.

153. Shie MY, Chang HC, Ding SJ. Effects of altering the Si/Ca molar ratio of a calcium silicate cement on in vitro cell attachment: Effects of Si/Ca molar ratio on cell attachment. *International Endodontic Journal*. 2012 Apr;45(4):337–45.
154. Chen C-L, Huang T-H, Ding S-J, Shie M-Y, Kao C-T. Comparison of Calcium and Silicate Cement and Mineral Trioxide Aggregate Biologic Effects and Bone Markers Expression in MG63 Cells. *Journal of Endodontics*. 2009 May;35(5):682–5.
155. Chen C-L, Kao C-T, Ding S-J, Shie M-Y, Huang T-H. Expression of the Inflammatory Marker Cyclooxygenase-2 in Dental Pulp Cells Cultured with Mineral Trioxide Aggregate or Calcium Silicate Cements. *Journal of Endodontics*. 2010 Mar;36(3):465–8.
156. Hung C-J, Kao C-T, Shie M-Y, Huang T-H. Comparison of host inflammatory responses between calcium-silicate base material and IRM. *Journal of Dental Sciences*. 2014 Jun;9(2):158–64.
157. Leal F, De-Deus G, Brandao C, Luna A, Souza E, Fidel S. Similar Sealability Between Bioceramic Putty Ready-To-Use Repair Cement and White MTA. *Brazilian Dental Journal*. 2013 Jul;24(4):362–6.
158. Damlar I, Ozcan E, Yula E, Yalcin M, CeliK S. Antimicrobial effects of several calcium silicate-based root-end filling materials. *Dental Materials Journal*. 2014;33(4):453–7.
159. Kohli MR, Yamaguchi M, Setzer FC, Karabucak B. Spectrophotometric Analysis of Coronal Tooth Discoloration Induced by Various Bioceramic Cements and Other Endodontic Materials. *Journal of Endodontics*. 2015 Nov;41(11):1862–6.
160. Shahabinejad H. Warm vertical obturation with three different sealers, effects of technique on sealing ability and potential for retreatment. *OpenBU*; 2020. Available from: <https://open.bu.edu/handle/2144/39301>
161. Merget R, Bauer T, Küpper H, Philippou S, Bauer H, Breitstadt R, et al. Health hazards due to the inhalation of amorphous silica. *Archives of Toxicology*. 2002 Jan;75(11–12):625–34.
162. Santra S, Zhang P, Wang K, Tapeç R, Tan W. Conjugation of biomolecules with luminophore-doped silica nanoparticles for photostable biomarkers. *Analytical Chemistry* 2001 Oct 15;73(20):4988–93.
163. Bharali DJ, Klejbor I, Stachowiak EK, Dutta P, Roy I, Kaur N, et al. Organically modified silica nanoparticles: A nonviral vector for in vivo gene delivery and

- expression in the brain. *Proceedings of the National Academy of Sciences*. 2005 Aug 9;102(32):11539–44.
164. Slowing II, Vivero-Escoto JL, Wu C-W, Lin VS-Y. Mesoporous silica nanoparticles as controlled release drug delivery and gene transfection carriers. *Advanced Drug Delivery Reviews*. 2008 Aug 17;60(11):1278–88.
 165. Barik TK, Sahu B, Swain V. Nanosilica-from medicine to pest control. *Parasitology Research*. 2008 Jul;103(2):253–8.
 166. Shinto H, Fukasawa T, Yoshisue K, Tezuka M, Orita M. Cell membrane disruption induced by amorphous silica nanoparticles in erythrocytes, lymphocytes, malignant melanocytes, and macrophages. *Advanced Powder Technology*. 2014 Nov;25(6):1872–81.
 167. Murdock RC, Braydich-Stolle L, Schrand AM, Schlager JJ, Hussain SM. Characterization of Nanomaterial Dispersion in Solution Prior to In Vitro Exposure Using Dynamic Light Scattering Technique. *Toxicological Sciences*. 2008 Feb;101(2):239–53.
 168. Warheit DB. How Meaningful are the Results of Nanotoxicity Studies in the Absence of Adequate Material Characterization? *Toxicological Sciences*. 2008 Feb;101(2):183–5.
 169. Schwartz MA, Ginsberg MH. Networks and crosstalk: integrin signalling spreads. *Natural Cell Biology*. 2002 Apr;4(4):E65–8.
 170. Boudreau N, Bissell MJ. Extracellular matrix signaling: integration of form and function in normal and malignant cells. *Current Opinion in Cell Biology*. 1998 Oct;10(5):640–6.
 171. Kumar CSSR, editor. *Nanotechnology for the life sciences*. Weinheim: Wiley-VCH; 2011.
 172. Singhvi R, Kumar A, Lopez GP, Stephanopoulos GN, Wang DI, Whitesides GM, et al. Engineering cell shape and function. *Science*. 1994 Apr 29;264(5159):696–8.
 173. Théry M, Racine V, Pépin A, Piel M, Chen Y, Sibarita J-B, et al. The extracellular matrix guides the orientation of the cell division axis. *Natural Cell Biology*. 2005 Oct;7(10):947–53.
 174. Keselowsky BG, Collard DM, García AJ. Integrin binding specificity regulates biomaterial surface chemistry effects on cell differentiation. *Proceedings of the National Academy of Sciences*. 2005 Apr 26;102(17):5953–7.

175. Ding S-J, Shie M-Y, Hoshiba T, Kawazoe N, Chen G, Chang H-C. Osteogenic differentiation and immune response of human bone-marrow-derived mesenchymal stem cells on injectable calcium-silicate-based bone grafts. *Tissue Engineering Part A*. 2010 Jul;16(7):2343–54.
176. Kou PM, Schwartz Z, Boyan BD, Babensee JE. Dendritic cell responses to surface properties of clinical titanium surfaces. *Acta Biomaterialia*. 2011 Mar;7(3):1354–63.
177. Stevens MM. Exploring and Engineering the Cell Surface Interface. *Science*. 2005 Nov 18;310(5751):1135–8.
178. Galli C, Collaud Coen M, Hauert R, Katanaev VL, Gröning P, Schlapbach L. Creation of nanostructures to study the topographical dependency of protein adsorption. *Colloids and Surfaces B: Biointerfaces*. 2002 Oct;26(3):255–67.
179. Barbucci R, Pasqui D, Wirsén A, Affrossman S, Curtis A, Tetta C. Micro and nano-structured surfaces. *Journal of Materials Science*. 2003 Aug;14(8):721–5.
180. Conti M, Donati G, Cianciolo G, Stefoni S, Samorì B. Force spectroscopy study of the adhesion of plasma proteins to the surface of a dialysis membrane: role of the nanoscale surface hydrophobicity and topography. *Journal of Biomedical Materials Research*. 2002 Sep 5;61(3):370–9.
181. Hung C-J, Hsu H-I, Lin C-C, Huang T-H, Wu B-C, Kao C-T, et al. The Role of Integrin αv in Proliferation and Differentiation of Human Dental Pulp Cell Response to Calcium Silicate Cement. *Journal of Endodontics*. 2014 Nov;40(11):1802–9.
182. An SSA, Ryu HJ, Seong N-W, So BJ, Seo H-S, Kim J-H, et al. Evaluation of silica nanoparticle toxicity after topical exposure for 90 days. *International Journal of Nanomedicine*. 2014 Dec;127.
183. Ismail IH, Wadhra TI, Hammarsten O. An optimized method for detecting gamma-H2AX in blood cells reveals a significant interindividual variation in the gamma-H2AX response among humans. *Nucleic Acids Research*. 2007;35(5):e36.
184. Lewis DJ, Bruce C, Bohic S, Cloetens P, Hammond SP, Arbon D, et al. Intracellular synchrotron nanoimaging and DNA damage/genotoxicity screening of novel lanthanide-coated nanovectors. *Nanomedicine*. 2010 Dec;5(10):1547–57.
185. Downs TR, Crosby ME, Hu T, Kumar S, Sullivan A, Sarlo K, et al. Silica nanoparticles administered at the maximum tolerated dose induce genotoxic effects through an inflammatory reaction while gold nanoparticles do not. *Mutation*

Research - Genetic Toxicology and Environmental Mutagenesis. 2012 Jun;745(1–2):38–50.

186. Cha KE, Myung H. Cytotoxic effects of nanoparticles assessed in vitro and in vivo. *Journal of Microbiology and Biotechnology*. 2007 Sep;17(9):1573–8.
187. Xu L, Li X, Takemura T, Hanagata N, Wu G, Chou L. Genotoxicity and molecular response of silver nanoparticle (NP)-based hydrogel. *Journal of Nanobiotechnology*. 2012;10(1):16.

CURRICULUM VITAE

